Titre: Title:	Synthesis of Metal-Polymer Nanocomposites for Fuel Applications
Auteur: Author:	Ricardo José Pontes Lima
Date:	2015
Type:	Mémoire ou thèse / Dissertation or Thesis
Référence: Citation:	Pontes Lima, R. J. (2015). Synthesis of Metal-Polymer Nanocomposites for Fuel Applications [Thèse de doctorat, École Polytechnique de Montréal]. PolyPublie. https://publications.polymtl.ca/1698/

UNIVERSITÉ DE MONTRÉAL

SYNTHESIS OF METAL-POLYMER NANOCOMPOSITES FOR FUEL APPLICATIONS

RICARDO JOSÉ PONTES LIMA

DÉPARTEMENT DE GÉNIE CHIMIQUE

ÉCOLE POLYTECHNIQUE DE MONTRÉAL

THÉSE PRÉSENTÉE EN VUE DE L'OBTENTION

DU DIPLÔME DE PHILOSOPHIAE DOCTOR

(GÉNIE CHIMIQUE)

MARS 2015

UNIVERSITÉ DE MONTRÉAL

ÉCOLE POLYTECHNIQUE DE MONTRÉAL

Cette thèse intitulée:

SYNTHESIS OF METAL-POLYMER NANOCOMPOSITES FOR FUEL APPLICATIONS

présentée par : PONTES LIMA Ricardo José

en vue de l'obtention du diplôme de : Philosophiae Doctor

a été dûment acceptée par le jury d'examen constitué de :

M. FRADETTE Louis, Ph. D., président

M. DUBOIS Charles, Ph. D., membre et directeur de recherche

M. STOWE Robert, Ph. D., membre et codirecteur de recherche

M. TAVARES Jason-Robert, Ph. D., membre

M. WEN John Z., Ph. D., membre

DEDICATION

This thesis is dedicated to

The memory of my parents: Raimundo and Alice.

To my lovely wife: Lidia.

ACKNOWLEDGMENTS

This work would never have been completed without the support of several people, to whom I wish to express my sincere gratitude for all the help they gave me during the last five years.

Professor Charles Dubois, thank you for your guidance, helpful suggestions, encouragement, and for the trust you have placed in me throughout this project. Also, I am deeply grateful for all valuable comments on this thesis.

Dr. Robert Stowe, my co-supervisor: thank you for supporting this project, and for all the efforts for improving the quality of the papers.

I would like to thank Dr. Sophie Ringuette for her help in carrying out the characterization analysis at DRDC, as well as he important and relevant comments on the articles.

I also thank the invaluable financial support from Defence Research and Development Canada.

Several members of the chemical engineering department of polytechnique offered technical assistance for this work, including Ms. Martine Lamarche, Ms. Claire Cerclé, Mr. Gino Robin, Mr. Jean Huard, Mr. Guillaume Lessard, Mr. Robert Delisle. My sincere thanks to all.

I would also like to thank important friends that were beside me during the development of this work: Millad, Omid, Jonathan, Jean-Christophe, Sahar, Paul, Patrice, and Babak.

I also wish to thank Dr. Josianne Lefebvre for the XPS measurements, M. Jean-Philippe Masse and M. Philippe Plamondon for their assistance with the morphological characterizations.

A special thanks to my family: my lovely wife Lidia, for her love and encouragement, as well as for the invaluable support during this endeavour. My daughter, Alice, and my son, Ricardo, thank you for your love and support. Dad loves you.

RÉSUMÉ

Les particules métalliques ont été d'intérêt comme combustibles et additifs de combustibles pour des propergols et explosifs, car ils possèdent une énergie à haute densité. En général, la densité d'énergie volumétrique est supérieure à celui de carburant conventionnel à base d'hydrocarbure. Cet avantage est clairement bénéfique pour les systèmes de propulsion fusée à volume limité, dans lequel le paramètre le plus important est l'impulsion spécifique. Il est bien connu que la réactivité des particules métalliques dépend de la taille des particules qui augmente lorsque la taille des particules diminue. Des améliorations significatives dans les comportements de combustion du propergol ont été attribuées à l'utilisation de particules métalliques de taille nanométrique, par exemple l'augmentation du taux de combustion et la réduction du temps de retard à l'allumage. Pour cette raison, l'application de particules de taille nanométrique comme combustible pourrait être préférable que les particules plus larges. Cependant, plusieurs difficultés limitent l'utilisation des particules ultrafines dans les applications de combustibles et carburants. La plupart d'entre eux sont attribuées à la formation d'une couche d'oxyde sur les particules qui empêchent un bon rendement dans le processus de combustion. Dans les applications de bore comme carburant, ces difficultés pratiques d'allumage et de la complète combustion ont jusqu'à présent limité l'utilisation extensive de bore pour la demande de carburant.

L’application des revêtements non oxydés sur les particules a été indiquée pour les protéger contre l'oxydation prématurée et à améliorer leurs propriétés de combustion. Un certain nombre de méthodes ont été proposées pour enrober des particules de métal avec une variété de composés organiques ou d'autres métaux. Les applications courantes suggèrent les enrobages par des hydrocarbures saturés ou des acides gras, tels que l'acide oléique, en tant que moyen de passivation des particules. Récemment, le broyage de haute énergie en combinaison avec des réactions chimiques a été appliqué à fabriquer des particules métalliques de taille nanométrique, enrobés par des composés organiques. Des avantages de cette technique c’est que la passivation est intégrée à la production de particules dans une seule étape. Par exemple, le broyage réactif de poudres de bore dans une solution d'acide oléique a causé une amélioration de leur réactivité. Toutefois, la polyvalence de la technique de broyage mécanique suggère la possibilité d’enrobage de particules avec des composés organiques variés. Ainsi, le changement de revêtement organique traditionnel par de nouvelles molécules qui peuvent encore améliorer les propriétés des particules est un exceptionnel défi.

La première contribution de ce travail est d'étudier le processus de broyage réactif de poudres métalliques, tels que le bore et l'aluminium, pour une meilleure compréhension de la méthode expérimentale, qu'on propose comme moyen d'obtenir des particules métalliques enrobées par de polymères énergétiques. À cet effet, une étude expérimentale comparative a été réalisée afin d'évaluer deux variantes du broyage mécanique. Dans une procédure typique, les poudres métalliques et les réactifs sont versés dans le flacon de broyeur au démarrage. Les réactions organiques se produisent en même temps que le procédé de broyage. Au contraire, dans la procédure alternative, les poudres sont broyées au préalable avant l'addition du réactif organique, donc un processus pas à pas est effectué. Pour les deux méthodes, un composé organique fonctionnalisé a été greffé sur les particules, par la suite ils ont été incorporés dans une matrice de polymère énergétique pour fabriquer le composite métal-polymère. Les résultats mettent en évidence les différences dans la forme et la taille des particules, l'identification des inconvénients pour les deux applications, ainsi que, l'analyse des effets sur les propriétés de combustion des poudres organiques enrobées et des métaux composites à base de liants.

Le polymère de l'azoture de glycidyl a été choisi le candidat pour enrober les particules en raison de ses bonnes propriétés énergétiques. Comme la viscosité du mélange augmente lorsque la taille des particules diminue, les réactifs de faible viscosité sont recommandés pour éviter la viscosité très élevée. Le poids moléculaire du GAP peut varier de 700 à 5500 et le nombre de groupes hydroxyles terminaux de 0 (GAP plastifiant) à 3. Parmi ces polymères, le GAP plastifiant (700 g mol^{-1}, à faible viscosité) possède de bonnes propriétés qui facilitent son emploi dans un procédé de broyage réactif. Toutefois, certains groupes fonctionnalisés sont nécessaires pour greffer le polymère sur les particules métalliques et le GAP plastifiant ne portent pas de groupes hydroxyle téléchélique. Pour obtenir une meilleure réactivité de ce polymère et la surface du métal frais, le GAP plastifiant a été modifiée chimiquement pour apporter quelques branches de fonction acides supplémentaires dans la chaîne principale. La méthode directe pour l'enrobage des particules métalliques avec le polymère de l'azoture de glycidyl modifié a montré plus d'efficacité pour former la couche énergétique, qui a influencé la dispersion des poudres dans des polymères et accrut la libération totale d'énergie par la combustion de composite métal-polymère.

La dernière phase de cette recherche concerne la production de composites bore polymère à des fins de combustion. Le bore a un très haute pouvoir calorifique sur un base massique, (58 kJ/g) mais aussi, et surtout, par unité de volume (136 kJ/ cc). Cela dépasse clairement l'autre métaux

ou autres combustibles hydrocarbonés classique en masse et volumétrique production de l'énergie. Malgré cette favorable énergie potentielle, le bore a rarement atteint son potentiel dans les systèmes de propulsion alors que l'aluminium est le métal le plus couramment employé dans la préparation des propergols solides composites. Un certain nombre d'études consacrées à la combustion de bore attribuent sa performance réduite à quelques propriétés du métal. La couche d'oxyde de bore (B_2O_3) sur les particules est très stable, ce qui conduit à longue durée de retard d'allumage. Ainsi, le bore élémentaire s'enflamme en deux étapes. La première étape correspond à la combustion de bore revêtue d'une couche d'oxyde, dans un second stage se donne l'achèvement de la combustion du bore particule nu.

L'utilisation de métaux légers, tels que le magnésium et l'aluminium en tant qu'additifs dans des formulations de bore ont été indiquée comme un moyen pour améliorer son efficacité de combustion. Récemment, des améliorations de l'efficacité de la combustion de bore ont été associées à l'utilisation du magnésium et de l'aluminium ajoutés à des formulations. Le mécanisme proposé pour ces améliorations est l'enlèvement de l'oxyde de bore par la réaction avec de l'aluminium et les dégagements de chaleur supplémentaires apportés par l'allumage rapide du magnésium.

Dans ce travail, il a été proposé l'application d'une couche de polymère énergétique sur les particules de bore, qui en plus de la libération d'une quantité importante d'énergie apporte d'autres avantages sur le plan de l'application finale des particules comme carburant (par exemple, la dispersion de particules dans un liant de polymère).

ABSTRACT

Metal particles have long been of interest as fuel and fuel additives for propellants and explosives because their high-density energy. In general, their volumetric energy density is higher as compared to conventional hydrocarbon-based fuel. This advantage is clearly beneficial for volume-limited rocket propulsion systems, in which the most important parameter is the density-based specific impulse. It is widely known that the reactivity of metal particles increases when particle size decreases. Significant improvements in combustion behaviors of propellant have been attributed to the use of nanosize metal particles, for example faster burning rates and shorter ignition delay time. For this reason the application of nanosize particles as fuel could be preferable than large particles. However, several difficulties limit the use of ultrafine particles in fuel applications and propellants. Most of them are attributed to the oxide layer formation on the particles that prevents good combustion performance. In boron applications, practical difficulties such as poor ignition and combustion performance, have so far limited extensive use of boron for fuel applications.

Indications are that application of non-oxide coatings on particles protects them against premature oxidation and enhances their combustion properties. A number of methods have been proposed to coat metal particles with a variety of organic compounds or other metals. Common applications provides coatings of saturated hydrocarbons or fatty acids, such as oleic acid as a means to passivation the particles. Recently, high-energy ball milling, in combination with chemical reactions, was applied to fabricate nanostructured metal particles coated with organic compounds. One of the advantages of this technique is that the passivation be integrated into the production of particles as a single step. For example, the reactive milling of boron in oleic acid solution showed an improved reactivity of as-milled powders. However, the versatility of the mechanical milling technique suggests that a vast range of organic compounds could be applied to the capping of particles. Thus, developing a new method to obtain metal nanosized particles coated with chemical substances that can further improve the properties of particles is a great challenge.

The first contribution of this work is to investigate the reactive milling process of metal powders, such as boron and aluminum, to better understand the experimental methodology as a means to obtain energetic-capped metal particles. To this end, a comparative experimental study was

performed to evaluate two variations of the mechanical milling. In a typical procedure, metal powders and the reagents are poured into the mill vial at the start of milling. The organic reactions occur simultaneously in the milling process. In the alternative procedure, the powders are milled prior the addition of the organic reagent, thus a stepwise process is done. For both methods, an organic functionalized compound was grafted onto the particles, followed by their incorporation into an energetic polymer matrix to create a metal-polymer composite. The results highlight the differences in shape in size of particles, identifying some drawbacks for both applications, as well as analyzing the effects on combustion properties of the organic-capped powders and the binder composites.

The analysis of the first results of the reactive milling showed that this way might lead to by-products and self-polymerization of organic coatings. That is the main drawback for the simultaneous milling process, preventing a better performance of as-milled powders. Considering this problem, it was necessary to modify the milling procedure to further improve the capping of metal particle. Thus, the second part of experiments applies an energetic polymer direct grafted onto particles as a means to further improvements in the energetic properties of powders.

Glycidyl azide polymer (GAP) was chosen as candidate to coat the particles because of its good energetic properties. Since the mixture viscosity increases as the size of particles decreases, low-viscosity reagents are recommended to avoid very high viscosity. The molecular weight of GAP can range from 700 to 5500 and the number of hydroxyl end groups from 0 (GAP plasticizer) to 3. Among these polymers, the GAP plasticizer (700 g mol^{-1}, low viscosity) has good properties to be applied in reactive milling. However, some functionalized groups are necessary to graft the polymer onto metal particles and the GAP plasticizer does not carry telechelic hydroxyl groups. To achieve a better reactivity of this polymer and the fresh metal surface, the GAP plasticizer was chemically modified to make some additional acid-functionalized branches in the main chain of the polymer. The direct method for coating the metal particles with the modified GAP was more effective in forming the energetic layer, which has influenced the dispersion of powders into polymers and increased the total energy release by the combustion of metal-polymer composites.

The last phase of this research addressed the production of boron-polymer composites for combustion purposes. Boron has a very high gravimetric (58 kJ/g) and volumetric (136 kJ/cc) heating value. This clearly exceeds other metal or other conventional hydrocarbon fuels in both

mass and volumetric energy production. Despite of this great potential energy, boron has rarely achieved its potential in propulsion systems, whereas the aluminum is the most common metal employed in the preparation of composite solid propellants. A number of studies addressed to the boron combustion attribute its reduced performance to a certain combustion property of the metal. The boron oxide (B_2O_3) layer, normally found on the particles is highly stable and leads to long ignition delay times. Therefore, the elemental boron ignites in a two-stage process. The first stage corresponds to the burning of boron covered with an oxide layer, and the second stage involves the completion of the combustion of the bare boron particle.

The use of light metals, such as magnesium and aluminum as additives in boron formulations, has been indicated as a means to enhance its combustion efficiency. Recently, improvements of the combustion efficiency of boron were associated with the use of magnesium and aluminum as additives. The mechanism proposed for these improvements was boron oxide removal by reaction with aluminum and the additional heat release by the easy ignition of magnesium.

In this work, it was proposed to apply of a layer of energetic polymer on the boron particles, which, in addition to releasing a significant amount of energy, brings other benefits in terms of the final application of the particles as fuel (i.e., the dispersion of particles into a polymer binder).

TABLE OF CONTENTS

LIST OF TABLES

LIST OF FIGURES

LIST OF ABBREVIATIONS AND ACRONYMS

AM	After-milling reactions
ASF	Atomic sensitivity factor
ATR-FTIR	Attenuated total reflectance – Fourier transform infrared spectroscopy
BCC	Body-centered cubic
BET	Brunauer-Emmett-Teller
BPS	Bis-propargyl-succinate
DEM	Discrete Element Modeling
DSC	Differential scanning calorimeter
DTA	Differential thermal analysis
EEW	Electrical explosion of wire
FT-IR	Fourier transformed infrared spectroscopy
GAP	Glycidyl azide polymer
GAPm	Modified glycidyl azide polymer
AN	Ammonium nitrate
HAP	Hydroxyl ammonium perchlorate
HCP	Hexagonal close-packed
HTPB	Hydrodroxyl-terminated polybutadiene
LOX	Liquid oxygen
PAc	Propiolic Acid
PE	Polyethylene
PCA	Process control agent
PGA	Propargyl alcohol

PU	Polyurethane polymer
SEM	Scanning electron microscopy
SDTA	Simultaneous differential thermal analysis
SR	Simultaneous Reactions
TGA	Thermal gravimetric analysis
TDI	Toluene diisocyanate
XPS	X-ray photoelectron spectroscopy

NOMENCLATURE

A	Peak area in the DTA curve [°C]
A_t	Transversal area [m^2]
C^*	Characteristic velocity [m/s]
C_{Al}	Aluminum content [%]
C_R	Charge ratio
I_s	Specific impulse [s]
M	Molecular weight [kg mol^{-1}]
m_i	Initial weight [mg]
m_0	Weight after first domain [mg]
m	Mass flow rate [kg s^{-1}]
P	Pressure [N m^{-2}]
S_{sp}	Specific surface area [m^2 g^{-1}]
T_{on}	Onset temperature [°C]
$T_{ox\ peak\ 1}$	Maximum temperature in the first peak of oxidation [°C]
V_{ox}	Maximum rate of oxidation [mg min^{-1}]
w/w	Mass fraction [%]
α	Degree of oxidation [%]
α_1	First degree of oxidation [%]
α_2	Final degree of oxidation [%]
ρ	Density [kg m^{-3}]
Δm	Rang of weight variation [mg]
Φ	Diameter [mm]
ρ	Density [g cm^{-3}]

INTRODUCTION

Metal powders, such as boron and aluminum, are attractive fuels and fuel additives for propellants and explosives because of their high energy density. Metal particles, to the exception of lithium, have much higher density than conventional hydrocarbon solid fuels, such as hydroxyl-terminated polybutadiene (HTPB), commonly used in hybrid and solid rocket motors.

Solid rocket motors and hybrid rocket propulsion systems use energy liberated from the combustion of fuel and oxidizer to generate thrust (Chiaverini, 2007). In fact, combustion of solid propellants results in formation of condensed combustion products (Meda et al., 2005). The hot product gases are then expelled out the nozzle to generate thrust (Chiaverini, 2007).

Solid rocket motors are composite materials, solid propellant, constituted by the major part of an oxidation agent, an inorganic salt such as ammonium perchlorate, and an organic binder, typically a polymeric matrix such as HTPB (Meda et al., 2005). In hybrid rocket propulsion, the oxidizer and fuel are both physically separated and stored in different phases. In this case, the solid-fuel grain normally not contents any oxidizing agent, which is a liquid or gaseous oxidizer that is injected into the head end of the solid-fuel grain (Altman and Holzman, 2007).

Metalized-polymer fuels can be applied to both rocket engines, solid rocket motors and hybrid rocket propulsion systems, as a means of enhancing their combustion performances. The key parameter influencing the rocket motor design is the solid-fuel regression rate. The regression rate, a velocity, is defined as the rate at which the solid-phase fuel is converted to a gas (Chiaverini, 2007). The term burning rate is more appropriated to define this velocity for solid propellants because the composite material contains the solid-fuel and oxidation agent mixed together.

Several previous studies are addressed to the use of metal particles in solid propellants and solid-fuels (Chiaverini et al., 2000; Evans et al., 2006; Galfetti et al., 2006; 2007; Liu et al., 2013; Meda et al., 2005; Mullen et al., 2008; Sabourin et al., 2008; Wood et al., 2009; Young et al., 2006;). Most of these researches have been focused on the effect of the addition of aluminum to solid propellants and solid fuels on the regression and burning rates. Significant improvements have been shown, and the advantage of using metal fuels is clearly beneficial for volume-limited rocket propulsion systems, in which the most important parameter is the specific impulse (Kuo et al.,

2004). However, several difficulties limit the use of metal particles in fuels and propellants. For example, the phenomenon of metal agglomeration unfortunately limits the actual performance of metalized propellants (Meda et al., 2005). In the case of boron, ignition problems and incomplete combustion have so far limited the extensive use of this metal (Yeh and Kuo, 1996).

It is has been well established that the size of particle plays an important role in the combustion process of metal powders. For instance, the use of nanoparticles in propellants enhances their combustion properties with shorter ignition delay, faster burning rate, and more complete combustion, as compared to micron-sized metal powders (Galfetti et al., 2006; Kuo et al., 2004; Yetter et al., 2009). In addition, enhanced heat-transfer rates from higher specific surface area; greater flexibility in designing new energetic fuel/propellants with desirable physical properties; the possibility using as a gelling agent to replace inert or low-energy gellants; the faster energy release from direct oxidation reaction in the high-temperature zone, and enhanced propulsive performance with increased density impulse have been attributed to the use of nanoparticles in fuels and propellants (Kuo et al., 2004).

Despite these numerous advantages, ultrafine metal powders without any protective layer can be easily oxidized by exposure to air, producing an oxide layer onto the particles. Under certain conditions (type of metal, size of particles, oxygen pressure and humidity) metal particles can be pyrophoric, for example, aluminum nanoparticles (5 to 80 nm) are highly pyrophoric in air (Martirosyan et al., 2009). Some conditions, such as: a sufficient mass and heating rate, insignificant heat release, and absence of dilution, intense self-heating of sample leads to self-ignition (Ivanov et al., 1999). A large particle under oxidative environment tends to form a protective oxide film layer that prevents further oxidation (diffusion-controlled conditions), whereas the diffusion rate of the oxidizer is much faster than the reaction rate at the particle surface (kinetically controlled conditions) in a small particle (Huang et al., 2009). As a consequence, fast oxidation reaction occurs releasing a high amount of heat in a short time, and the conditions for self-ignition are attained at normal atmospheres and temperature. This drawback could be prevented by the passivation of metal particles with a controlled flow of air in other gases or solvents (Fedorov et al., 2010; Kwon et. al, 2007). However, due to the fact that nanoparticles have a high specific surface area (S_{sp}, [m^2 g^{-1}]), the oxidation process tends to consume a significant portion of the active metal in the particles, with the immediate consequence of diminishing their

energetic potential. Also, the presence of a thick oxide layer complicates the combustion process, retarding the ignition and leading to an incomplete combustion. These findings highlight the need to protect the nanoparticles for reducing possible hazards associated with their handling, as well as their undesirable premature oxidation.

A variety of methods have been proposed for the passivation of metal particles. Conventional methods apply a controlled slow stream of dry gas (Ar + 0.1 vol.%) (Grumov et al., 2006; Kwon et al., 2003; 2007), mixed with saturated hydrocarbons (paraffin) or stearic acid solution in toluene (Kwon et al., 2003). A polyolefin coating produced by in-situ polymerization has been proposed by Dubois et al. (2007) as a means of improving aging characteristic of aluminum powders. In Devener et al. (2009), high-energy ball milling has been applied to fabricate stearic-capped boron particles obtaining a fuel-soluble boron nanoparticles. Modification of the reactivity of micrometer-sized aluminum by coating with poly(carbon monofluoride) and polytetrafluoroethylene, using mechanical activation is reported by Sippel and co-workers. (Sippel et al., 2103[a]; 2013[b]). Sossi et al. (2013) point out the effects of the coatings of nanosized aluminum with hydrocarbons and fluoro hydrocarbons on non-isothermal oxidation behavior.

The passivation layer determines the reactivity, the stability of particles, and the interaction between the coating and the polymer binder. Thus, developing a coating process in which these properties are enhanced presents a formidable challenge. The main goal of this study is to investigate the use of an energetic polymer as a protective layer over metal particles to improve the ignition and combustion characteristics of nanosized metal powders. It is widely believed that the use of the energetic polymer could enhance the reactivity of metallic powder because of its additional and localized energy release during combustion. In addition, a lower enthalpy of the mixture could be reached from polymer-capped particles resulting in easier dispersion in polymer binders.

To fabricate the metal-nanosized powders, we chose to investigate the so-called “mechanical attrition” method combined with chemical reactions between the surface of the particles and the organic reagents. When a metal powder is ball milled, its original surface coated with oxide is destroyed, and a new surface is produced. For milling performed in an inert environment, this new surface is not oxidized (Zhang et al., 2013). Organic compounds added to milling coats the freshly generated metal surface. For a better understanding of the reactive milling approach and for

facilitating the interpretation of the findings presented in this PhD thesis, a literature review is presented in Chapter 1. It concerns the review of solid rocket motors and solid propulsion systems, the application of metal particles as a fuel and fuel additives for solid propellants, and the mechanical milling by high-energy ball milling as a method to obtain functionalized-metal particles. The coatings and passivation methods of metal particles are also reviewed. Chapter 2 presents the materials and methods for all experiments using the high-energy ball milling, as well as the methodology supporting the analysis and validation of combustion parameters. Chapter 3 summarizes the three papers concerning the findings of this work. Chapter 4 presents the results of the organic-coated aluminum particles obtained from high-energy ball milling by two different methods. The simultaneous milling and reactions are compared to a stepwise process. The findings show the differences in the shapes of particles obtained from the two methods. The effect of the new characteristics of particles on the combustion properties is analyzed and discussed. In Chapter 5, the effects of the energetic capping of aluminum particles on the combustion process are presented. It introduces a new energetic polymer synthesis that included chemical modification of glycidyl azide polymer. The modified GAP was used to graft the energetic molecules onto aluminum particles. Chapter 6 presents the evaluation of the effects of the energetic capping of the boron and boron-magnesium alloy powders on non-isothermal oxidation behavior and combustion energy release from the composites. A critical review of the findings of this PhD thesis, focusing on the application of the metal-polymer composite as a fuel, is presented in the chapter 7. Finally, the most important conclusions are given in chapter 8, as well as the perspectives and recommendations for new research in the field of metal-composite for fuel applications.

CHAPTER 1 LITERATURE REVIEW

The literature review is focused on the use of metal particles as a means of improving combustion behaviors of solid fuels. Other important aspects including the production of metal particles, in which the mechanical milling process is emphasized, and the protective coating of metal particles.

1.1 Solid rocket motors and solid propulsion systems

Classical solid rocket motors are composite materials, in which the oxidizer and the fuel-binder are intimately mixed in the single solid phase. However, in hybrid rocket propulsion the propellants are both physically separated and stored in different phases (Figure 1-1) (Altman & Holzman, 2007; Chiaverini, 2007). Consequently, the operation of a hybrid rocket is distinctly different from solid motors. In the solid rocket, since the single solid phase contents the fuel and oxidizer, the combustion occurs when the exposed surface is heated by the combustion flame to the ignition temperature (Altman & Holzman, 2007). In hybrid motors, combustion usually occurs in the boundary layer above the fuel surface rather than at the fuel surface itself (Chiaverini, 2007).

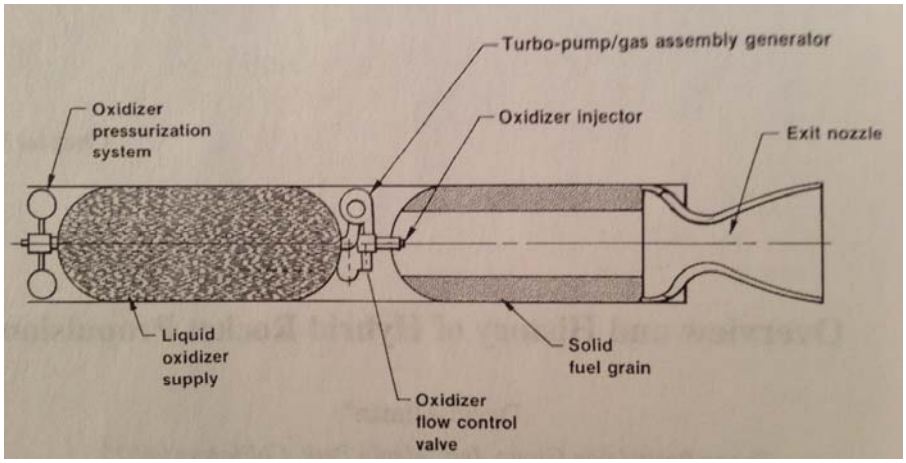

Figure 1-1: Hybrid rocket Schematic (Altman & Holzman, 2007).

The combustion process of hybrid rocket involves the phenomenon of sublimation and or pyrolysis of the solid fuel. Sublimation in the usual sense is the phase change from a solid to a gas without first passing through a liquid phase. Whereas, pyrolysis relates the chemical change, such as the polymer chain breaking, cyclization, and re-organization that can occur while polymer-based fuel degrades and regress.

Polyurethane polymer (PU) is one of the most fuel-binder materials used in composite solid propellants. The PU composite propellant is a heterogeneous mixture of polymer binder, inorganic oxidizer and metallic fuel as the major ingredients. Large portions of oxidizer (68-82 wt.%) is embedded in a polymeric matrix. It can be classified as a highly filled PU system in which the three dimensional elastomeric matrix binds the oxidizer and metallic fuel to form a rubbery material (Mahanta & Pathak, 2012). The binder polymer accounts for 10-15 wt.% of the composite propellant. It usually consists of components: a liquid polyol (HTPB is the most commonly used), an isocyanate (e.g., toluene diisocyanate TDI) as a curator agent, a chain extender (1,4 butenodiol), and cross-linking agent, as the trimethylol propane.

PU composite is a fuel often considered for application to large rocket motors, but other polymer-based fuels could be used, as polyethylene (PE), which can be considered as a reference material for laboratory testing and also can be used for small motors with simple perforations, as well as glycidyl azide polymer (GAP), a fuel which is of interest because of its potential for high regression rates due to its exothermic decomposition (Lengellé, 2007).

Table 1-1: PU composite propellant's performance.

Oxidizer	Composite propellants	ρ (g cm^{-3})	T_1 (K)	C^* (m s^{-1})	M (kg mol^{-1})	I_s (s)	k (c_p/c_v)
Ammonium Nitrate 82 %	11 % PU binder 7 % additive	1.51	1282	1209	20.1	192	1.26
Ammonium Perchlorate 78 – 66 %	18 % PU binder 4 – 20 % Al	1.69	2816	1590	25.0	262	1.21
Ammonium Perchlorate 78 – 66 %	12 % PU binder 4 – 20 % Al	1.74	3371	1577	29.3	266	1.17

Adapted from Sutton & Biblarz (2010)

Table 1-1 summarizes the theoretical values of the specific impulse (I_s), and other performance parameters of some of solid propellant formulations. It includes the characteristic velocity (C^*) that is basically a function of the propellant characteristic (P_1, combustion chamber pressure and

mass flow rate) and combustion chamber design (A_t transversal chamber area). Thus, it is widely used to compare the performance of propellant combinations and combustion chamber designs (Sutton & Biblarz, 2010). It can be calculated from experimental data of P_1, A_t and mass flow rate by using the expression:

Equation 1-1 $$C^* = P_1 \cdot A_t / \dot{m}$$

The specific impulse (I_s) is defined as the total momentum per unit weight of the propellant. This is a very important parameter of the performance of a rocket propulsion system. It can be summarized as time (s) during which a rocket engine can provide at the level of the sea, a thrust equal to a kilogram-force, or 9.81 N per kilogram of propellant consumed.

The theoretical values of I_s, C^*, and propellant density (ρ) of aluminized-binder (Table 1-1) can exemplify the benefits brought by the aluminum addition to solid fuel compared to PU-binder fuel. Considering these improvements, the inclusion of particulate metal materials in solid fuels is great interest in performance enhancement techniques on their physical and thermal properties.

Regression rate is considered the key parameter in hybrid rocket propulsion (Chiaverini et al. 2000). Relatively low mass and linear regression rates of solid fuels have been among the major drawbacks of classical hybrid rocket engine technology due to low density, inertness of conventional solid fuels, and diffusion-controlled combustion process (Risha et al., 2007). Thus, several researches have been focused on this subject, showing significant enhancement techniques of hybrid-propulsion systems (Chiaverini et al., 2000; Evans et al., 2006; Galfetti et al., 2006; 2007; Liu et al., 2013; Meda et al., 2005; Mullen et al., 2008; Sabourin et al., 2008; Wood et al., 2009; Young et al., 2006).

As discussed by Risha et al. (2007), performance enhancement techniques of hybrid-propulsion systems can be divided into three possible categories: (1) adding energetic particles into the solid-fuel grain, (2) replacing the virtually inert HTPB binder with more energetic polymers, e.g., GAP (Hori, 2009; Wada et al., 2009), (3) substituting liquid oxygen (LOX) with more energetic and dense liquid oxidizers such as hydroxyl ammonium perchlorate (HAP) or Hydroxyl ammonium nitrate (HAN). The focus of this work is in the application of the first category, adding energetic particles into the solid-fuel grain, regarding the uses of special coatings to increase their reactivity and energy release during their ignition and combustion process.

1.2 Nanosized material from mechanical attrition

Nanosized materials from mechanical attrition are produced by a “top-down” process, in which a coarse-grained powder is reduced to smaller particles (Castro and Mitchell, 2002). The process is considered very simple, versatile, and interesting to produce new materials that can be quickly obtained in quick laboratory experiments. It may be used to create particles of a certain size and shape, to increase the surface area, and to induce defects in solid structures (Ward et al., 2005). Many researchers have reported significant progress in the preparation of new materials from mechanical attrition techniques. For example, to produce nanocrystalline metals (Fecht et al., 1995; 1990), supersaturated solid solutions of intermetallic compounds (Davis et al., 1988; Umbrajkar et al., 2005), micro/nanocomposites of metallic oxides (Nagashima et al., 2001), to provide a mechanical activation on the thermal explosion in Al-Ni system (Shteinberg et al., 2010; White et al., 2009) and on the thermal synthesis of boron-rich solids of light metals (e.g. Al, Mg, Ca) by subsequent annealing of as-milled powder precursors (Abe et al., 2003; Hacler et al., 2003; Urakaev et al., 2004).

The term “mechanical attrition” can be subdivided into “mechanical alloying” that was developed in 1970’s to prepare oxide dispersion superalloys, amorphous alloys, solid solutions and many classes of metastable materials, and into “mechanical milling” which is the milling of single composition powders to obtain nanocrystalline species or ultrafine amorphous powders (Koch et al., 2010).

The fundamental principle of size reduction in mechanical attrition devices is attributed to the energy transmitted to the sample during collisions between milling media. When using mills in which balls are applied as the milling media, different motions of the balls can be observed (Fig. 1-2).

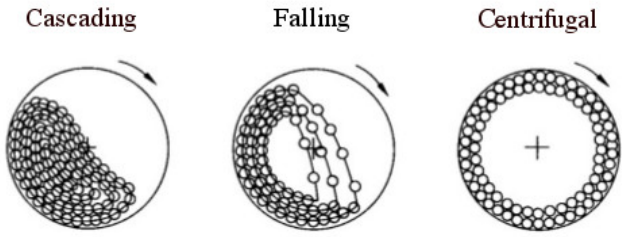

Figure 1-2: Type of motion

The collisions between the balls and the vial cause a plastic deformation by slip, twinning, and re-twinning at high strain rates and, as a result, produce complex dense networks of dislocations (Hwang et al., 2001). The main stress types applied are compression, shear (attrition), impact (stroke) and impact (collision) as depicted in Figure 1-3 (adapted from Balaz, 2008).

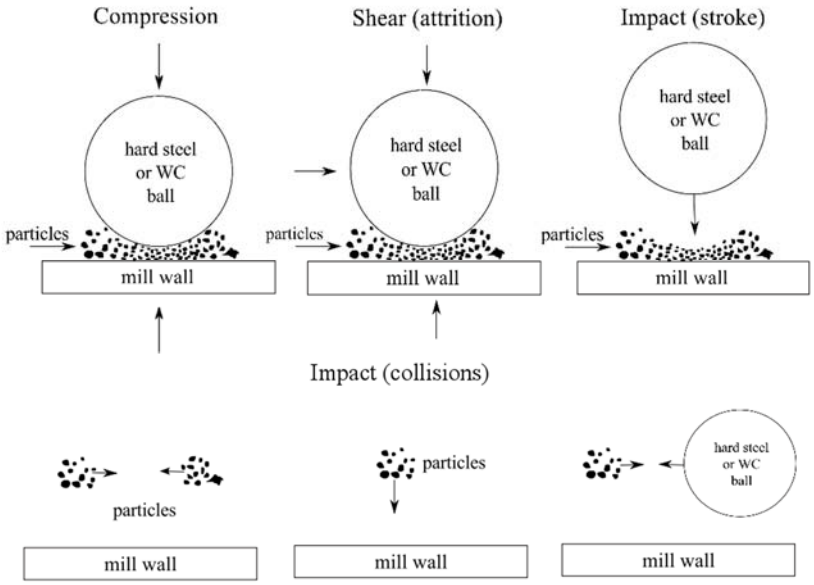

Figure 1-3: The main stress types applied for reducing particle sizes

There are several variables that influence the milling process. Figure 1-4 shows an overview of the main factors that should be considered in the milling process.

Figure 1-4: An overview of the main factors to be considered in the milling process [adapted from Balaz, (2008)]

Type of mill

A variety of types of mills (ball; planetary; vibration; attritor-stirring ball, pin, and rolling mills) with different milling media (balls, rods and cylpebs) are available for high-energy milling. The most frequently used mill for laboratory investigations is a special shaker mill that has been developed in the US under the trade name SPEX mills. The common variety of this mill has one vial containing the sample and milling media, secured in the clamp and swung energetically back and forth several times a minute. According to the specifications of the manufacturer of SPEX 8000M, the mill operates at 1060 cycles/minute (clamp speed) with back-and-forth amplitude of 59mm and side-to-side amplitude of 25mm. The ball velocities are high (5 m s^{-1}) that consequently generate high forces of impact ball-to-ball and ball-to-inner-walls. Therefore, these mills can be considered as the high-energy variety (Koch 1993). Low energy mill operates at low rotation, for example, US Stone-ware roller mill rotating at 290 RPM (Sippel et al., 2013).

Mill materials

A wide variety of the mill materials (vial and milling media) are available. The specific gravity of these materials plays an important role in the milling process. High density materials are commonly used to fabricate balls and mills, including tungsten carbide (14.5 g cm^{-3}), stainless steel (7.8 g cm^{-}

^{3}), hardness steel (7.9 g cm^{-3}), and Zirconium oxide (5.7 g cm^{-3}). Some specific materials can also be employed for more specialized purposes. It has been predicted that high impact forces lead a better results, and the balls should be denser than the material to be milled. The properties of materials commonly used as milling media are given in Table 1-2.

Table 1-2: Milling media for high-energy ball milling

Material	**Main composition**	**Density [g cm^{-3}]**	**Hardness [mohs]**	**Abrasion resistance**
WC	W, C, Co	14.5	8	Very high
Hardened steel	Fe, Cr	7.9	5 - 6	Good
Stainless steel	Fe, Cr, Ni	7.8	5 - 5	Fairly good
Zirconium oxide	ZrO_2	5.7	8	Extremely high

Environment

The milling environment can influence the results significantly. The study conducted by Eckert et al. (1993) evaluates the influence of the milling atmosphere on the melting point temperature of the resulting material. Aluminum powders were milled under different atmospheres (argon, hydrogen, and oxygen) and compared to aluminum powders synthesized by inert gas condensation. The finding reveals that the grain size decreases rapidly to less than 30 nm in the initial hours, and tends to reach a steady state after 30 hours for the samples under argon and hydrogen. Milling of samples under an oxygen environment presents a different refinement of grain that was strongly influenced by the considerable oxide formation resulting in a strong decrease of particles to 13nm after 80h. The final diameter of particles milled under argon attained to 22 nm, and 24 nm for Al under hydrogen.

Wet milling appears more efficient than dry milling in the investigation conducted by Devener et al. (2009). Moreover, severe caking of the boron powder was observed, and the dry milling required

two times longer to reach the same results. In fact, for wet milling, the solvent and reagents can act as a process control agent (PCA) resulting in lubrication of the milling media and the mill walls by a decrease in the surface tension. The easy dispersion of powders increases the trapping of particles in the collisions, augmenting the ball milling efficiency.

Milling time

Milling time is considered the most important factor in the milling process. According to many researchers, the dependence of the milling time on particle refinement usually takes the form of exponential decay, as is depicted in Figure 1-5. Additionally, for long milling times the level of contamination will increase (Balaz, 2008).

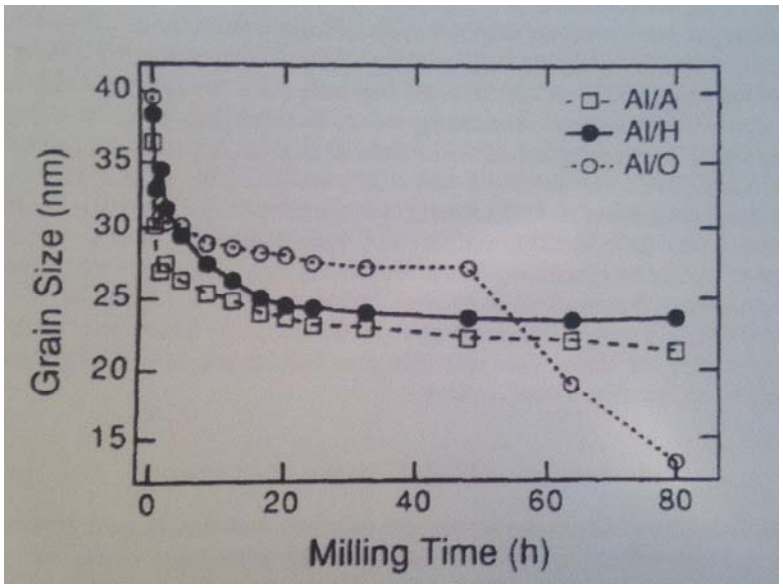

Figure 1-5: Average grain size of aluminum powders as function of milling time

(Eckert et al., 1993)

Temperature of mill

The temperature in ball mill results from oblique collisions and friction. The rise in temperature depends on the speed, the size of the balls, and the stress types. Local temperature rises due to ball collisions and the overall temperature in the vial (Balaz, 2008). The ball temperature remains below 100 °C in a SPEX mixer mill.

1.2.1 Nanosized metal particles from high-energy ball milling

Mechanical milling is widely used for the preparation of metastable amorphous powders, quasi-crystalline, and nanocrystalline materials. The grain size refinement of an elemental metal can be understood following the mechanism proposed by Fecht et al. (1995; 1990) in their report on the synthesis of nanocrystalline metals with body-centered cubic (BCC) and hexagonal close-packed (HCP) structures subjected to ball milling. According to this work, the refinement of the grain size can be summarized in three stages:

(i) Initially, the internal strain increases due to the increasing dislocation density;

(ii) At a certain dislocation density within these heavily strained regions, the crystals disintegrate into sub-grains with low angle boundaries;

(iii) Finally, the sub-grains undergo additional deformation and subsequent disintegrations decreasing the sub-grain sizes.

As a result, the final material obtained by high-energy ball milling consists of nanosized grains, increases in atomic level internal strains, stored enthalpy, and excess specific heat that strongly influence the properties of such materials (Eckert, et al., 1993; Fecht et al., 1990, 1995). As a consequence of the high surface-to-volume ratio for a very fine particle the surface energy may qualitatively change the bulk properties of the material, including the melting temperature, enthalpy of fusion, and boiling temperature (Huang et al., 2009). Theoretical and experimental studies on the melting behavior of aluminum particles (Eckert et al., 1993; Sun et al., 2007) have been shown that the melting temperature decreases gradually with decreasing particle size up to 10 nm (Fig. 1-6). When the particle size is smaller than this critical value, a drastic decrease in the melting temperatures occurs.

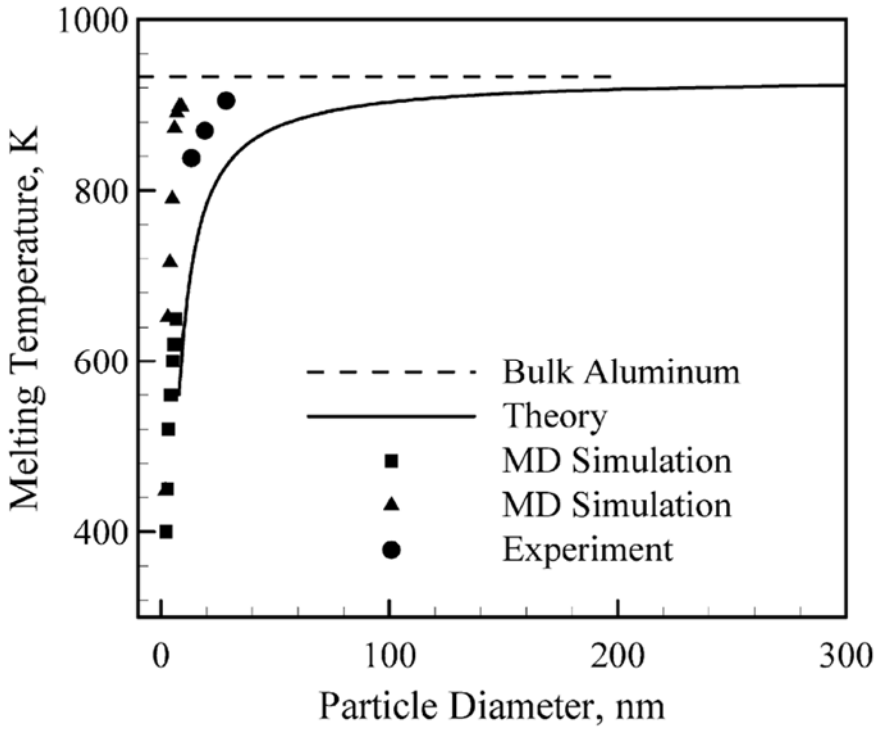

Figure 1-6: Aluminum melting temperature as a function of particle diameter

(Adapted from Huang, 2009)

Numerous research has shown the preparation of nanostructured materials from mechanical attrition and mechanical alloying. Most of it focuses on the synthesis of new materials and alloys, for example, the synthesis of nanocrystalline magnesium (Hwang et al., 2001); the preparation of MgB_2 (Hacler et al., 2003; Gumbel et al., 2002); the preparation of nanocrystalline metals (Fecht et al., 1995; 1990), supersaturated solid solutions of intermetallic compounds (Umbrajkar et al., 2005; Davis et al., 1988), and micro/nanocomposites of metallic oxides (Nagashima et al., 2001). Also, as intermediate process, for example: to provide a mechanical activation on the thermal explosion in Al-Ni system (Shteinberg et al., 2010; White et al., 2009) and on the thermal synthesis of boron-rich solids of light metals (e.g. Al, Mg, Ca) by subsequent annealing of as-milled powder precursors (Abe et al., 2003; Hacler et al., 2003; Urakaev et al., 2004). Other research addressed the study of new properties (Eckert et al., 1993) and the enhancement of materials by the addition of other metals and alloys as is presented in: Koch et al., (2010); Zhang et al., (2013).

A number of experimental and theoretical studies focused on mathematical descriptions of mechanical milling and mechanical alloying (Davis and McDermott, 1998; Maurice and Courtney, 1990; Jiang et al., 2008; Ward et al., 2005). The reactive milling process was described theoretically using the discrete element model (DEM), in a planetary mill (Jiang et al., 2008), and in a SPEX mill (Ward et al., 2005). The theoretical concept of specific milling dose (Dm) was introduced to describe the effect of different parameters on the milling process. An expression for the milling dose, defined as the product of charge ratio (C_R) and milling time (t), is used as an experimental parameter to track the progress of the material refinement (Eq. 1-2).

Equation 1-2 $D_m = C_R\, t$

The usefulness of the DEM model was established in predicting the milling conditions for various process parameters of mechanical alloying or reactive milling (Jiang et al., 2008). Although it provides a good prediction of the rate of material refinement, some side effects that can occur during milling are not considered. For example, the contamination caused by attrition increases significantly as a function of increasing milling time, thus showing the disadvantage of a long process (Balaz et al. 2008).

1.2.2 Other methods of production of metal nanoparticles

Large-scale production of nanoparticles is possible by the electrical explosion of wires (EEW) technology (Sossi et al., 2013). The method is highly productive, provides more than 200 kg/h of powders with an average particle size between 20 to 100 nm, and requires an energy consumption of about 25 kWh/kg (Kotov, 2003).

The method is fully described in Kotov (2003; 2009), but briefly it could be summarized following the schematic diagram depicted in Figure 1-7. When a high-density (10^4–10^6 A/mm^2) current pulse, which is usually produced by the discharge of a capacitor bank, passes through a wire, the density of the energy in the wire may considerably exceed the binding energy because of a high rate of the energy injection and an expansion lag of the heated material. As a result, the material boils up in a burst, a bright light flashes, and a mixture of superheated vapor and boiling droplets of the exploding wire material and a shockwave scatter to the ambient atmosphere.

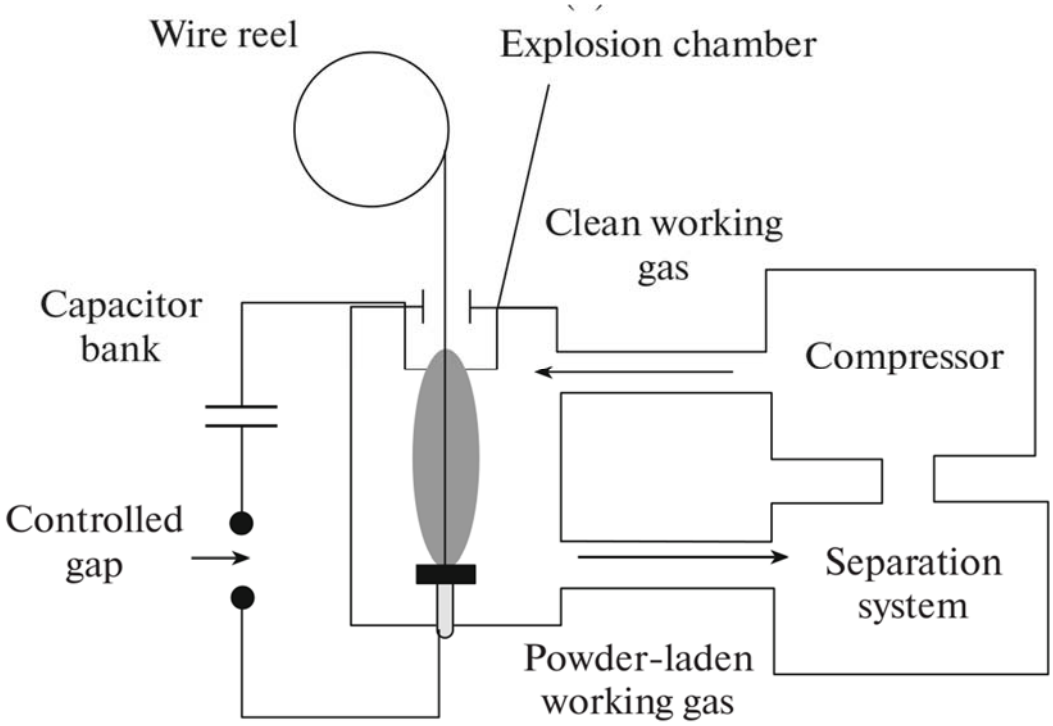

Figure 1-7: Functional diagram of the EEW (Kotov, 2009)

Chemical synthesis can also be used to obtain metallic nanoparticles. For example: the arc-decomposition of diborane (Si et al., 2003), the synthesis of boron nanoparticles by reduction of halides (Lima et al., 2010; Pickering et al. 2007), the pyrolysis of the alkyl aluminum (Cheng, 2005), and the hydrogels synthesis (Hussain et al., 2003).

Very small particles of boron can be obtained by the method described in Pickering et al. (2007). The synthesis of the boron particles follows a synthetic route based on a halogenated precursor (e.g., BBr_3) to produce functionalized boron nanoparticles. The method provides the boron nanoparticles with an average particle size of 5 nm, as shown by the TEM images in Figure 1-8. In Lima et al. (2010), the original route was adapted to produce hydroxyl functional end groups on the surface of the boron particles. These end groups make it possible to insert the boron nanoparticles into the energetic polymer matrix by a further in-situ polymerization step (Lima et al., 2010)

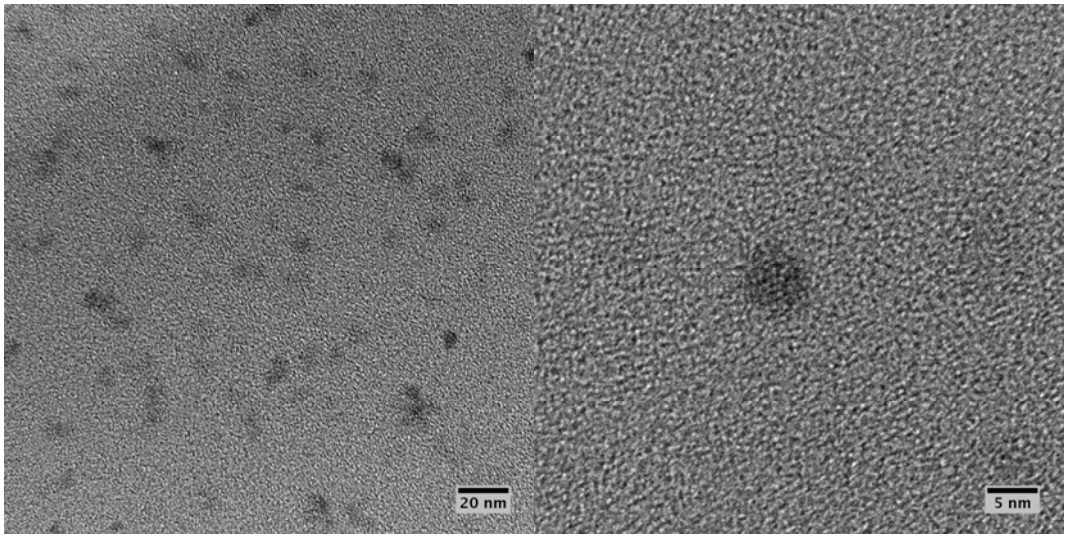

Figure 1-8: TEM images of boron nanoparticles (Lima et al., 2010)

1.3 Coatings of metal particles

Numerous research has been conducted to study methods that provide coatings on metal particles to protect particles against oxidation and aging. The passivation of metal nanopowders is an obligatory stage of production that results in the chemical stability of powders in storage and high reactivity in high-energy condensed system compositions (Fedorov et al., 2010).

Passivation with air

Conventional methods apply oxide films layered onto particles with an amorphous and crystalline structure, such as γ-Al_2O_3 deposed in aluminum nanopowders. Such processing of the oxide layer formation is conducted under slow surface oxidation in a controlled oxidative atmosphere that should be called “passivation-up-to-self-saturation” (Kwon et. al, 2007). (Eq. 1-3) and (Eq. 1-4).

Equation 1-3 $$2Al_{(s)} + 3/2\ O_{2\,(g)} \rightarrow Al_2O_{3\,(s)}$$

Equation 1-4 $$2Al_{(s)} + 3H_2O_{(g)} \rightarrow Al_2O_{3\,(s)} + 3H_{2(s)}$$

According to the data from transmission electron microscopy from Gromov et al. (2006), aluminum particles, passivated by air, are covered with an oxide layer of amorphous and crystalline Al_2O_3, which reaches several nanometers (4-8 nm), as is depicted in Figure 1-9. The already formed oxide

layer on particles of powders can reach 10 – 15 wt. % of γ-Al_2O_3 for particles of ~ 100 nm, and cannot be removed or substituted by any kind of after-passivation treatment (Kwon et al., 2007).

In general, aluminum nanopowders contain 10 wt. % of aluminum oxide, whereas its content in micro powders are only 1.5 – 5.0 wt.% (Fedorov et al., 2009). This drawback limits the application of this technique for passivation of nanopowders with air for application in high-energy condensed systems because of the diminished active metal content.

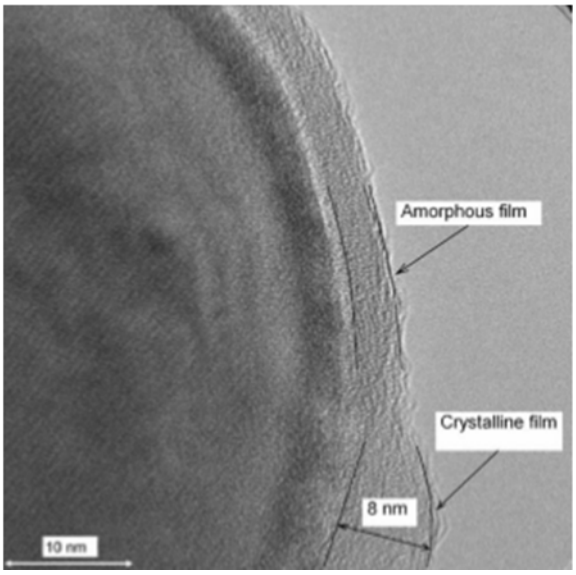

Figure 1-9: TEM images of aluminum nanoparticles (diameter ~100 nm) passivated by air (Gromov et al., 2006)

Passivation by other gases

Passivation directly in the process of production of aluminum nanoparticles could be applied to reduce the risk of pyrophoric effects of powders, and to shorter passivation because the coating of particles is formed during the process. Usually it is applied to the process of electrical explosion of wire (EEW) by using of additives of reactive gases (O_2 or N_2) to argon during the process, which leads to the formation of passivating films (Kwon et al., 2003). Nitrogen gas reacts with aluminum to form aluminum nitride (AlN) films on the particles, however AlN is oxidized and hydrolyzed during storage in air (Kwon et al., 2002). The data presented by Kwon et al. (2003) showed a mass percent of aluminum oxides at 16.0 – 19.1 % for aluminum particles produced by EEW using Ar + 10 vol.% N_2 and passivated with air. On the contrary, aluminum oxide content is 1.1 – 3.7 % for powders produced under Ar + 10 vol.% H_2 gas media.

Kwon et al. (2002) have presented an alternative to a protective film of oxide by the use of aluminum diboride (AlB2). The boride-coated aluminum particles were obtained by EEW of aluminum wires with a boron-containing coating. The advantage offered for this process is the high heat of combustion of aluminum diboride at 41,337 kJ/kg. The table 1-3 summarizes some of the results of this research.

Table 1-3: Characteristics of superfine aluminum powders

SFAP (cover film)	Gas-media	S_s (BET) [$m^2 g^{-1}$]	Al^0 [mass%]	Al2O3 [mass%]
Al (AlB_2)	Ar	17.0	78.0 +18.0(AlB_2)	>1.0
Al (Al_2O_3)	Ar	9.3	88.5	5.5
Al (Al_2O_3)	Ar + N_2	16.0	89.0	5.0
Al (Al_2O_3)	Ar	12.1	94.8	4.0

Adapted from Kwon et al. (2002)

Organic substances coating deposition

The technique of coating particles with organic compounds before their contact with air has been applied as a means to form non-oxide coating films on particles, and to protect against excessive oxidation and aging. Usual methods apply organic substances in solvents. The solution for passivation is added to the fresh powder immediately after production and the powder solution is mechanically stirred for approximately 2 hours (Grumov et al. 2006). The solvent is then evaporated, and the powders dried. The solvents are selected to better disperse the powders and not to interact with the metal powders. The organic substances commonly used to passivate aluminum powders are stearic acid in ethanol or kerosene, and oleic acid in ethanol, (Gromov et al., 2006; Kwon et al., 2007). Other compounds usually applied for organic deposition are nitrocellulose in ethanol, palmitic acid in hydrocarbons, and fluoro-polymers in isopropyl alcohol (Sossi et al., 2013).

Recently, Sossi et al. (2013) have compared fluorohydrocarbon coatings with hydrocarbon acids, such as stearic and palmitic acid. Two diameter sizes of aluminum particles (100 and 50 nm)

produced by EEW and dry air passivated were treated with a solution of the hydrocarbons and fluorohydrocarbons, and compared to one sample without additional coating of organic compounds. From the data of the aluminum content that was measured by alkaline digestion (evaluated after 30 min reaction time in a 5 wt.% NaOH solution), it can be observed that the aluminum content diminished after coating passivation as a result of the mass added from the organic coating. The samples were analyzed by DSC-TGA techniques under non-isothermal oxidation. They concluded that almost no effect on slow non-isothermal oxidation was noted from particles covered by fatty acids, while fluoroelastomer coatings shifted the oxidation to higher temperatures. The authors highlight that fluoroelastomer coatings seem to be better to protect the particle metal core from oxidation, even at high temperatures.

Organic coating by chemical reactions

As an alternative to the process of protective organic coatings by deposition, Roy et al. (2004) and Dubois et al. (2007) investigated the in-situ polymerization process using a thermoplastic and thermoset coatings. Polyolefins such as polyethylene and polypropylene were produced by a modified Ziegler-Natta reaction scheme. Dubois et al. (2007) argue the benefits bring of this method as an efficient barrier against aging and degradation of metal powders, thus polyethylene-coated particles showed a better resistance to aging under stringent conditions of temperature and humidity.

The coating of boron with oleic acid has been presented in Devener et al. (2009). High-energy ball milling has been used to produce boron coated with organic compounds and cerium oxide. They used a SPEX M8000 mill with WC balls and jars for the milling resulting in ~50 nm particles protected against room temperature oxidation by oleic acid functionalization, which also provides an additional solubility in hydrocarbons. The catalyst coating by cerium oxide (CeO_2) is also reported.

In this method, the coating is formed in simple one-step process to produce the nanoparticles and coat them with organic substances, which prevents further oxidation of powders. Various kinds of reagents could be applied that makes it possible for different end uses.

The main drawback of this methodology is the level of contamination from the milling media and the atmosphere. In fact, the authors report contamination with W, Co and Fe from tungsten carbide

milling jars and balls. As boron is very hard and abrasive, the parameters such milling time and ratio powders-to-balls-mass become crucial to prevent high levels of contamination.

The versatility of this method can be exemplified by the findings presented by (Gao et al., 2012). The changing of the oleic acid layer for dopamine hydrochloride provides water-dispersible boron nanoparticles.

The advantages of the applications of non-oxide coatings on metal particles may go beyond these goals since the coating layer can bring other beneficial properties depending of its nature.

Metallic additives and alloys

Another way to enhance the combustion properties of metal powders, such aluminum and boron, is by the addition of other metals or alloys in which the metal added has higher reactivity, for example magnesium. Several applications can be found in the literature.

Liu et al. (2014) studied the effects of the magnesium on the burning characteristics of boron. In their investigation, micron sized magnesium powders (~1μm) and amorphous boron powders (~1μm) were mixed in a mortar to produce five Mg/B mixtures (ratios of 0.1 to 0.5). The samples were analyzed by thermal gravimetric analysis. Combustion studies were carried out in a laser ignition/combustion facility.

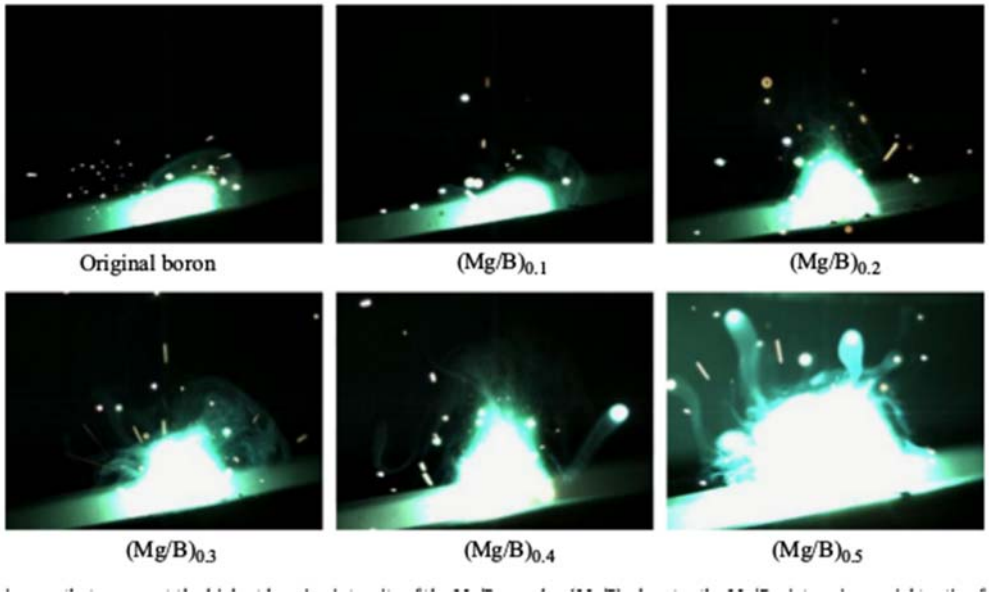

Figure 1-10: Flame images of the Mg/B (Liu et. al, 2014)

The results showed by the authors lead to a conclusion that since magnesium ignites more easily than boron, it induces boron ignition. It was shown by the frame images recorded by a high-speed camera (Fig. 1-10), to be a bright plume surrounded by green radiation, which was interpreted as BO_2 emission.

The faster ignition of boron can be explained by the fact that magnesium reacts with oxygen quickly and releases a significant amount of heat (24.7 kJ g^{-1}). This additional heat can help in the removal of the oxide layer on boron surface and promoting its ignition. However, the reduced ignition delay times for (Mg/B) 0.1 and (Mg/B) 0.2 as compared to original boron (Fig. 1-11), then increase for higher concentration of magnesium. The authors argue a mutual completion in relation between the magnesium-oxygen and boron-oxygen reaction explains this behavior. However, for mixtures prepared in a mortar from a coarse starting material, Zang et al., 2013 showed that the effect of magnesium addition, compared to the powder produced by the use of high-energy milling could be mitigated.

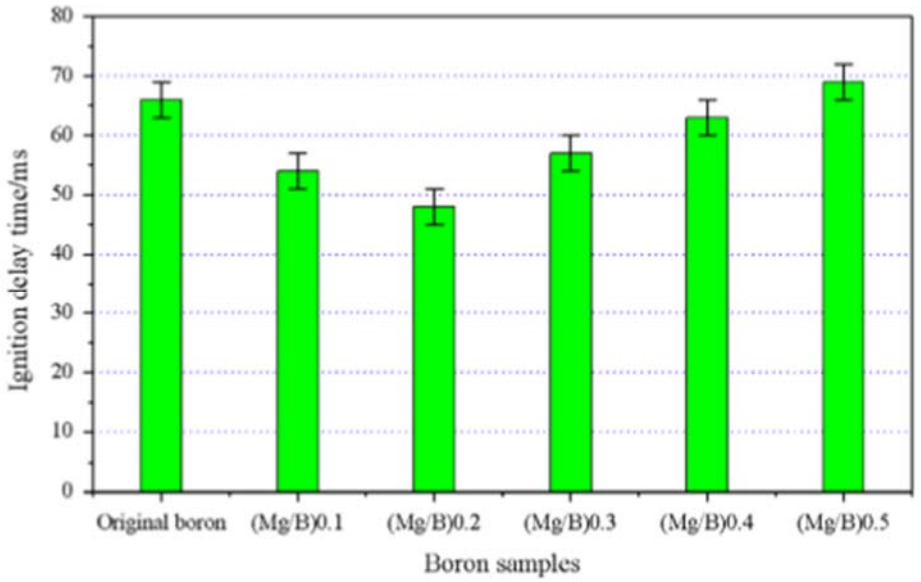

Figure 1-11: Boron ignition delay time of different samples (Liu et al., 2014)

From TGA data, they conclude that the adding of magnesium reduces the initial temperature of boron oxidation, but the mass ratios of up to 0.2 Mg/B decrease in temperature changes insignificantly with respect to an increase in magnesium content. The initial temperatures of the Mg/B samples varied between 600 °C and 630 °C instead ~ 758 °C for the original boron.

Enhanced boron combustion by adding other reactive metals was also demonstrated in the investigation carried out by Zhang et al. (2013). They showed that aluminum and boron milled together improved the activity of boron. The authors claim that this improvement is caused by the reaction between aluminum and the boron oxide following the schematic reaction in eq. 1-5. However, there are not further explanations that can prove if this reaction occurs removing the liquid boron oxide.

Equation 1-5 $2Al + B_2O_3 = 2B + Al_2O_3$

In this research, wet high-energy milling was used to produce the boron/aluminum composite powder by the addition of nanosized aluminum (200 nm) to the raw boron powder (2 – 4 μm) in ethanol as the solvent. In addition, boron powder was milled in pure ethanol as a means to purify the long-term storage boron. The researchers argue that this method is helpful to prevent further oxidation of the boron and dissolve the B_2O_3 deposited on the particles. From the results of TGA-DSC analysis, they concluded that the addition of aluminum is helpful for the reactivity of boron, which is demonstrated by the decrease in the initial temperature of boron oxidation by 133°C, the mass gain increased by 121%, and the heat release increase by 444%. However, there was not any significant improvement for the boron milled with ethanol. From the results of the combustion tests, the burning rate increased by 2.4 – 3.4 times for the boron/aluminum composites.

The importance of high-energy milling was demonstrated by the comparison between as-milled powders and a single mixture of precursors. Faster ignition was observed from as-milled powders.

It has been well established that the passivation layer determines the reactivity, the stability of particles, and the interaction between coating and polymer binder. It improves the particle dispersion in the polymer matrix during mixing. Moreover, the coating process to apply an energetic layer onto particles can provide enhanced combustion.

1.4 Problematic

It is well known that metal particles are attractive fuels for solid propellants and additives for propellants and explosives. Similarly, the use of nanosized metal powders is known to enhance several combustion properties. However, the high reactivity of nanoparticles also leads to some undesirable characteristics, such as the easy oxidation under oxygen-rich environments. A passivation under controlled low oxidative atmospheres can prevent self-ignition of the material;

but at the price of reducing the metal content. Additionally, the oxide layer on the particles is considered the main drawback in the combustion process.

Another shortcoming found in nanoparticle applications is their easy agglomeration and incompatibility with binders during the compounding process. In view of these findings, developing a new method to obtain metal nanosized particles coated with a chemical substance that could protect against oxidation while improving their combustion properties would be a real asset for the future use of these materials in high energy density formulations.

1.5 Objective

The literature review showed that metal particles can be produced and successfully coated with organic ligand by high-energy ball milling. In addition, of the best protection against premature oxidation of particles, some characteristics of the metal combustion would be enhanced (e. g. burning rate, ignition delay time) by the application of an energetic ligand onto particles.

The main goal of this PhD thesis is to develop the method to cap metal particles with an energetic polymer to improve their combustion properties. The high-energy ball milling is proposed as an experimental tool to fabricate the energetic-coated metal particles.

1.6 Specific objectives

The specific objectives of this research are to:

(i) Develop a method to fabricate energetic-capped metal particles using the High-energy ball milling based-process.

(ii) Analyze the effect of energetic coatings on the oxidation of as-milled metal powders.

(iii) Fabricate metal-rich composite materials that could be employed as solid fuels in rocket propulsion applications.

(iv) Assess the effect of energetic coatings on the combustion behavior of metalized-binders.

CHAPTER 2 MATERIALS AND METHODS

2.1 Materials

Micrometric metal powders, such as boron, aluminum, and magnesium, were used as starting materials to produce nanostructured powders and alloys. These powders were then capped with organic compounds to obtain organic-metal nanocomposites. Table 2-1 summarizes the physicochemical properties and supplier of the starting powders.

Table 2-1: Physicochemical properties of metal powders.

Material properties *					Powders characterization	
Metal powders	Density [g cm^{-3}]	Oxide form	Gravimetric heat of Oxidation [kJ g^{-1}]	Volumetric heat of oxidation [kJ cm^{-3}]	Average particle size [μm]	Supplier
Aluminum	2.70	Al_2O_3	31.1	83.9	60	Valimet, Inc.
Boron	2.34	B_2O_3	58.7	137.0	1-2	US Research Nanomaterials, Inc.
Magnesium	1.74	MgO	24.7	43.0	96	—

* Refers to bulk metal. Data from Risha et al., 2007

The organic compounds employed for the coating of particles, propargyl alcohol and propiolic acid, were both supplied by Sigma-Aldrich and used as received. Most particle production was carried out with a triazole modified glycidyl azide polymer (GAP) that was fabricated in our laboratory from GAP plasticizer (3M) and propiolic acid. Bis-Propargyl-Succinate (BPS) used as a curing agent in the polymerization of azide binders, was synthesized in our laboratory following the method described in Keicher et al., 2009.

N-hexane (anhydrous grade, 95%) and toluene (anhydrous grade, 99.8%) procured from Sigma-Aldrich were used as solvents to pour in metal powder mixtures to prevent caking of the powders.

All the solvents were previously dried by molecular sieve (type 3A). Starting materials and milling balls were placed in a milling vial and sealed under argon to avoid contamination. In order to reduce fire hazard, all chemicals and materials were handled in an argon-filled glove box at all times. Since the nanosized powders formed have a higher risk of ignition upon first contact with oxygen-rich environments, it is highly recommended that rigorous laboratory safety practices be carefully followed when handling as-milled metal powders (Bretherick, 1990).

2.2 High-energy ball milling

The SPEX M 8000 series high-energy ball mill (Figure 2-1) using a set of tungsten carbide balls and the container was applied to produce all the samples in this study. The vial temperature during the ball milling process was kept constant by air-cooling. In order to increase the cooling of milling vial, the original shaker mill was modified by the addition of a new external fan to cool the chamber containing the vial. Moreover, a set of finned aluminum heat sinks was placed to enhance the heat transfer from the original tungsten carbide vial, as shown on Figure 2-1b.

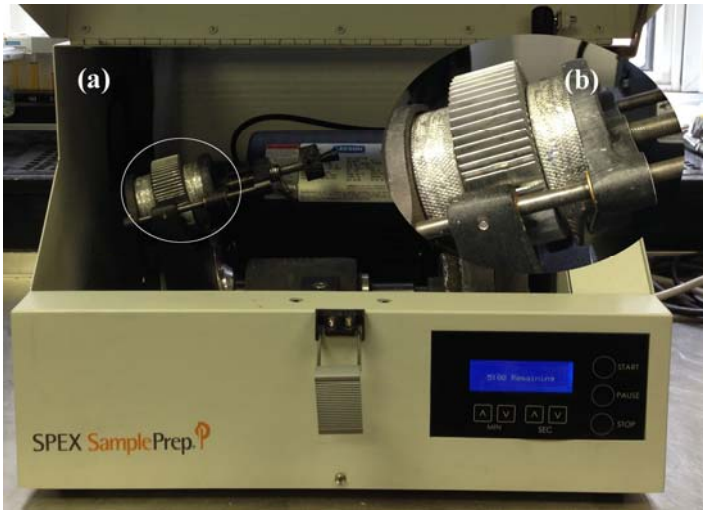

Figure 2-1: (a) Modified SPEX M 8000 (b) detail of finned aluminum heat sink

This study required a variety of milling times leading to a range of different samples, which varied in shape and size as a consequence of processing time. As shown in the literature review, the milling time is the most important factor in the process. While longer milling times bring a more extensive size reduction, they also come with a more significant occurrence of contamination by abrasion of

the vial and balls. Since boron is a very abrasive material, at the beginning of this study, the milling tests were carried out in order to determine an upper limit for the milling time to avoid high contamination.

2.3 Synthesis of modified glycidyl azide polymer

The synthesis of modified glycidyl azide polymer was done by the 1,3 dipolar cycloaddition reaction between azide groups of GAP and alkynes bonds of propiolic acid, which results in the formation of 5-membered heterocyclic groups (triazole rings). The main objective for modifying the original GAP molecules is the addition of hydroxyl groups on the polymer chain, which are necessary to graft it onto metal particles. For a partial substitution of azide groups [N_3], the molecular ratio between these functional groups and the triple bonds of alkynes [-C≡C-] was 0.20 molar equivalent.

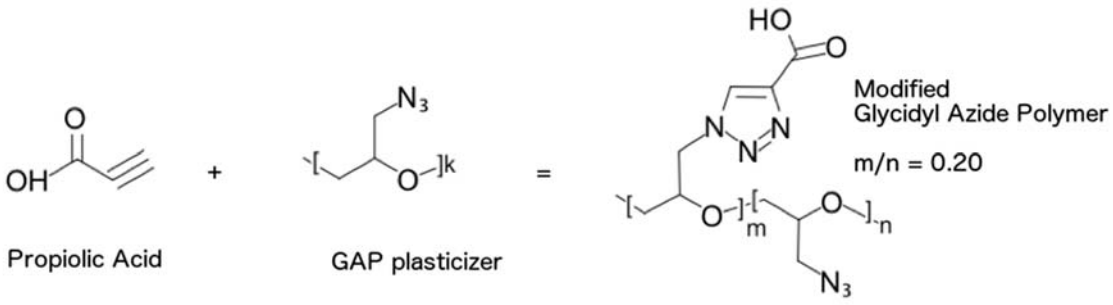

Figure 2-2: Schematic of 1,3 dipolar cycloaddition reaction to produce the modified GAP.

The GAP plasticizer (GAP700 – 700g mol^{-1}) was degassed and dry under vacuum at 70°C for 24h prior to its reaction with propiolic acid (HCCCOOH, Sigma-Aldrich, >95% purity), which was used without further purification.

The procedure to obtain the partially triazole-substituted GAP is as follows:

An amount of 15g of GAP plasticizer (21.43 mmol) was poured into a 50ml round-bottom flask equipped with a mechanical stirrer and placed in thermostatic bath. The starting material was heated under stirring until the mixture temperature attains about 60°C. Propiolic acid was slowly added to the reaction flask using a small syringe (500 μl) equipped with a thin needle (22 ga x 5 cm). The acid was injected very slowly by dripping it until the complete addition of an amount of 2.1 g (29.97 mmol). This procedure was sufficient to dissipate the heat of reaction (247.2 $kJmol^{-}$

[1]), thus avoiding a self-heating that could lead to the violent decomposition of GAP. The mixture temperature was kept at 60°C at all times. The advancement of reaction can be observed by the rise of the mixture viscosity, which increases when the new functionalized branches are added to the main chain of GAP. The rise in viscosity can be attributed to the intermolecular hydrogen bonds formed by the ends of new branches in the GAP chain. The final product is a very viscous liquid. The recovered product was degassed prior to its characterization.

2.4 Fabrication of metal-polymer energetic binders

Several samples of energetic binders enriched by organic-coated metal powders were fabricated using the polymerization reaction between the glycidyl azide polymer (GAP-0700 Plasticizer) and Bis-propargyl succinate following the procedure adapted from Keicher et al. (2009). Thus, the solid fuels were produced using the metal powders incorporated in a GAP-BPS binder (molar ratio 1:0.25).

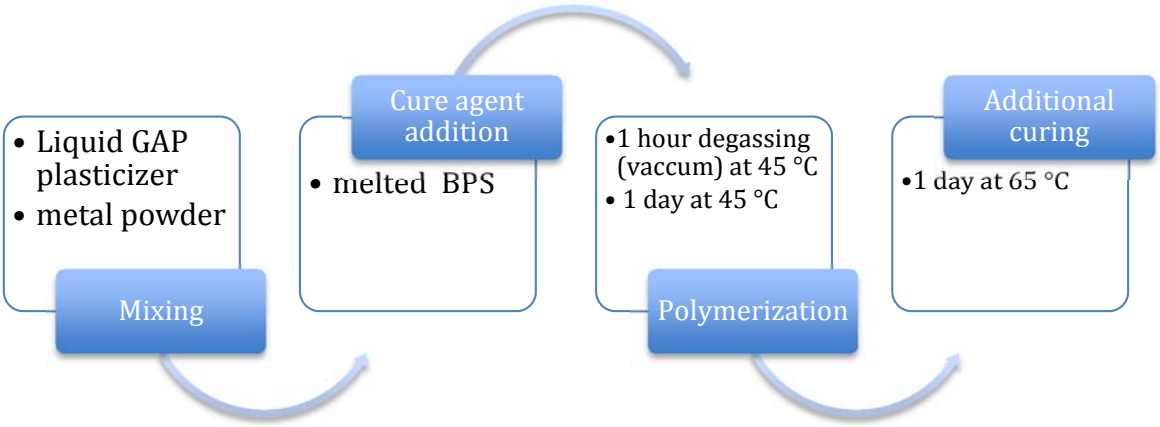

Figure 2-3: The schematic flow of polymerization reactions to produce metalized-binders.

First, a sufficient amount of powders has dispersed into the liquid GAP plasticizer and homogenized for 30 min by manual stirring at ambient temperature. Then, the melted BPS was added to the mixture and mixed until complete homogenization. The final formulation was cast

into plastic molds, degassed during 1 hour at 45°C and cured during one day at 45°C. The initial curing at 45°C was necessary to avoid self-heating and decomposition of GAP mixture. Complete curing was achieved at 65°C for an additional period of one day.

2.5 Characterization techniques

Several experimental techniques were applied to characterize the samples of organic-capped metal powders and metal-polymer energetic binders. Among these techniques, the non-isothermal oxidation of powders conducted in TGA experiments and the measurements of the heat of combustion carried out in an oxygen bomb calorimeter are considered the most important.

2.5.1 Thermal analysis TGA-SDTA

Thermal analysis experiments were conducted in a Mettler Toledo apparatus, model TGA/SDTA 851e. A heating rate of 10 °C/min and a flow rate of 50 ml/min of pure dry oxygen or oxygen/argon mixtures (50/50 and 75/25) were used. For each non-isothermal experiment carried out over the 25 – 1050 °C temperature range, approximately 3 mg of the samples were placed in a 70µl alumina crucible. The initial oxidation temperature, the weight gain rate, and the temperature at a maximum oxidation rate of metal samples were determined using thermal gravimetric and differential thermal analysis.

2.5.2 Oxygen bomb calorimeter

The heat of combustion of metal-rich energetic composites and inert powders composite were measured using a PARR bomb calorimeter under pure dry oxygen. An oxygen pressure of 30 atmospheres was used for all experiments. The thermal mass of the calorimeter was determined to be 10,482±101 JK^{-1} prior to the calorimetric measurements through the combustion of standardized benzoic acid (Fluka, Benzoic acid for calorimeter determination, 26,470 ± 20 J g^{-1}) in a pure oxygen atmosphere. The samples of metal-polymer binders were ignited in a ceramic crucible by a fuse wire in the form of a small loop close to the sample surface.

2.5.3 Surface characterizations XPS and SEM

The chemical composition of particle surfaces was carried out using X-ray photoelectron spectroscopy (XPS). XPS spectra were collected using the Mg Kα X-ray source on a VG Scientific ESCALAB 3 M KII XPS spectrometer. The electron beam power was 216 W (12 kV, 18mA). Both low-resolution survey and high-resolution scans of energy ranges were done. High-resolution spectra were taken with 20 eV pass energy and a resolution of 0.05 eV. The Shirley method was used to subtract background noise and Wagner sensitivity factors for quantitative analysis. Scanning electron microscopy (model JEOL JSM7600TFE) was used for morphological study of powders.

2.5.4 ATR – FTIR and DSC

In order to confirm the new postulated structure of GAPm, ATR-FTIR spectra were obtained using a Perkin Elmer Spectrum 65 – FTIR Spectrometer. The differential scanning calorimetry (DSC) was done using TA instruments Q2000. Scans were carried out using hermetic aluminum pans at scan rates of 5°C min^{-1}, under nitrogen flux, in the range of 40 – 400°C. The study of GAPm decomposition was carried out using thermal analysis (differential gravimetric analysis and thermal analysis).

2.5.5 Physical properties: BET (Brunauer-Emmett-Teller), pycnometer, and physicochemical analysis

As-milled powders were also characterized using additional techniques such as chemical analysis, and BET specific surface area. A simple digestion procedure in a 2M NaOH ethanol/water (20% v/v) solution was used to measure the aluminum content of the samples. Measurements were done according to a gas evolution technique described in Dubois et al., (2007). Adsorption-desorption measurements were performed using a nitrogen/helium mixture as the test gas with a Micromeritics instrument.

CHAPTER 3 ORGANIZATION OF ARTICLES

The following three chapters contain the articles corresponding to the main findings of this work. Each article is presented as a separate chapter.

The first manuscript is found in Chapter 4: "*High-Energy Ball Milling: A comparative Study of Simultaneous and Stepwise Process to Prepare Propargyl-Capped Aluminum Nanoparticles"*. This work investigates the process to prepare aluminum nanoparticles capping by propargylic species, such as propargyl alcohol and propiolic acid. The goal of this work is to compare the effect of the organic coating on the combustion properties of nanoparticles that were produced by two different variations of the high-energy ball milling process. In the first method, the preparation of nanoparticles occurs simultaneously with the coating by the reaction of propargyl alcohol on the fresh surface of the particles. The second method consists in a stepwise process, in which as-milled powders are subjected to reaction with propiolic acid for the formation of an organic layer on the particles. The results shown that the two methods produced particles of different shapes, which influences the combustion behavior. This article has been submitted to the *Journal of Energetic Materials* in 2014 and received correction.

The article: "*Enhanced Reactivity of Aluminum Powders by Capping with A Modified Glycidyl Azide Polymer*" is presented in chapter 5 as the second contribution of this thesis. Following the method applied to obtain aluminum nano flakes coated with organic compounds presented in the first article, this work is focusing on the capping of aluminum particles with energetic polymers as a means to enhance their combustion properties. The findings show that the proposed procedure has been successfully applied to enhance the reactivity of aluminum powders. The coating of modified GAP was grafted onto the aluminum surface, thus it was helpful for the combustion of powders. This article has been submitted to the *International Journal of Energetic Materials and Chemical Propulsion* in 2014 and received minor correction.

The third article: "*Reactivities of Boron and Boron-Magnesium Alloy Powders Coated with a Modified Glycidyl Azide Polymer"* discusses other important metallic fuels: the boron and boron-magnesium alloy powders. The powders were produced from micrometric boron and magnesium by high-energy ball milling followed the coating with modified glycidyl azide polymer. This paper

highlights the significant effect of the energetic coating of metal particles on the final properties of metal-polymer composite. This article has been submitted to the *Journal Energy and fuels* in 2015.

CHAPTER 4 ARTICLE 1: HIGH-ENERGY BALL MILLING: A COMPARATIVE STUDY OF SIMULTANEOUS AND STEPWISE PROCESS TO PREPARE PROPARGYL-CAPPED ALUMINUM NANOPARTICLES

Ricardo J. Pontes Lima[1], Charles Dubois[1], Robert Stowe[2], Sophie Ringuette[2].

1) École Polytechnique de Montréal, Montreal, Canada

2) Defence R&D Canada, Quebec City, Canada

This paper has been submitted to Journal of Energetic Materials

Abstract

High-energy ball milling has been applied to successfully produce on an industrial scale, new alloys, intermetallic compounds and phase mixtures. In nanomaterial research, this technique is often used to produce nanosized particles from much larger ones. This work is focused on the use of this technique to synthesize aluminum-functionalized nanoparticles by the chemical reactions with propargyl groups. It is expected that the propargyl-capped aluminum nanoparticles produced by high-energy ball milling provide a functionalized surface area on metallic particles that can react with azide bearing energetic polymers. In this work, a comparative study of two variants of ball-milled aluminum powders show the influences of simultaneous reaction milling *versus* after-milling reactions on the thermal behavior of powders and on the heat of combustion of binders enriched with milled aluminum powders. Propargylic compounds, such as propargyl alcohol and propiolic acid, were employed to cap milled particles obtained from micrometric aluminum powders. The propargyl functional groups on the particles were then used to graft an energetic polymer, glycidyl azide polymer - GAP, by the formation of triazole rings, and then produce a metal-rich energetic polymer matrix cured with bis-propargyl-succinate. The heat of combustion of binders was measured in a bomb calorimeter. Aluminum-milled powders were characterized by BET (Brunauer-Emmett-Teller) surface area and scanning electron microscopy (SEM). Thermal analysis (thermal gravimetric and differential thermal analysis, TG-DTA) was used to carry out a

comparative study on the reactivity of as-milled powders. As a result, propargyl-capped aluminum powders obtained by after-milling reactions show the highest aluminum content, faster oxidation and attain the highest conversion degree, but the first oxidation occurs at highest temperature. Also, the organic protective coating has not influenced their thermal properties. On the contrary, simultaneous reaction milling gradually reduces aluminum content in the samples and the coating may have influenced the thermal stability of aluminum powders in their oxidation process.

4.1 Introduction

Mechanical attrition by high-energy ball milling has proven to be an effective processing technique to produce nanocrystalline metals (Fecht et al., 1995; 1990), supersaturated solid solutions of intermetallic compounds (Davis et al., 1988; Umbrajkar et al., 2005), micro/nanocomposites of metallic oxides (Nagashima et al., 2001), and to provide a mechanical activation on the thermal explosion in Al-Ni system (Shteinberg et al., 2010; White et al., 2009) and on the thermal synthesis of boron-rich solids of light metals (e.g. Al, Mg, Ca) by subsequent annealing of as-milled powder precursors (Abe et al., 2003; Hacler et al., 2003; Urakaev et al., 2004). The term “mechanical attrition” can be subdivided into “mechanical alloying” that was used to prepare oxide dispersion superalloys, amorphous alloys, solid solutions and many classes of metastable materials, and “mechanical milling” which is the milling of single composition powders to obtain nanocrystalline species or ultrafine amorphous powders (Koch et al., 2010).

During mechanical attrition, the metal powders are subjected to severe mechanical deformation from collisions between the balls and the vial that cause a plastic deformation by slip, twinning and re-twinning at high strain rates, and as a result produce complex dense networks of dislocations (Hwang et al., 2001). For this, high-energy milling forces should be applied by using high frequencies and relatively small amplitude vibrations of balls as produced in shaker mills (e.g. SPEX 8000M).

The grain size reduction of an elemental metal can be understood following the mechanism proposed by Fecht et al. (1995) in their report on the synthesis of nanocrystalline metals with body-centered cubic (BCC) and hexagonal close-packed (HCP) structures subjected to ball milling. According to this work, the refinement of the grain size can be summarized in three stages: initially the internal strain increases due to the increasing dislocation density; at a certain dislocation density

within these heavily strained regions, the crystals disintegrate into sub-grains with low angle boundaries; and finally the sub-grains undergo additional deformation and subsequent disintegrations decreasing the sub-grains size. As a result, the final material obtained by high-energy ball milling consists of nanosized grains, increases in atomic level internal strains, stored enthalpy, and excess specific heat strongly influence the properties of such materials. For example, in the study conducted by Eckert et al. (1993) on the melting behavior of nanocrystalline aluminum powders prepared by ball milling, it was found that they exhibit a lower melting temperature than the bulk melting point as a consequence of the instability due to nucleation of disorder/melting at grain boundary interfaces.

Mechanical milling is a very versatile method of obtaining metastable amorphous powders, quasi-crystalline, and nanocrystalline materials. It can be applied to diverse fields of nanotechnology. Such a method can be employed to produce organic-capped nanoparticles, in which the coating of the particles occurs simultaneously with the milling process. For example, this technique has been used to obtain fuel-soluble and air-stable boron nanoparticles for combustion purposes (Devener et al., 2009). A similar procedure was also used to fabricate water-dispersible boron nanoparticles as a potential boron delivery agent for cancer treatments (Gao et al., 2012) by ligand exchange with dopamine hydrochloride.

The main goal of our research is to evaluate the combustion properties of metallic particles capped by an organic ligand layer. Coating the particles with an energetic polymer can bring additional heat closer to the particles' surface, thus facilitating ignition (Dubois et. al, 2007). For this, in the present study mechanical attrition – ball milling of powders – was used as a method to prepare nanostructured metals capped with an organic ligand layer. This layer, from a subsequent reaction with an energetic polymer, leads to a metal-rich energetic polymer matrix. It is most important that the particles achieved a large surface area while keeping a high fraction of non-oxidized metal content. Since the capping occurs by a reaction between metal particles and an organic compound, which acts as an oxidant, a good balance between milling and reaction time is necessary. In order to provide a better procedure to achieve these goals, we present a comparative study in which we compare two variants of the high-energy ball milling, a simultaneous reaction milling and an after-milling reaction scheme. The approach chosen to determine the reactivity of powders was the non-

isothermal oxidation carried out in the thermogravimetric analysis. Several thermal parameters were measured following a methodology that is fully described in Ilyin et al., (2002).

Also, aluminized energetic binder composites were fabricated from the propargyl-capped aluminum nanoparticles using glycidyl azide polymer, as an energetic binder, cured with bis-propargyl-succinate (BPS) (Keicher et al., 2009). The composites were analyzed in a bomb calorimeter to determine the heat of combustion in an oxygen environment.

4.2 Experimental Methodology

4.2.1 Ball Milling

Commercial aluminum powder (Aluminum H60 Valimet Inc., nominal diameter 60 μm containing a minimum 99.7% of weight aluminum) was used as starting material. A SPEX 8000 series shaker mill using a tungsten carbide vial and balls (Φ = 3.16 mm, ρ = 14.5 g cm^{-3}) was employed to prepare the ball-milling powders. In previous milling tests, we observed that the milling-time and ball-to-powder mass ratio (charge ratio, C_R) influences directly the grain size reduction. Based on those previous results, we decided to set this ratio to 20:1 for all experiments and varying the milling time, which allows evaluating the effect of grinding on the same amount of aluminum powder. For this purpose, in each milling test 4.5 g of aluminum powder were added to 15 ml of toluene (Sigma-Aldrich) previously dried in a molecular sieve.

Starting materials and milling balls were placed in a milling vial and sealed under argon to avoid premature oxidation of the metal. All chemicals and materials were handled in an argon-filled glove box. In order to establish a reasonable comparison study, two series of experiments were carried out with a progressive variation of milling times. The first set of tests was the simultaneous milling and chemical reaction by the addition of 6.5 ml of propargyl alcohol (Sigma-Aldrich) into the starting materials. Six samples were produced for milling times ranging from 30 to 360 minutes. In the second group of experiments, only the initial mixture of powders and solvent was milled and the milling time was varied between 180 to 360 minutes. At the end of each milling, an amount of 1ml of propiolic acid (Sigma-Aldrich) was added to the sample prior to a further milling step of 30 min.

4.2.2 Processing of Energetic Aluminized-Binders

Several samples of energetic composites enriched by propargyl-capped aluminum powders were fabricated using glycidyl azide polymer (GAP-0700 Plasticizer). Composites were produced using either 10 or 30wt% Al powders in a GAP-BPS binder (molar ratio 1:0.25). In order to investigate the heat of combustion of aluminum powders in the composite, which is proportional to the aluminum content in the samples, some composites containing an inert material (alumina (Al_2O_3)) were also produced. The general procedure for the preparation of compositions was as follows:

The appropriated amounts of GAP and BPS for a molar ratio of 0.25 ([C≡C]/[N_3]) were weighed together and then homogenized by mixing for 30 min. at ambient temperature. The clear solution was slowly poured over the propargyl-capped aluminum powder and mixed until complete homogenization. The mixture was then cast into a plastic mold, degassed during 30 min at 45°C and then cured during one day at 45°C. The pre-curing at 45°C is applied to avoid a self-heating reaction that could lead to decomposition of GAP mixture. Complete curing was conducted at 65°C for one additional day.

4.2.3 Characterizations

Oxidation of the as-milled powders was studied by differential thermal analysis (DTA) in an oxygen/argon (75/25) environment with thermogravimetry analysis and simultaneous differential temperature analysis (TGA/SDTA) using a METTLER TOLEDO apparatus operating over a 25°C – 1050°C range. In order to establish the difference between aluminum powders produced by simultaneous reaction milling and after-milling reaction, thermal characteristic properties of aluminum powders were compared. To this end, TGA/SDTA data of non-isothermal oxidation experiments was obtained. Thermogravimetric analysis was done under conditions programmed for the oxygen/argon flow rate of 50 ml/min at a heating rate of 10 K/min. The following performance factors were retained for characterization and discussion purposes:

a) The temperature of the onset of intensive oxidation (t_{on} ,°C)

b) The maximum rate of oxidation (v_{ox}, mg/min)

c) The degree of oxidation of Al in a given temperature range (α, %)

d) The relative thermal effect (defined as the peak area under the SDTA curve divided by weight gain, (A/Δm, relative units).

The degree of oxidation of aluminum was calculated from the initial mass increase corresponding to the first stepwise oxidation (α_1) and to the final degree of oxidation (α_2) at 1050 °C. The weight loss starting at the initial temperature up to 350 °C was also noted as an additional parameter that was associated to the organic layer decomposition.

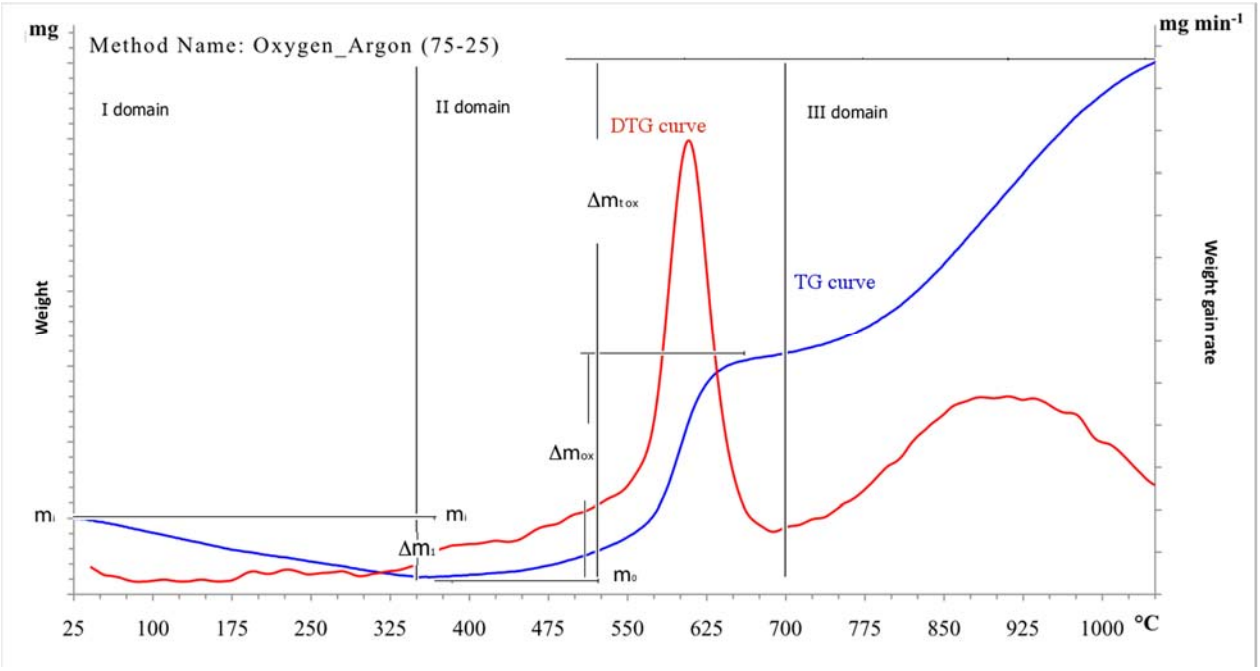

Figure 4-1: Typical TGA-DTG curves

These parameters are shown schematically in Figure 4-1 using a typical TGA/DTG curves. The first domain is denoted by a significant weight loss (Δm_1) from initial temperature up to 350°C. This initial weight loss is mainly due to organic layer degradation and oxidation, though weight loss from the beginning up to 120°C is probably due to water and some residual solvents evaporation and gas desorption from the surface particles. In the second domain of TGA curve a mass gain is observed related to the aluminum oxidation by oxygen that results in solid alumina (Al_2O_3). The slope of the TGA curve is attenuated before the second oxidation begins, in which oxidation rate is less pronounced.

Ball-milled powders were also characterized using additional techniques such as chemical analysis, scanning electron microscopy (SEM), and BET specific surface area. A simple digestion procedure in a 2M NaOH ethanol/water (20% v/v) solution was used to measure the aluminum content of the samples. Measurements were done according to a gas evolution technique described in Dubois et al., (2007). Adsorption-desorption measurements were performed using a nitrogen/helium mixture as the test gas with a Micromeritics instrument. Scanning electron microscopy (model JEOL JSM7600TFE) was used for the morphological study of the powders.

The combustion behavior of aluminum-rich energetic composites (Al-GAP/BPS) and inert powders composite were investigated using a PARR bomb calorimeter to measure the heat of combustion in pure dry oxygen at 30 atm. In order to calculate the volumetric heat of combustion, composite densities were measured with a gas pycnometer (AccuPyc 1340 MICROMERITICS apparatus) operated under helium at room temperature.

4.3 Results and Discussions

The results of specific surface area, as measured by the Brunauer-Emmett-Teller method (BET) and reported in Table 4-1, show that aluminum powders produced by simultaneous milling have specific surface areas much larger than those produced by an after-milling reaction scheme.

Table 4-1: High-Energy Ball Milling Parameters

Powder Abbreviation	Milling Time (min)	Reactant	Coating Reaction	BET (m^2 g^{-1}) (±3%)
Al_PGA_SR30	30	Propargyl alcohol	Simultaneous	30.94
Al_PGA_SR60	60	Propargyl alcohol	Simultaneous	40.72
Al_PGA_SR120	120	Propargyl alcohol	Simultaneous	44.89
Al_PGA_SR180	180	Propargyl alcohol	Simultaneous	49.97
Al_PGA_SR240	240	Propargyl alcohol	Simultaneous	56.15
Al_PGA_SR360	360	Propargyl alcohol	Simultaneous	66.57
Al_PAc_AM180	180	Propiolic acid	After-milling	3.52
Al_PAc_AM240	240	Propiolic acid	After-milling	2.33
Al_PAc_AM300	300	Propiolic acid	After-milling	2.60
Al_PAc_AM360	360	Propiolic acid	After-milling	3.16

The sample Al_PGA_SR360 has the highest value of specific surface area measured at 66.57±2.00 m^2 g^{-1}. Also, specific surface area increases when milling time increases in the first series, whereas

random variations are found in the second series. This suggests that the grain size reduction was much more effective in the simultaneous milling (Fig. 4-2) than with after-milling reactions.

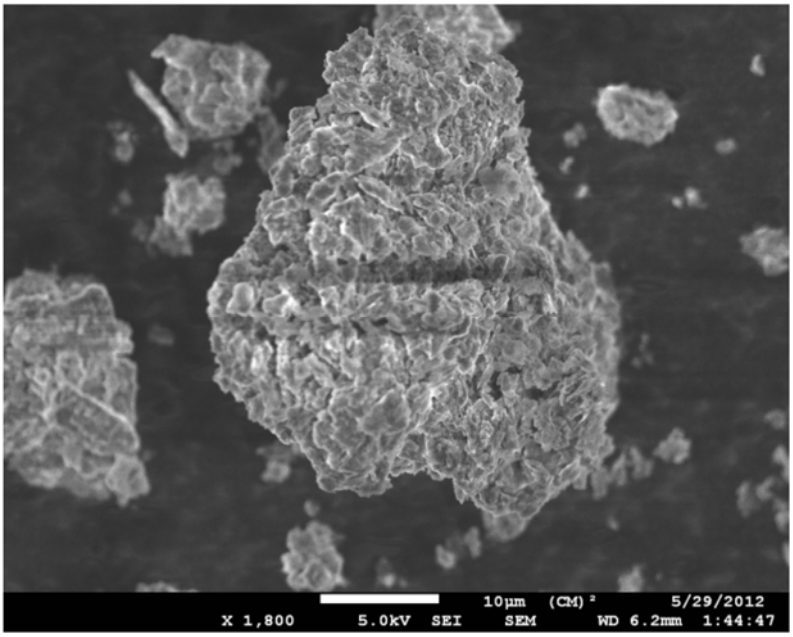

Figure 4-2: The SEM images of Aluminum-polymers agglomerate formed after simultaneous milling

However, mechanical milling is a very energetic method that can help activate chemical reactions. According to Umbrajkar et al. (2005), milling temperatures increases rapidly during the initial 20-30 min and continues to change gradually after 1h of milling. Milling temperatures can reach 80°C in certain circumstances. Since propargyl alcohol (HO-CH2C≡CH) has two reactive groups, a hydroxyl (OH) and an alkyne (C≡C) it can undergo a self-polymerization under these conditions. A sample of propargyl alcohol was polymerized in a laboratory scale test by heating at 70 °C for three hours, in a toluene solution. It resulted in a viscous yellow liquid after removing the solvent. FT-IR spectra (Fig. 4-3) show the differences in the organic chain before and after treatment. It is clear that alkynes bond has been reacted, as it can be seen by a decreasing in the absorption bands at 2123 and 3296 cm^{-1}, respectively attributed to an alkyne bond and a hydrogen bond with C^3. The intense band from 3500-3100 cm^{-1} that can be associated to the hydroxyl group (O–H) and the stretching band near to 1025 cm^{-1} attributed to –C–O (primary alcohols) were diminished. Also, the more intense absorption bands in the region 2861–2929 cm^{-1} correspond to increasing –C–H bonds. The new absorptions at 1624 and 1731 cm^{-1} can be attributed to carbonyl and alkene groups

reflecting the different structures of the two compounds. Clearly, the observed infrared spectra are consistent with the polymerization of propargyl.

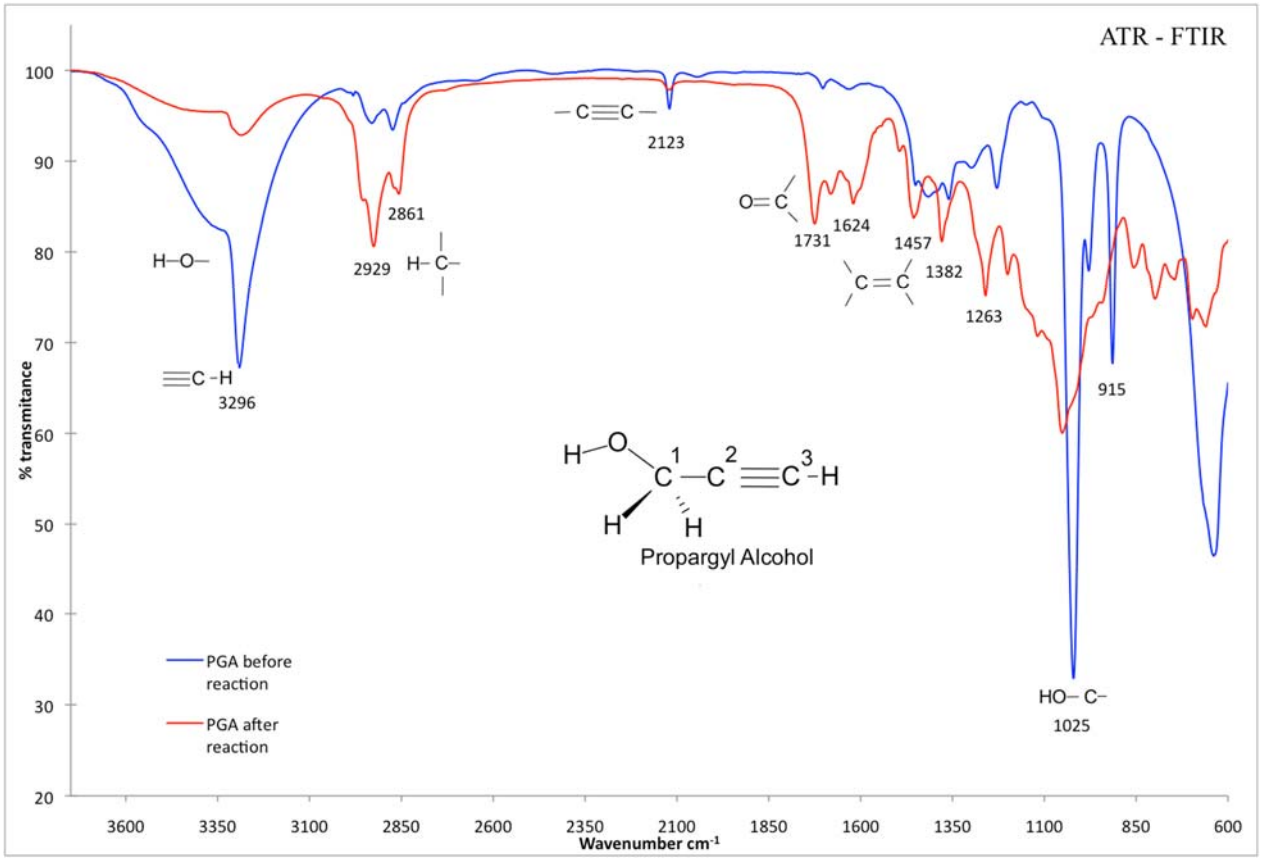

Figure 4-3: ATR-FTIR spectrograph from commercial propargyl alcohol (bleu line) and polymerized sample (red line).

We observed that simultaneous milling made a very viscous slurry mixture at the end of experiments while the second method produced a more fluid mixture. This change in behavior suggested that self-polymerization of the propargyl alcohol has occurred. Furthermore, a rise in mixture viscosity is given by the strong particle-to-particle interactions that increase with decreasing particle size. In fact, the SEM-images (Fig. 4-2) of samples in the first series of experiments show large clusters that are formed by small metal particles and organic compounds. As shown by the micrograph, the particles are very small and the agglomerate seems porous. Considering the hypothesis that self-polymerization of propargyl took place and that the polymer chains act as a binder between the aluminum particles, both phenomena contribute to the high viscosity of the mixture.

In contrast to these SEM-images, the micrographs taken from the second series of milling experiments look quite different. Instead of the large clusters, they show large thin flakes as reported in Fig. 4-4A. The average flake thickness is about 85 nm according to measurements shown in Fig. 4-4B.

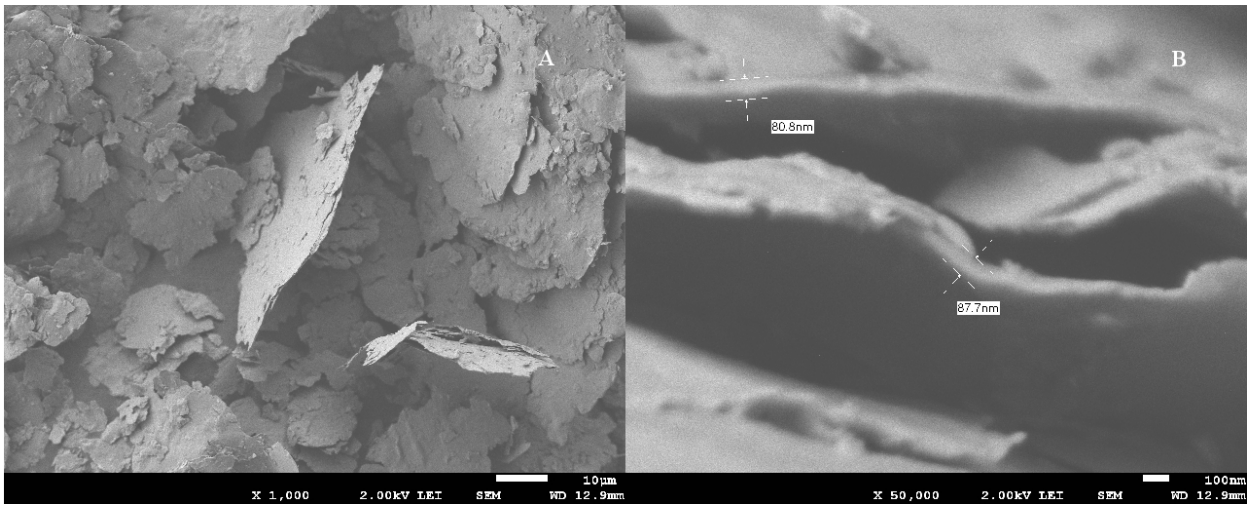

Figure 4-4: The SEM images of aluminum particles after ball milling (A), measurement of flake thickness (B)

According to the above analysis, the BET specific surface areas for the samples of simultaneous milling process could be strongly influenced by the clustering of particles caused by an excessive coating of propargyl polymers, which could result in a porous agglomerate. However, this does not mean that this method is not effective and does not produce ultrafine particles. The first oxidation peak of all the samples produced by simultaneous milling reaction appears before the Al melting point (660°C). This thermal behavior is typical of what is normally observed with nanosized aluminum particles, as reported in Sossi et al., (2013). However, BET measurements from the stepwise process samples are more representative of actual specific surface areas, they also reveal low values of specific surface, varying between 2.33 and 3.52 $m^2 g^{-1}$.

As mentioned in the introduction, the main characterization technique for the materials produced in this study is thermal analysis. The results and calculations of the experimental parameters of ball-milled powders are given in Table 4-2.

Table 4-2: Thermal parameters obtained from TGA

Powder abbreviation	Parameter Value T_{on} (°C)	$T_{ox\ peak1}$ (°C)	V_{ox} (mg min^{-1})	Δm_1 (%)	α_1 (%)	α_2 (%)	$A/\Delta m$ (abs.)	C_{Al} (%)
Al_PGA_SR30	566.08	603.95	0.10	-8.36	35.27	82.34	28.36	84.75
Al_PGA_SR60	568.06	596.75	0.09	-13.97	36.93	68.88	26.17	74.93
Al_PGA_SR120	546.86	593.37	0.09	-16.71	35.45	57.24	26.63	68.48
Al_PGA_SR180	553.61	587.94	0.07	-27.18	31.40	50.88	22.53	60.44
Al_PGA_SR240	543.53	587.24	0.07	-33.66	31.66	51.02	22.33	57.60
Al_PGA_SR360	546.64	587.20	0.05	-43.77	22.83	39.21	21.08	49.67
Al_PAc_AM180	648.35	689.03	0.12	-7.19	36.58	79.24	22.28	84.16
Al_PAc_AM240	646.14	690.94	0.13	-9.48	39.26	84.13	19.57	84.43
Al_PAc_AM300	651.89	684.45	0.14	-5.41	38.71	89.04	24.33	90.32
Al_PAc_AM360	643.38	688.81	0.12	-3.63	37.80	78.12	22.10	86.67

A typical TGA thermograph is shown on Figure 4-1, along with the parameter values used in this work. The results of both series of samples analyzed in this study are in good agreement with a thermograph of aluminum flakes in Trunov et al., (2005), which summarized the aluminum oxidation in three stages. At temperature below ~ 550 °C, the oxidation is relatively slow. The second one over a narrow temperature range from 550 to 650 °C results in accelerated oxidation. The oxidation slows down just before the melting point of aluminum (660 °C) to form the third stage over which the oxidation rate continuously increases from about 650 to 1000–1100 °C. Other studies on the thermal properties of aluminum particles (Ilyin et al., 2002; Rufino, B. et al. 2007; Trunov et al., 2005) suggest that the oxidation of aluminum powders can occur in four steps as a

result of polymorphic phase transformations during the growth of the oxide film. These stepwise oxidations were observed when the coarse aluminum powders were heated up to 1600 °C (Rufino B. et al., 2007; Trunov et al., 2005) while for ultrafine powders, as aluminum flakes, nearly all the aluminum content was oxidized before 1000 °C (Trunov et al., 2005). The same thermal behavior was observed for nanosized aluminum particles in Sossi et al., (2013), in which an exothermal peak and an increase in the mass were observed between 400 and 660°C.

Note there are several differences in the thermal parameters between the first and second series of aluminum powders samples. The onset and peak temperatures of intensive first oxidation in the first series of experiments are lower than the second ones, but the degree of oxidation of Al in this domain (α_1) decreases when milling time increases. On the contrary, weight loss increases with increasing milling time from 8.4 to 43.8wt%. This seems to have directly influenced the maximum oxidation rate and the relative thermal effect ($A/\Delta m$) measured in these experiments that decreases from 0.1 to 0.05 mg/min and from 28.4 to 21.1 respectively. According to Sossi et al., (2013) an incomplete oxidation of Al can occur even at high temperatures due to the presence of residual products from the elastomer decomposition. This fact can support the assumption of self-polymerization of propargyl alcohol that seems was gradually intensified with the milling time. TGA results have shown that powder oxidation begins at a temperature of 450 ^{o}C with the appearance of an exothermal peak that reaches a maximum at 600 °C.

Propargyl-capped aluminum powders from the after-milling method exhibit high aluminum content for all samples in the experiments and the maximum value achieves 90wt% of active aluminum for the sample Al_Pac_AM300. All samples exhibit a first oxidation peak in a DTA curve between 660 and 750°C for higher oxidation rates.

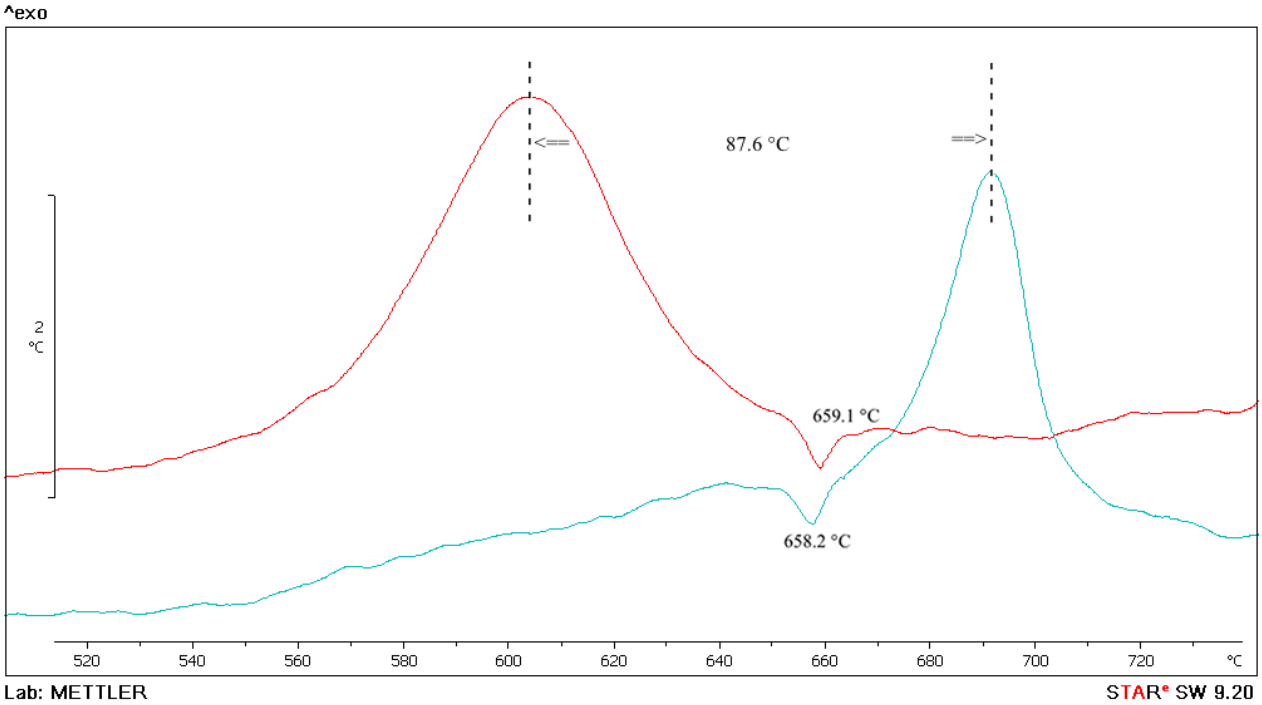

Figure 4-5: Comparative DTA curve between simultaneous milling (red line) and after milling powders (green line)

The oxidation is characterized by a high conversion degree (i.e. 0.12 mg min^{-1}) and it occurs after the melting temperature of aluminum, which can be seen by endothermic peaks in DTA curves at ~ 660 °C. Comparative DTA curve in Figure 4-5 indicates a gap of 87.6 °C between the maximum of the oxidation peaks at 603.8 °C for the first series of experiments and the second series at 691.4 °C. It also shows a slight difference in the aluminum-melting peak between the two samples that is very close to the theoretical value for the aluminum. This thermal behavior is quite different from what has been reported in the literature. It is most interesting that the first oxidation stage in the series of stepwise process begins immediately after the melting point of aluminum. There is no record of such a behavior in the literature for flakes or nanosized aluminum. Furthermore, it is known that micrometric powders have a small growth of the oxide layer in vicinity of 600°C and no weight increase was detected in the melting point or immediately after it, as was shown in Trunov et al. (2005 and 2006) and Rufino et al. (2007). This might be explained by the presence of the protective propargyl-coating layers that shifted the process of aluminum core oxidation until the melting process start and creates a stress in the amorphous aluminum oxide.

Table 4-3: Active aluminum content in the milled-powders.

Powder abbreviation	C_{Al} Active Al content (%)		
	NaOH[1] (± 1.20)	Calorimeter Bomb [2] (± 1.40)	TGA [3] (± 0.05)
Al_PGA_SR30	71.06	81.34	84.75
Al_PGA_SR60	52.75	74.40	74.93
Al_PGA_SR120	42.87	70.80	68.48
Al_PGA_SR180	34.34	72.45	60.44
Al_PGA_SR240	33.42	54.10	57.60
Al_PGA_SR360	24.31	44.36	49.67
Al_PAc_AM180	79.36	86.01	84.16
Al_PAc_AM240	76.93	84.73	84.43
Al_PAc_AM300	79.01	81.89	90.32
Al_PAc_AM360	74.04	81.10	86.67

[1]Active aluminum content measured by alkaline digestion method
[2]Active aluminum content estimated from oxygen calorimeter bomb assuming that sample containing 100% of Al releases of 31.05 kJ g^{-1}.
[3]Active aluminum content calculated from TGA results based on the amount of mass oxide produced.

The active aluminum content (C_{Al}), as reported in Table 4-3, was measured by three different methods. The first approach was a simple digestion in a concentrate NaOH solution. It was found

that this technique is strongly affected by the presence of polymer coatings, for both sets of samples, even if ethanol (20% v/v) was used as a tensoactive agent.

In the other two methods, active aluminum was estimated from the parameters measured by the TGA and bomb calorimeter. The final weight of oxides (m_{Tox}) in TGA curves was used to calculate active Al following the stoichiometry of the reaction $2\,Al_{(s)} + 3/2\,O_{2(g)} => Al_2O_{3(s)}$ where the weight of oxidation product $Al_2O_{3(s)}$ should be 1.89 g if there is 1 g of aluminum in the reactive powder,. For the bomb calorimeter, the heat of combustion of aluminized energetic composites was compared with the heat of combustion of inert powders composites measured at the same conditions. Alumina (Al_2O_3) replaces aluminum powders at the same proportions into the energetic binder (10 and 30wt%) in order to provide the same thermal properties as a heat transfer during combustion process. Since alumina powders are inert in oxygen environments, the amount of energy measured correspond to the combustion enthalpy of a portion of the energetic binder. The aluminum content was calculated as follows: the difference between the combustion enthalpy of aluminized and neat binders, in which aluminum was replaced by alumina powders, is assumed to be the combustion energy release of aluminum in the samples. This value was compared with the standard combustion enthalpy of pure aluminum (i.e. $Al_{enthalpy.} = 31.05\ kJ\ g^{-1}$) to estimate the aluminum content in the samples. This approach enhances accuracy in the measurements.

Calorimetry results testify to the great potential of propargyl-capped aluminum powders as energetic composites. Compared to non-metallic binders (i.e. GAP/BPS sample), the energetic polymers, including propargyl-capped aluminum, enhance both volumetric and gravimetric heats of combustion (Table 4-4).

Table 4-4: Heat of combustion of aluminized-binders

Aluminized-binder abbreviation GAP/BPS: POWDERS	Parameter Values				
	% Powder Weight	Theoretical Density ($kg\ m^{-3}$)	Measured Density ($kg\ m^{-3}$) (± 10)	Heat Combustion $Q_{comb.\ Corr.}$ ($kJ\ g^{-1}$) (± 0.40)	Volumetric Heat combustion ($MJ\ L^{-1}$) (± 0.50)
Binder 1:0.25	-	-	1305	21 907.14	28.59
Alumina (Al_2O_3)	10	1400	1401	19 660.71	27.04
Alumina (Al_2O_3)	30	1640	1620	15 285.62	24.77
Al_PGA_SR30	10	1376	1374	22 186.30	30.48
Al_PGA_SR60	10	1376	1368	21 970.98	30.06
Al_PGA_SR120	10	1376	1369	21 858.98	29.92
Al_PGA_SR180	10	1376	1368	21 910.28	29.97
Al_PGA_SR240	10	1376	1367	21 340.36	29.18
Al_PGA_SR360	10	1375.9	1369	20 853.37	28.56
Al_PGA_SR360	30	1538	1462	19 298.17	28.21
Al_PAc_AM180	30	1538	1504	23 297.28	35.04
Al_PAc_AM240	30	1538	1503	23 178.08	34.85
Al_PAc_AM300	30	1538.3	1521	22 922.49	34.86
Al_PAc_AM360	10	1375.9	1374	22.171.48	30.46
Al_PAc_AM360	30	1538.3	1537	22 840.25	35.10

However, the simultaneous milling method wherein organic compound was added prior to the initial milling process was less effective, probably influenced by higher percentages of coating on the aluminum particles which was itself caused by the polymerization of propargyl alcohol. In fact, we observed that the percentage of the coating increases with the increasing of milling-time, as can be noted by an increasing in the weight loss before 350 °C in TGA. The products resulting of these polymerization reactions on aluminum particles were not identified, but the active aluminum content was decreased showing that aluminum was consumed. As a consequence, the heat of combustion decreases in the series of experiment as a function of milling-time (Fig.4-6).

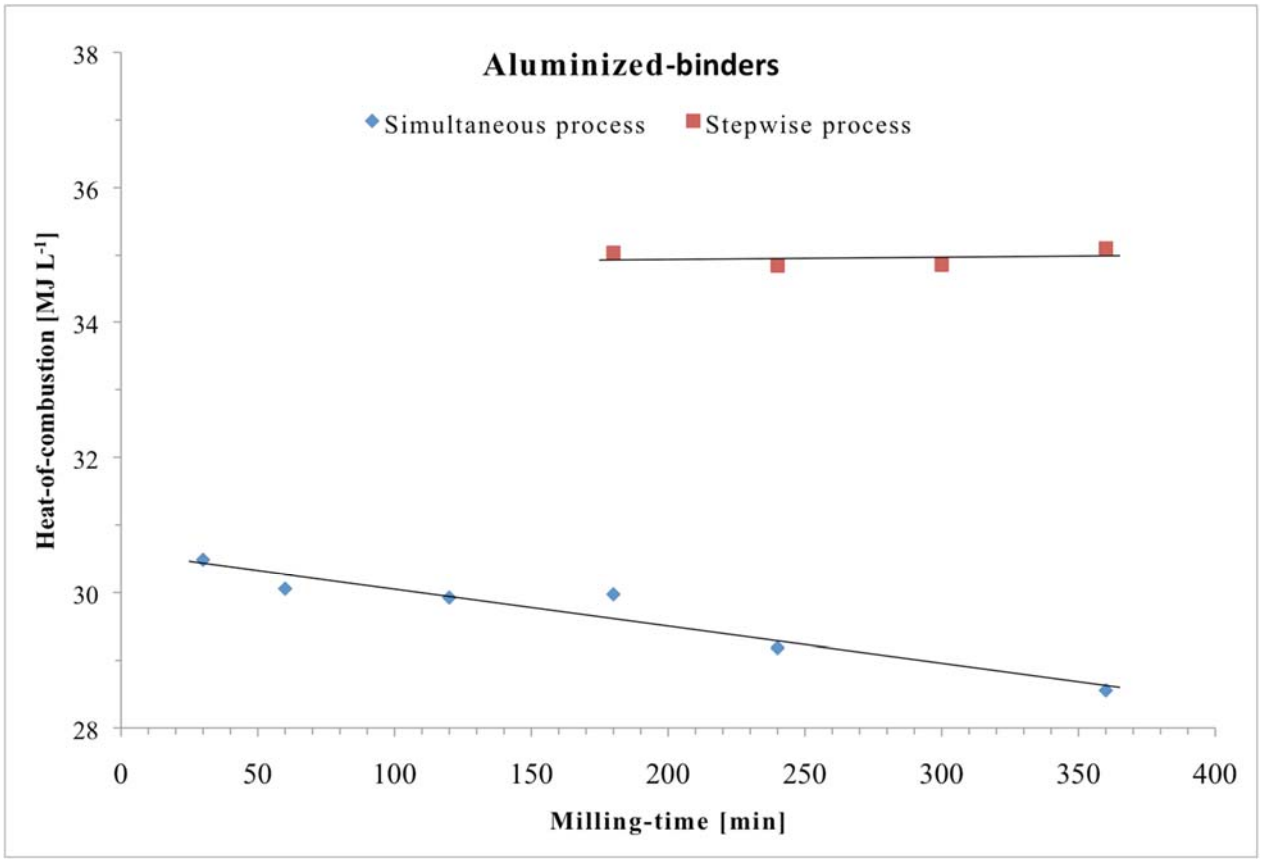

Figure 4-6: The heat of combustion of aluminized-binders

The lowest value measured from the sample GAP/BPS:Al_PGA_SR360 (28.55, 28.21 MJ L^{-1} respectively to 10 and 30wt%) is actually smaller than the pure binder, which has 28.59 MJ L^{-1}. On the other hand, almost the samples from after-milling reaction exhibit a great value that exceeds this value by 23wt% on average.

4.4 Conclusions

High-energy ball milling of aluminum powders was studied experimentally in two different ways to produce propargyl-capped aluminum powders. Simultaneous reaction milling and after-milling reactions schemes using propargyl species as a reactant were investigated. Thermal analysis was used to investigate the oxidative behavior of powders in the oxygen/argon environment. It was experimentally shown that propargyl-capped aluminum powders produced by the after-milling reactions method exhibit a better stability of powders than those produced by simultaneous reaction milling. This method produces nanosized aluminum flakes with a higher content of metal that could provide an increased heat of combustion when incorporated into an energetic binder. Heats of combustion of aluminized energetic composites obtained from propargyl-capped aluminum powders were measured in a bomb calorimeter. Volumetric heat of combustion of the composites reached a value of 35.1 MJ/L. Comparative values of heats of combustion were used to estimate the aluminum content of the powders. The highest value of 86wt% of active aluminum is achieved by the Al_Pac_AM360 powder (See tables 4-2 – 4-3).

Both capping methods produce propargyl-functionalized aluminum powders but some particularities of ball milling prevented a better performance of simultaneous milling reactions. Future work will continue to explore high-energy ball milling as a way to produce functionalized aluminum powders, as well as focusing on the influence of milling temperature.

4.5 References

Abe, H., Naito, M., Nogi, K., Matsuda, M., Miyake, M., Ohara, S., et al. (2003). Low temperature formation of superconducting MgB2 phase from elements by mechanical milling. *Physica C: Superconductivity and its Applications*, 391(2), 211-216.

Davis, R. M., McDermott, B., & Koch, C. C. (1988). Mechanical alloying of brittle materials. *Metallurgical Transactions A*, 19(12), 2867-2874.

Dubois, C., Lafleur, P. G., & Roy, C. (2007). Polymer-grafted metal nanoparticles for fuel applications. *Journal of Propulsion and Power*, 23 (4) 651- 658.

Eckert, J., Holzer, J. C., Ahn, C. C., Fu, Z., & Johnson, W. L. (1993). Melting behavior of nanocrystalline aluminum powders. *Nanostructured Materials*, 2(Compendex), 407-407.

Fecht, H. J., Hellstern, E., Fu, Z., & Johnson, W. L. (1990). Nanocrytalline metals prepared by high-energy ball milling. *Metallurgical Transactions A*, 21A, 2333-2337.

Fecht, H. J. (1995). Nanostructure formation by mechanical attrition. *Nanostructured Materials*, 6, 33-42.

Gao, Z., Walton, N. I., Malugin, A., Ghandehari, H., & Zharov, I. (2012). Preparation of dopamine-modified boron nanoparticles. *Journal of Materials Chemistry*, 22(3), 877-882.

Hacler, W., Rodig, C., Fischer, C., Holzapfel, B., Perner, O., Eckert, J., et al. (2003). Low temperature preparation of MgB2 tapes using mechanically alloyed powder.

Hwang, S., Nishimura, C., & McCormick, P. G. (2001). Mechanical milling of magnesium powder. Materials Science & Engineering A (Structural Materials: Properties, Microstructure and Processing), A318(1-2), 22-33.

Ilyin, A., Gromov, A., An, V., Faubert, F., De Izarra, C., Espagnacq, A., et al. (2002). Characterization of aluminum powders I. Parameters of reactivity of aluminum powders. *Propellants, Explosives, Pyrotechnics*, 27(6), 361-364.

Keicher, T., Kuglstatter, W., Eisele, S., Wetzel, T., & Krause, H. (2009). Isocyanate-free curing of glycidyl azide polymer (GAP) with bis-propargyl-succinate (II). *Propellants, Explosives, Pyrotechnics*, 34(3), 210-217.

Koch, C. C., Scattergood, R. O., Youssef, K. M., Chan, E., & Zhu, Y. T. (2010). Nanostructured materials by mechanical alloying: new results on property enhancement. *J Mater Sci*, 45, 4725-4732.

Nagashima, M.; Maji, K.; Hayakawa, M. (2001). Fabrication of Al2O3/ZrO2 micro/nano-composite prepared by high energy ball milling. *Materials Transactions*, 42, (6), 1119-1123.

Rufino, B., Boulc,Äôh, F., Coulet, M. V., Lacroix, G., & Denoyel, R. (2007). Influence of particles size on thermal properties of aluminium powder. *Acta Materialia*, 55(8), 2815-2827.

Shteinberg, A. S., Lin, Y.-C., Son, S. F., & Mukasyan, A. S. (2010). Kinetics of high temperature reaction in Ni-Al system: Influence of mechanical activation. *Journal of Physical Chemistry A*, 114(20), 6111-6116.

Sossi, A., Duranti, E., Paravan, C., Deluca, L. T., Vorozhtsov, A. B., Gromov, A. A., et al. (2013). Non-isothermal oxidation of aluminum nanopowder coated by hydrocarbons and fluorohydrocarbons. *Applied Surface Science*, 271, 337-343.

Trunov, M. A., Umbrajkar, S. M., Schoenitz, M., Mang, J. T., & Dreizin, E. L. (2006). Oxidation and melting of aluminum nanopowders. *Journal of Physical Chemistry B*, 110(26), 13094-13099.

Trunov, M. A., Schoenitz, M., Zhu, X., & Dreizin, E. L. (2005). Effect of polymorphic phase transformations in Al2O3 film on oxidation kinetics of aluminum powders. *Combustion and Flame*, 140(4), 310-318.

Trunov, M. A., Schoenitz, M., & Dreizin, E. L. (2005). Ignition of aluminum powders under different experimental conditions. *Propellants, Explosives, Pyrotechnics*, 30 (1), 36 - 43.

Umbrajkar, S. M., Schoenitz, M., Jones, S. R., & Dreizin, E. L. (2005). Effect of temperature on synthesis and properties of aluminum-magnesium mechanical alloys. *Journal of Alloys and Compounds*, 402(1-2), 70-77.

Urakaev, F. K., & Shevchenko, V. S. (2004). Synthesis of boron-rich solids of light metals in mechanochemical reactors. *Journal of Materials Science*, 39, 5507-5509.

Van Devener, B., Perez, J. P. L., Jankovich, J., & Anderson, S. L. (2009). Oxide-free, catalyst-coated, fuel-soluble, air-stable boron nanopowder as combined combustion catalyst and high energy density fuel. *Energy and Fuels*, 23(Compendex), 6111-6120.

White, J. D. E., Reeves, R. V., Son, S. F., & Mukasyan, A. S. (2009). Thermal explosion in Ni-Al system: Influence of mechanical activation. *Journal of Physical Chemistry A*, 113(48), 13541-13547.

CHAPTER 5 ARTICLE 2: ENHANCED REACTIVITY OF ALUMINUM POWDERS BY CAPPING WITH A MODIFIED GLYCIDYL AZIDE POLYMER

Ricardo José Pontes Lima[1], Charles Dubois[1], Robert Stowe[2], Sophie Ringuette[2].

[1] *École Polytechnique de Montréal, Montreal, Canada*

[2] *Defence R&D Canada, Quebec City, Canada*

This paper has been submitted to International Journal of Energetic Materials and Chemical Propulsion.

Parts of this work have been presented 10th International Symposium on Special Topics in Chemical Propulsion and Energetic Materials.

Abstract

Aluminum powder is a significant component of many energetic formulations for rocket propellants and explosives due to its high combustion enthalpy on both a mass and volumetric basis. The combustion properties of these formulations can be enhanced further through the use of aluminum nanoparticles including shorter ignition delay, shorter burning time, and more complete combustion. High-energy ball milling was used as a method to produce aluminum-functionalized nanoparticles. This method is based on the reaction of the new metallic surface generated by grinding with an organic functionalized compound. In order to enhance the reactivity of aluminum powders coated by organic layer, we replace the organic functionalized compound by an energetic polymer - glycidyl azide polymer (GAP). To achieve a desirable reactivity of GAP with aluminum particles, GAP plasticizer has been chemically modified by the partial reactions of azide groups on the polymer chain. The modified glycidyl azide polymer (GAPm) was grafted onto the aluminum particles by the reactions of acid groups and aluminum in a simultaneous reaction milling. The aluminum particles coated with GAPm were characterized by the BET (Brunauer-Emmett-Teller) surface area analysis technique and scanning electron microscopy. Thermal gravimetric and differential thermal analyses were also used to carry out a study on the reactivity of the coated

powders. Several different formulations of these coated powders combined with a binder were produced to investigate the influence of energetic capping of nanoparticles on the heat of combustion of these novel solid fuels.

5.1 Introduction

Mechanical attrition, initially developed as a method to synthesize materials, amorphous alloys, intermetallic compounds and phase mixtures (Fecht et al., 1990; 1995), has been used to produce nanosized metal particles from coarser feedstock. Nanosized materials have been fabricated by mechanical milling, which is the milling of single composition powders to obtain nanocrystalline species or ultrafine amorphous powders (Koch et al., 2010). However, metal nanoparticles having a high specific surface area can be easily oxidized by exposure to air, which produces a native oxide layer.

Simultaneous milling and chemical reactions can be applied to produce ultrafine metal powders coated by an organic ligand layer (Devener et al., 2009) to protect metal surface against premature oxidation. The organic layer takes the place of the native oxide layer formed on the metal particles. In addition, the organic coatings lead to new properties due to the chemical properties of organic compound applied. For example, the surface of the boron nanoparticles was modified by replacing the native oxide layer by oleic acid ($CH_3(CH_2)_7CH=CH(CH_2)_7COOH$) to synthesize ligand-protected hydrocarbon-soluble boron nanoparticles (Devener et al., 2009). In another application, water-dispersible boron nanoparticles were produced by the same procedure, but the ligand was exchanged for dopamine hydrochloride (Gao et al., 2012). Other benefits can be obtained by organic coatings, for example, by improving the particle dispersion in the polymer matrix during mixing, preventing particle agglomerations in the combustion chamber, and reducing the aging of particles in storage (Dubois et al., 2007). Although coating metal particles lead to these benefits, the method applied and the choice of organic-protective capping might be investigated for specific applications.

The strategy applied in the simultaneous reaction milling is to increase the surface-area-to-volume ratio by grinding, which enhances the reactivity of the metal for combustion, and to protect the surface of the particles through the reaction of the fresh metal surfaces generated by milling with

the organic functionalized compounds. According to Devener et al., (2009) the organic layer makes covalent bonds with metal particles on the freshly-exposed metal surface (e.g. B – O – C).

In this paper, we present recent advances obtained for this approach to produce an energetic coating around aluminum particles. Following the strategy cited above, we produced nano-aluminum flakes protected by an organic layer. With respect to the protection of the particle surfaces, the organic coating works well and, in fact, different chemical species (e.g. hydrocarbons, fluorocarbons) could be applied. However, a drawback to this is that it is limited by the fact that the decrease in particle size leads to an increase in the surface-area-to-volume ratio, and as a consequence the organic coating reaction consumes a greater mass percentage of the aluminum in the particle. Although the organic compound participates actively in the combustion process, the energy released by coating layer is not sufficiently high to replace the energy lost by the reduction of active aluminum in the powder for small particles. Recently, the reactivity of micrometer-sized aluminum powders was modified with selective inclusion of fluoride species (carbonmonofluoride and polytetrafluoroethyene) through mechanical activation (Sippel et. al, 2013[a], 2013[b]). Aluminum particles with a modified surface prepared by cryo-milling aluminum and cyclooctane (Zhang et al., 2013) have been showed as a good method to enhance ignition and combustion of aluminum particles.

In this work, it was hypothesized that since the organic coating participates actively in the combustion process, the use of energetic polymers as a coating layer of aluminum particles could enhance the metal reactivity because of the high release of energy from them.

Glycidyl azide polymer (GAP) was originally developed as an energetic binder (22.4 kJ g^{-1}) that could be used in explosives, pyrotechnics or composite propellants formulations. GAP is characterized by the functional group of C-N_3 (azide group). The molecular weight can range from 700 to 5500 and the number of hydroxyl end groups from 0 (GAP plasticizer) to 3. In our work, GAP plasticizer (700g mol^{-1}) is a logical candidate ingredient to coat the aluminum particles by simultaneous milling reactions because of its good properties such as low viscosity, low molecular weight, mild sensitivity to impact and friction, and good solubility in several organic solvents. Also, it is expected that the coating of aluminum particles by the GAP plasticizer facilitates their dispersion in an azide-based binder in the final composite material because of a smaller enthalpy of mixing. However, some functionalized groups are necessary to graft the polymer onto aluminum

particles and the GAP plasticizer does not carry telechelic hydroxyl groups. To achieve a better reactivity of this polymer and the fresh aluminum surface, the GAP plasticizer was chemically modified to make some additional acid functionalized branches in the main chain of polymer. The branches are formed following the Huisgen cycloaddition that is the reaction of a dipolarophile with a 1,3 dipolar compound leading to 5-membered heterocyclic groups. The 1,3 dipolar cycloaddition reactions, included as an important route to many organic synthesis, are identified as a class of chemical transformations that fulfill the criteria of click chemistry approach (Sharpless et al., 2001), in which the reaction must be modular, wide in scope, give high yields, enable simple product isolation with byproducts that can be removed by non-chromatographic methods, and be stereospecific. Figure 5-1 shows the general reactions of azide-alkynes cycloaddition.

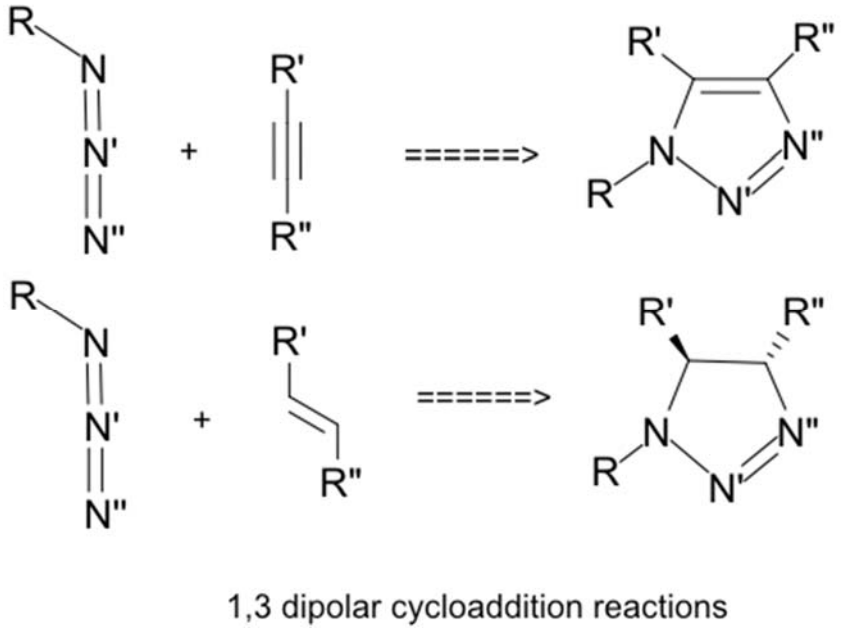

Figure 5-1: 1,3 Dipolar cycloaddition reactions from alkynes and alkenes.

In the field of energetic compounds, the azide-alkynes cycloaddition is an important route to obtain triazoles and tetrazoles compounds for the synthesis of nitrogen-rich energetic compounds. For example, the method was used to synthesize an energetic polymer by intermolecular cycloaddition of the propargyl azide ($HC{\equiv}CCH_2N_3$) formed from propargyl bromide and sodium azide in alcohol-water solution (Houser T. J. and Humbert D. K., 1973). Also, the reaction was applied successfully to the curing reaction of azide binders, using bis-propargyl compounds, as an alternative of cross-linked polyurethane reaction for an isocyanate-free curing system (Keicher et al., 2009). The curing

reaction of azide binders by the 1,3 dipolar cycloaddition reaction was first claimed by Manzara (1997) using acrylic and acetylenic compounds and later in the patents from Reed Jr. (2000) and Ciaramitaro (2005).

In this study, the 1,3 dipolar cycloaddition was applied to functionalize the GAP by addition of few acid-functionalized branches in the main chain of polymer. The azide groups presents in the GAP chain, which can be described as having at least one mesomeric structure that represents a charged dipole, react with the dipolarophiles compounds, in this case, the triples bonds of the alkynes group of the propiolic acid (HC≡CCOOH). If a molecular ratio between triple alkynes bonds and azide groups is adjusted for a non-stoichiometry mixture, in which the organic acid is a limiting reactant, only few branches are formed in the main chain. The ends of these branches have the organic acid groups that could use to graft the new polymer onto the aluminum particles.

The reactivity of aluminum powders capped with modified GAP (GAPm) and the amount of capping was thoroughly investigated by thermal gravimetric and differential thermal analyses, x-ray spectrometer analysis and TEM images. The results confirm the presence of the energetic polymer around the aluminum particles and the formation of Al-O-C bonds. The mass percentage of this organic capping as found by the TGA/DSC experiments was about 20 percent of the final mass of the aluminum powders.

Several formulations of binders, combined with aluminum powders capped by GAPm and PAC, were prepared to investigate the influence of this energetic capping on combustion behavior. The combustion energies were determined using a Parr oxygen bomb calorimeter in pure oxygen at 30 atm for both formulations.

5.2 Experimental Procedures

This section explains the steps undertaken in this work: the synthesis of the modified glycidyl azide polymer, the capping of aluminum particles in simultaneous ball milling and chemical reactions, and the formulation of azide binders with GAP-capped aluminum powders.

5.2.1 Experimental Synthesis of Modified Glycidyl Azide Polymer

The GAP plasticizer (GAP700 – 700g mol^{-1}) was degassed under vacuum at 70°C for 24h prior to react with propiolic acid (HCCCOOH, Sigma-Aldrich, >95% purity), which was used in the given purity without further purification. The synthesis of modified glycidyl azide polymer was done by the 1,3 dipolar cycloaddition reaction between azide groups of GAP and alkynes bonds of propiolic acid. The molecular ratio between triples bonds of alkynes [-C≡C-] and azide groups [N_3] was 0.20 molar equivalent that resulted in a partially substituted glycidyl azide polymer (Figure 5-2).

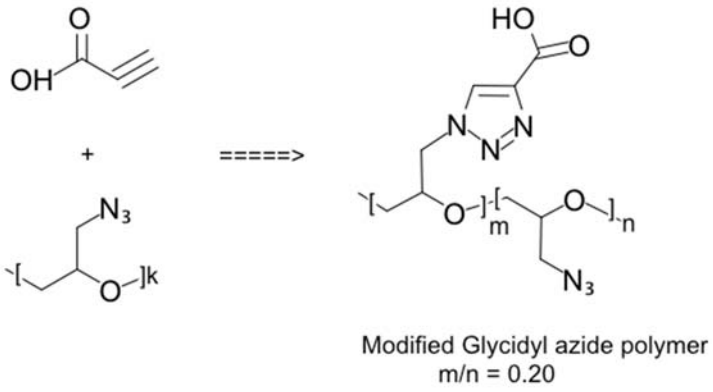

Figure 5-2: Schematic of the azide-alkyne reaction to produce the modified GAP.

An amount of 15g of GAP plasticizer (21.43 mmol) was poured into a 50ml round-bottom flask equipped with a mechanical stirrer and placed in thermostatic bath. The starting material was heated under stirring until the mixture temperature attains around 60°C. Propiolic acid was slowly added to the reaction flask using a small syringe (500 μl) equipped with a thin needle (22 ga x 5 cm). The azide-alkyne reaction is exothermic enough to lead to hazardous conditions during the GAP modification process (Dubois et al., 2003). Therefore, the acid was injected very slowly by dripping it until complete addition of an amount of 2.1 g (29.97 mmol). This procedure was sufficient to dissipate the heat of reaction (247.2 $kJmol^{-1}$), thus avoiding a self-heating that could lead to the decomposition of GAP. The mixture temperature was kept around 60°C at all times. The advancement of reaction can be observed by the rise of the mixture viscosity, which increases when the new functionalized branches are added to the main chain of GAP. The rise in viscosity can be attributed to the intermolecular hydrogen bonds formed by the ends of new branches in the

GAP chain. The final product is a very viscous liquid. The recovered product was degassed prior to characterization.

In order to confirm the new postulated structure of GAPm, ATR-FTIR spectra were obtained using a Perkin Elmer Spectrum 65 – FTIR Spectrometer. The differential scanning calorimetry (DSC) was done using TA instruments Q2000. Scans were carried out using hermetic aluminum pans at scan rates of 5°C min^{-1}, under nitrogen flux, in the range of 40 – 400°C. The study of GAPm decomposition was carried out using thermal analysis (differential gravimetric analysis and thermal analysis). The thermal study were performed using a METTLER Toledo apparatus operated under argon gas flow with heating rate of 10 K min^{-1}.

5.2.2 Capping of Aluminum Particles

Commercial aluminum powder (Valimet Inc., nominal diameter 60 μm contain a minimum 99.7% of weight aluminum) was used as starting material. Modified glycidyl azide polymer obtained by the procedure above was employed to cap the aluminum particles in the first experiment. Neat propiolic acid (HC≡CCOOH, Sigma-Aldrich, >95% purity) was used at the given purity for a second experiment. A SPEX 8000 series shaker mill using tungsten carbide vial and balls (Φ = 3.16 mm, ρ = 14.5 g cm^{-3}) was retained to prepare the ball-milled powders. A ball-to-powder mass ratio (charge ratio, C_R) was set to 20:1 for all experiments. For comparison purposes, two series of experiments were performed. In the first one, an amount of 3.5 g of aluminum powder was added to 20 ml of toluene (> 99.5%, Certified ACS reagent grade - Fisher Chemical) to help disperse the powders and prevent caking. At the same time, an amount of 1.5 g of GAPm was stirred into 10 ml of dichloromethane (Certified ACS reagent grade - Fisher Chemical) until complete dissolution. The clear solution of GAPm was poured into the milling vial and mixed with aluminum powders and toluene.

A second experiment was performed in order to produce samples without energetic capping, and then GAPm was replaced by propiolic acid (PAC). An amount of 2 g of the acid was dissolved in 20 ml of toluene and poured into the same amount of aluminum powder (3.5 g). All other conditions of the first milling were otherwise maintained.

All the solvents used were previously dried in a molecular sieve. Starting materials and milling balls were placed in a milling vial and sealed under argon to avoid premature oxidation. In order to reduce contamination, all chemicals and materials were handled in an argon-filled glove box at all times.

The milling process duration was set to 180 min for both experiments. The vial temperature during the ball milling processing was kept constant by air-cooling. In order to increase the cooling of milling vial, the original shaker mill was modified by addition of a new external fan to cool the chamber containing the vial. Moreover, a set of finned aluminum heat sinks was placed to enhance the heat transfer from the milling vial (Figure 5-3).

Figure 5-3: Milling vial adapted to improved heat transfer.

The organic coating grafted onto aluminum powders was investigated by TGA, DSC, XPS and TEM analysis. The thermal gravimetric analysis (TGA) experiments were carried out using a Mettler Toledo apparatus for both samples recovered of these two sets of experimentations. The amounts of the coatings were determined in a non-isothermal experiment (10°C min^{-1}) operated over the 25 – 500°C temperature range under argon flow. The oxygen/argon flow was used to investigate the non-isothermal oxidative process of new aluminum powders. Heating rate of 10°C min^{-1} was applied to over the 25 – 1050°C temperature range. Thermal properties of GAPm coatings were determined in a TA instruments Q2000 DSC apparatus using hermetic aluminum pans over a 25 – 400°C temperature range. The chemical composition of particle surfaces was carried out using X-ray photoelectron spectroscopy (XPS). XPS spectra were collected using the Mg Kα X-ray source on a VG Scientific ESCALAB 3 M KII XPS spectrometer. The electron beam

power was 216 W (12 kV, 18mA). Both low-resolution survey and high-resolution scans of energy ranges were done. High-resolution spectra were taken with 20 eV pass energy and a resolution of 0.05 eV. The Shirley method was used to subtract background noise and Wagner sensitivity factors for quantitative analysis.

5.2.3 Energetic Aluminized-binders

Several formulations of binders were fabricated in order to investigate the influence of GAPm coatings on the combustion properties and evaluate the relative enhance on combustion efficiency in comparison to the non-energetic coatings. The binders were composed of GAP plasticizer and aluminum powders cured with bi-propargyl succinate (BPS). Two series of binders were synthesized, each one from a different aluminum coated powder. A set of formulations was fabricated by the addition of 7.5, 15 and 30% w/w of aluminum powders into a mixture of GAP/BPS (molar ratio 1:0.25). Sufficient amounts of GAP and BPS to give a molar ratio of 0.25 ($[C\equiv C]/[N_3]$) were weighed separately. The amount of aluminum powders was poured into the GAP and homogenized for 30 min at ambient temperature. The BPS was added into the mixture and mixed until complete homogenization. The final formulation was cast into nylon molds, degassed during 1 hour at 45°C and cured during one day at 45°C. The initial curing at 45°C was necessary to avoid self-heating and decomposition of GAP mixture. Complete curing was achieved at 65°C for another 1 day.

The combustion properties of aluminized-binders were investigated in an oxygen calorimeter bomb (PARR calorimeter bomb) operated at 30 atmospheres. The thermal mass of the calorimeter was determined to be 10482 ± 101 JK^{-1} prior to the calorimetric measurements through the combustion of standardized benzoic acid in a pure oxygen atmosphere.

In order to calculate the volumetric heat of combustion, the densities of aluminized binders were measured with a gas pycnometer (AccuPyc 1340 MICROMERITICS apparatus) operated under helium at room temperature.

5.3 Results and Discussion

5.3.1 Modified GAP Characterization

The modified glycidyl azide polymer was characterized by attenuated-total-reflectance FT-IR spectroscopy (ATR-FTIR), thermal gravimetric analysis and differential scanning calorimeter. The infrared spectrum appears consistent with that expected on the modification chain of GAP (Figure 5-4). The two absorptions at 1553 and 1426 cm^{-1} are very close to the ring stretching vibrations of 1,2,3–triazoles that cannot be observed on the pure GAP plasticizer IR spectrum. The absorption at 1445 cm^{-1} that appears to both IR spectrum could be attributed to azide structure (N-N=N), but from modified GAP curve the absorption is shown as a large pick because the carbon bonds of 5-membered heterocyclic ring influence it. In addition, the absorptions at 853, 1050 and 1235 cm^{-1} are in the range related for ring skeletal vibrations of triazoles. Finally, the absorptions at 781 and 732 cm^{-1} could be attributed to C-H out-of-plane deformations for nitrogen containing heterocyclic compounds. A slight decrease in the absorption of the azide band at 2093 cm^{-1} in comparison of GAP spectrum denotes the amount of azide groups consumed by the azide-alkynes cycloaddition.

The new absorption bands at 1736 and 3160 cm^{-1} could be attributed to carbonyl stretch (1600–1900 cm^{-1}) and hydroxyl groups of organic acid on the branches of polymer from the propiolic acid respectively, and the non-appearance of the terminal alkynes band at 3310 and 2160 cm^{-1} is a good evidence of the formation of triazole compounds. Thus, the observed infrared spectra are consistent with the new structure added to GAP by 1,2,3 triazole acid-functionalized branches.

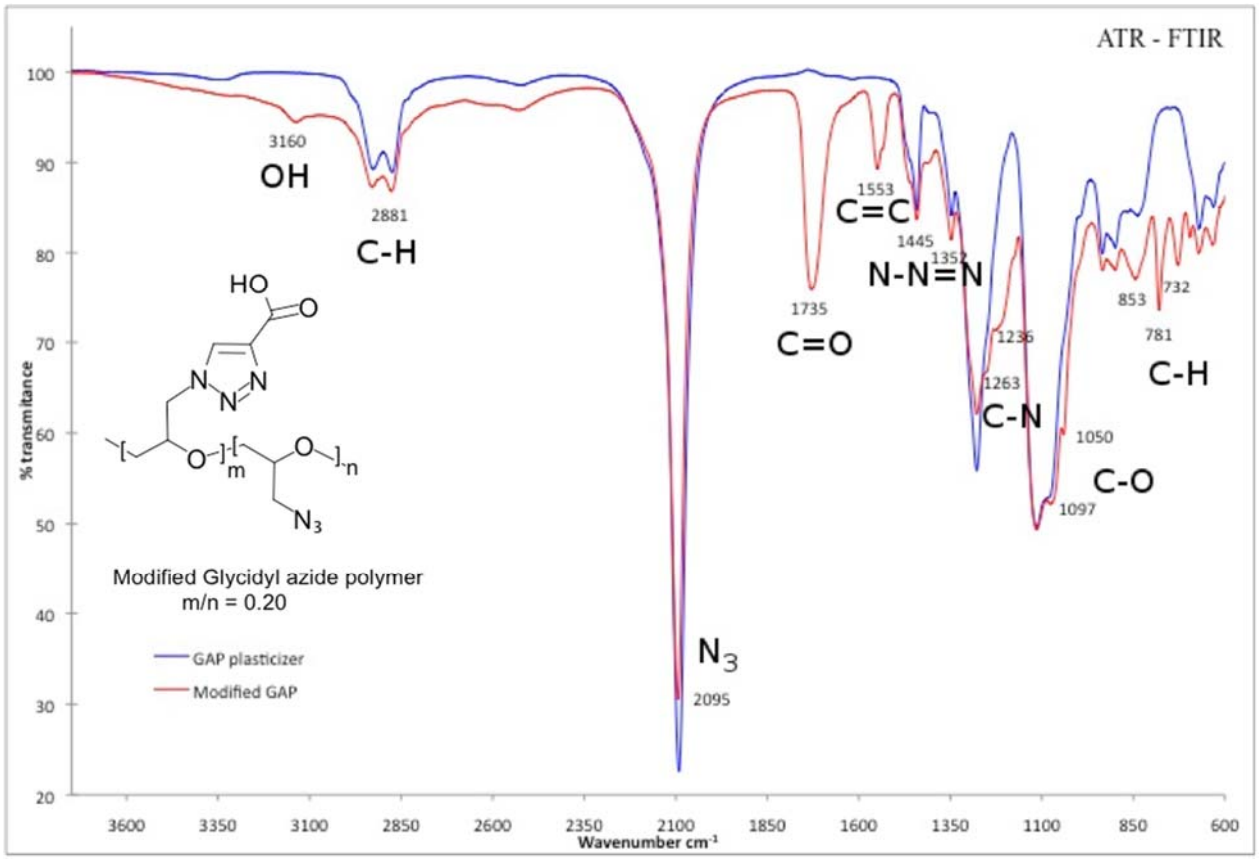

Figure 5-4: ATR-FTIR spectrograph from modified GAP (red line) in comparison to GAP plasticizer (blue line). It shows the chemical structure of modified GAP (detail).

The thermal analysis results for the modified GAP and commercial GAP plasticizer in argon and oxygen-rich environment are compared in Figure 5-5 (A) and (B). Comparative thermal decomposition under argon gas (blue lines) of modified GAP and commercial GAP plasticizer denotes the differences between the analyzed samples. The main decomposition of the GAP plasticizer sample appears as a single peak that has the higher T_{onset} at 240°C. The decomposition appears to occur in two steps with 48.5% mass loss to the first one in a very fast reaction. That was already expected for the conversion of azide to cyano group releasing $N_2 + H_2$ species (Feng et al., 1998; Ringuette et al., 2006). In contrast, the modified GAP shows a more complex decomposition and the first stage seems to subdivide into two steps. It is first shown as a double peak that has a gradual onset at 153.7°C. Then, it increases quickly to attain the same maximum temperature as observed from GAP plasticizer sample at 250°C. This smaller peak (9.4% mass loss) suggests that the acid branches incorporated onto the main chain of the GAP decompose first. Towards the end

of experiment (650°C), the modified GAP has almost the same mass loss of the commercial GAP that is slightly higher for GAPm (83,6 %) than for the one from GAP (78.8%).

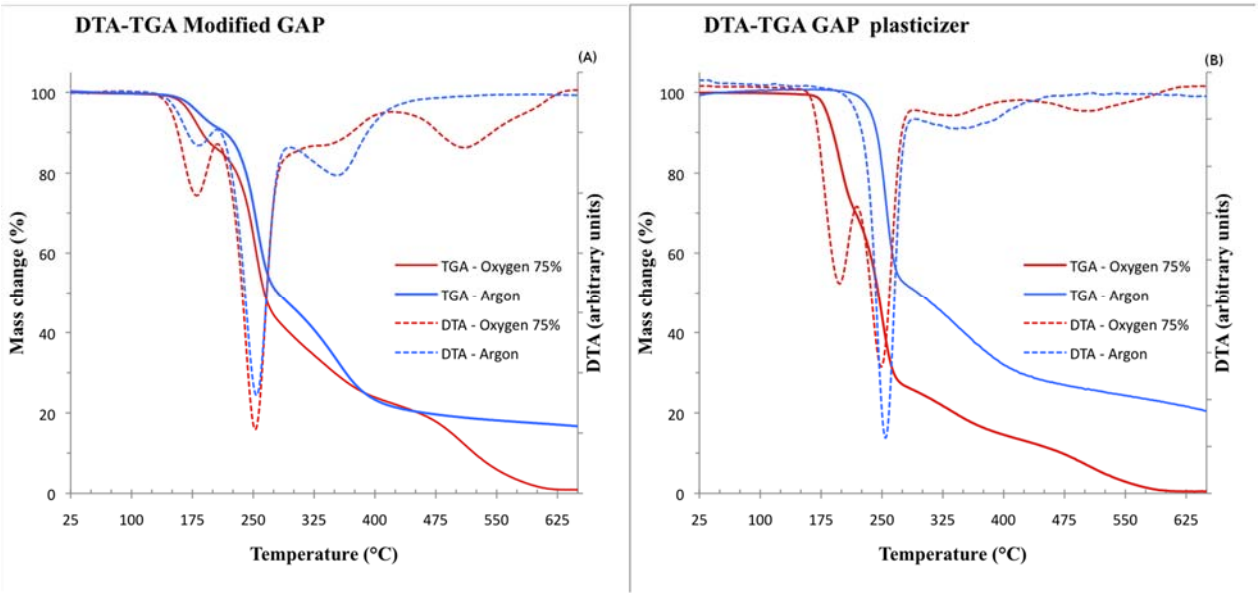

Figure 5-5: Comparison of experimental DTA-TGA curves of modified GAP (A) and GAP plasticizer (B) under argon and oxygen environments.

The thermal analysis curves in oxygen-rich environments (75%) for both samples are illustrated in red lines in Figure 5-6. As expected, the reactions under oxidative ambient were faster and completed up to 650°C because the fast oxidation process take place. The biggest change was recorded for GAP plasticizer that had a higher weight loss under oxygen-rich environment than the decomposition in argon. The DTA peak was divided in two peaks, which seem that, an easy and fast initial oxidation of hydrogen species (H_2) and azide groups released from GAP molecules facilitated by lowest viscosity. Between 450 and 650°C, for both samples, a combustion reaction of carbonaceous residues took place. The reaction was more accentuated in GAPm sample that corresponding to about 20% mass loss. This observation is most important to the understanding of the combustion behavior of GAPm-capped aluminum powders in TGA analysis due the complexity of simultaneous cracking reactions of the organic chain and the oxidation of aluminum particles, as discussed hereinafter.

Finally, the DSC analysis completes the modified GAP characterization. A typical DSC curves for GAPm is shown in Figure 5-6 (green line). An exothermic peak expected for the conversion of azide to cyano groups appears between 170 and 300°C, then a second stage took place up to 400°C.

The energy released from this first transformation was measured at 1.76 kJ g^{-1} that corresponds to about 70% of full energy released by commercial GAP plasticizer.

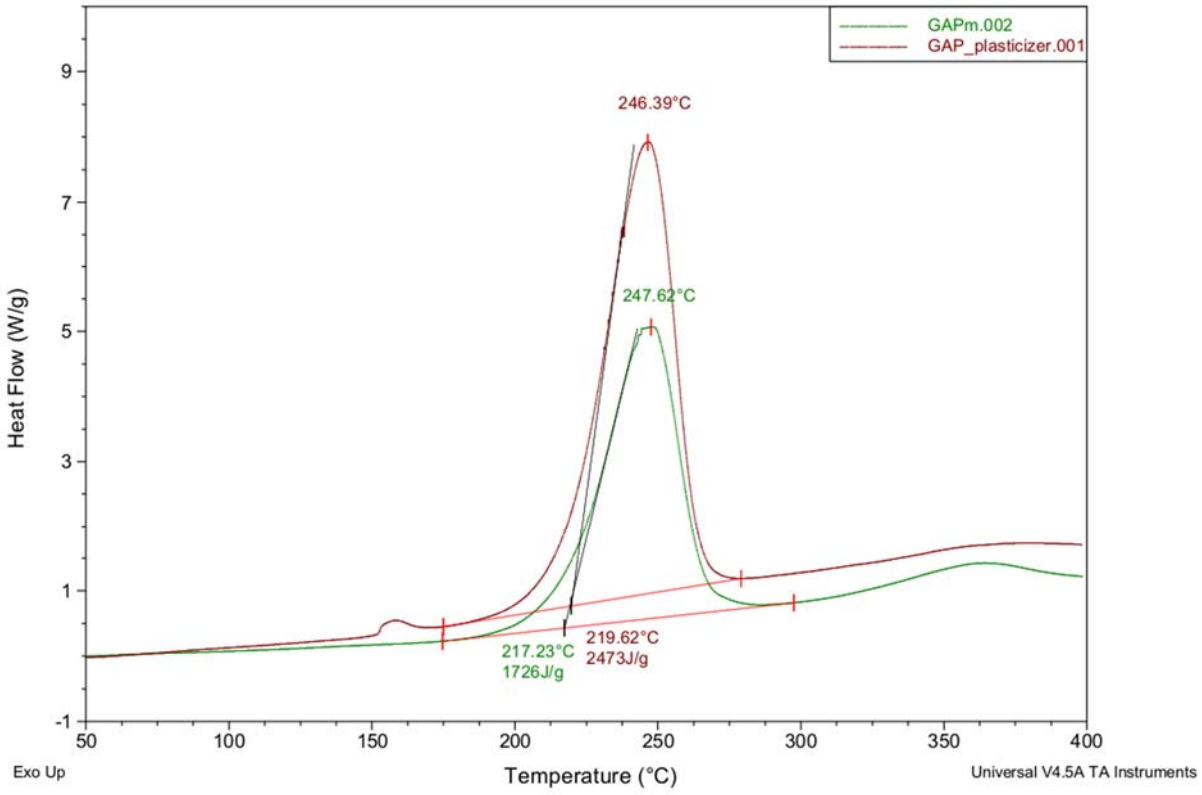

Figure 5-6: Comparative DSC thermographs between modified GAP (green line) and GAP plasticizer (red line).

Comparative DSC curves of GAPm and GAP plasticizer is shown in Figure 5-6. According to previous researches (Feng et al., 1998; Tang et al., 1999; Wang et al., 2007), the GAP has a complex decomposition in which many reactions take place and several radical species are formed; for example, the amides, amines, imines, acetonitrile, ammonia, oxygen containing species and the hydrocarbons. It is reasonable that the modification on the GAP chain by incorporation of acid-functionalized branches influences the decomposition process to provide a new radical species that could be cause the considerable difference in the enthalpy of decomposition.

5.3.2 Aluminum Particles Coated with Energetic and non-energetic compounds

Table 5-1 summarizes the properties and composition of the aluminum powders coated with modified GAP and propiolic acid.

Table 5-1: Description of aluminized milling samples.

Metal powders abbreviation	Milling time (min)	Coating description	Composition of the coating	BET (m^2/g)
Al_GAPm_M180	180	Modified Glycidyl Azide Polymer	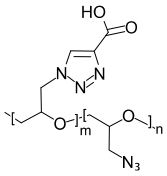	8.31 (±0.03)
Al_PAC_M180	180	Propiolic Acid	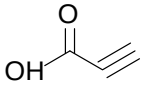	10.40 (±0.02)

Transmission Electron Microscopy (TEM) was applied to investigate as-milled aluminum morphology. Figure 5-7 contains TEM micrographics at two different magnifications obtained from aluminum particles coated with modified GAP. According to TEM results, particles have flake morphology formed from agglomerates of particles. Despite the larges aggregates small particles irregularly shaped could be identified. The particles agglomeration was possible determined by cold welding. According to Umbrajkar et al., (2005) aluminum flakes are expected, generally large, because great ductility of aluminum.

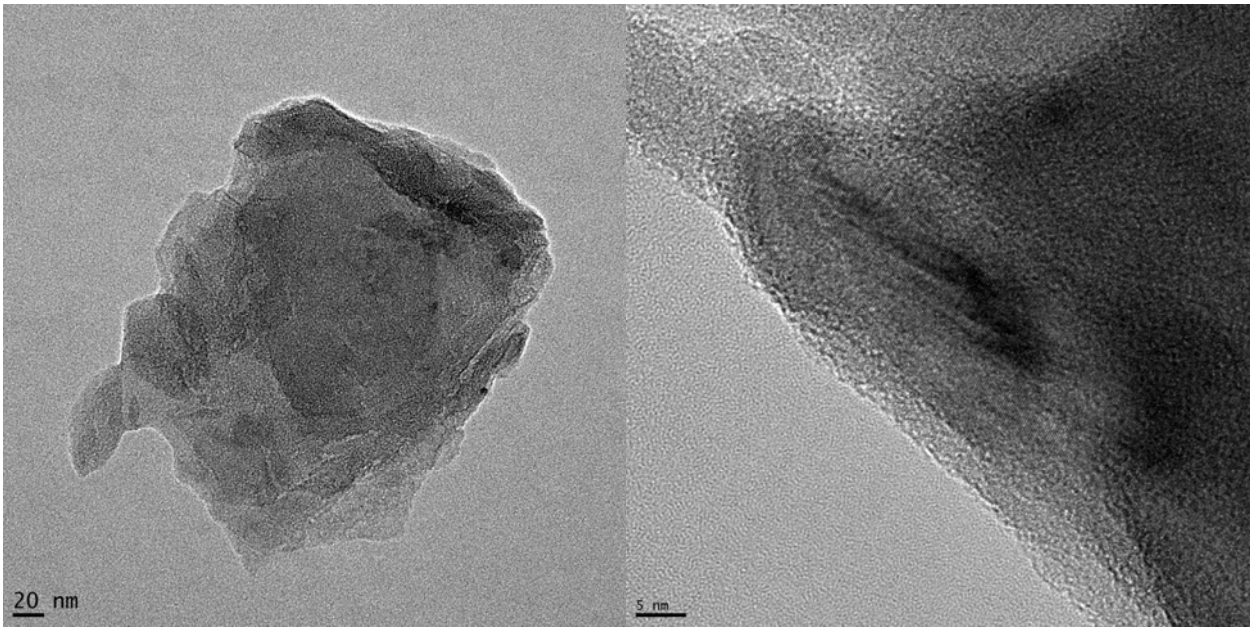

Figure 5-7: TEM-image of substructure of agglomerates of aluminum nanoparticles.

Aluminum powders capped by the acid-functionalized glycidyl azide polymer were further investigated to confirm the presence of the energetic coating. An exothermic behavior was observed in the DSC results obtained from a non-isothermal experiment of this aluminum powders. The exothermic peak with an onset of temperature about of 136°C and ΔH=0.24 kJ g^{-1} can be considered the main energy release from the azide bonds decomposition.

The DSC thermograph of Al_GAPm_M180 sample is shown in Figure 5-8. The DSC result agrees with the initial mass loss observed in TGA experiments carried out in an argon environment that also confirms the decomposition in two main steps. According to Wang et al., (2007) the thermal decomposition of GAP at low pressure begins at about 70°C (under vacuum), compared to about 170°C in the air. The products are basically with low molecular weight. This decomposition behavior was observed in the DSC and TGA experimental curves measured for GAPm-capped aluminum powder, but the main peak of decomposition was recorded at about 180°C.

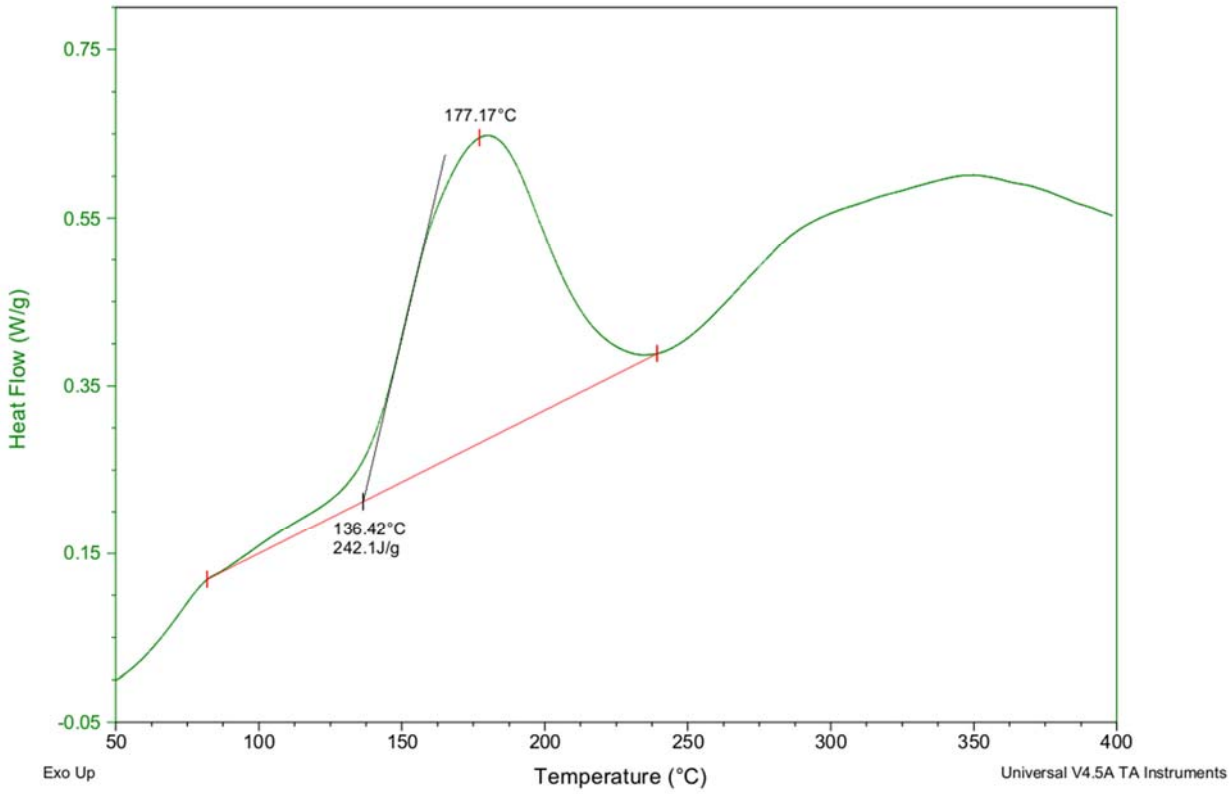

Figure 5-8: DSC thermograph of GAPm-capped aluminum powders.

The total mass percentage loss up to 500°C observed in the TGA thermogram (Fig. 5-9) was about 13.50 %, and can be attributed to the percentage of GAP grafted onto aluminum particles. This percentage can be evaluated by DSC measurements from the energy released of Al_GAPm_M180 sample (0.242 kJg^{-1}). Assuming that this energy corresponds to azide group decomposition from GAPm, it reflects a percentage of 14.02% of the total energy measured from the pure GAPm sample (1.726 kJ g^{-1}) as shown in Figure 5-6. However, while this evaluation is quite close to the real capping mass, it is not accurate. According to what has already been discussed before, the thermal decomposition of GAP is a complex system of chemical reactions in which many chemical species are formed. It is highly possible that some of these products are absorbed on the surface of aluminum particles and make some surface reactions resulting in residual mass up to 500°C. In addition, as was discussed in the GAPm characterization, the mass decreases up to 650°C in an oxygen-rich environment, but it is clearly noted in the TGA curves (Fig. 5-10) that the mass increase begins at 450°C as a result of aluminum oxidation. Simultaneous processes of combustion of the protective residual coating from GAPm decomposition and aluminum oxidation took place

in the range of 450 to 650°C. After the aluminum melting point temperature (660°C) the oxidation slows down.

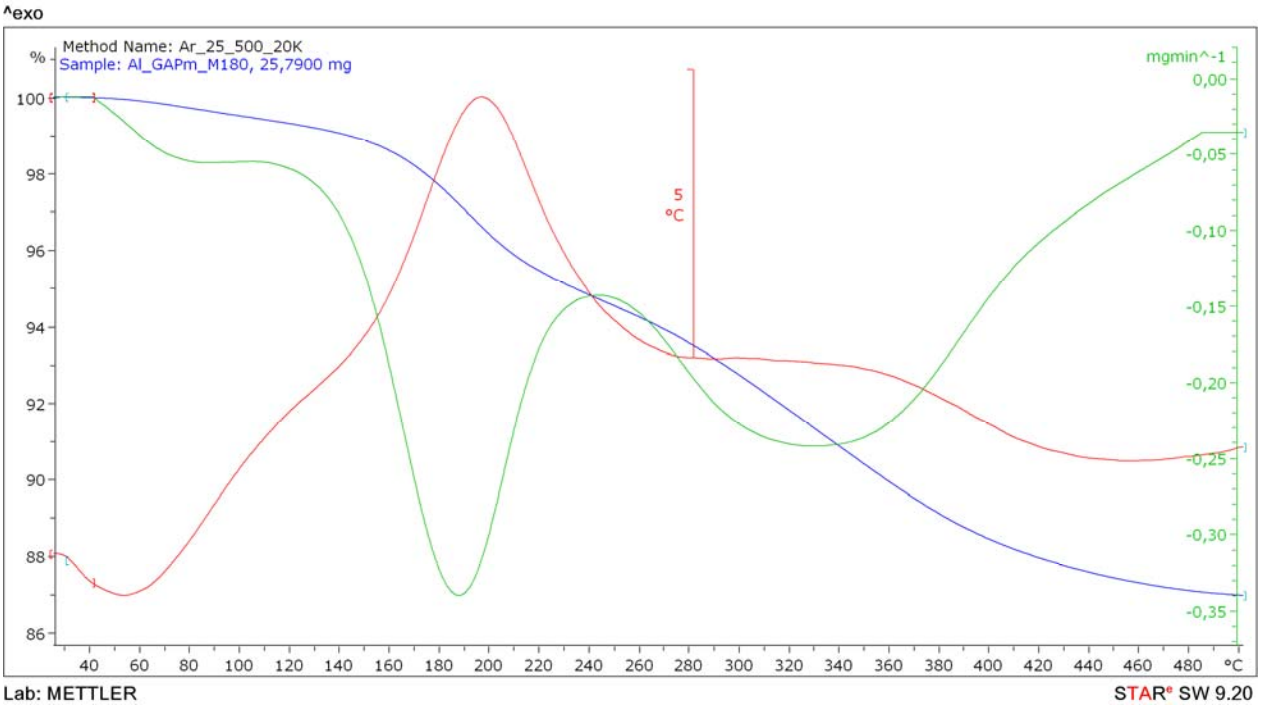

Figure 5-9: TGA thermogram of GAPm-capped aluminum powders measured in argon. Red line correspond to SDTA measurements (exothermic up)

According to other studies on thermal properties of aluminum particles (Rufino et al. 2007; Trunov et al. 2005), the oxidation of aluminum flakes could be summarized to three stages. At temperature below ~ 550°C, the oxidation is relatively slow. The second stage of aluminum oxidation, over a narrow temperature range from 550 to 650°C, results in accelerated oxidation. The oxidation slows down just before the melting point of aluminum to form the third stage of which the oxidation rate continuously increase from about 650 to 1100°C..

The complexity of those processes leads to non-accurate values based in TGA techniques. However, the comparison between two or more organic coatings could be evaluated.

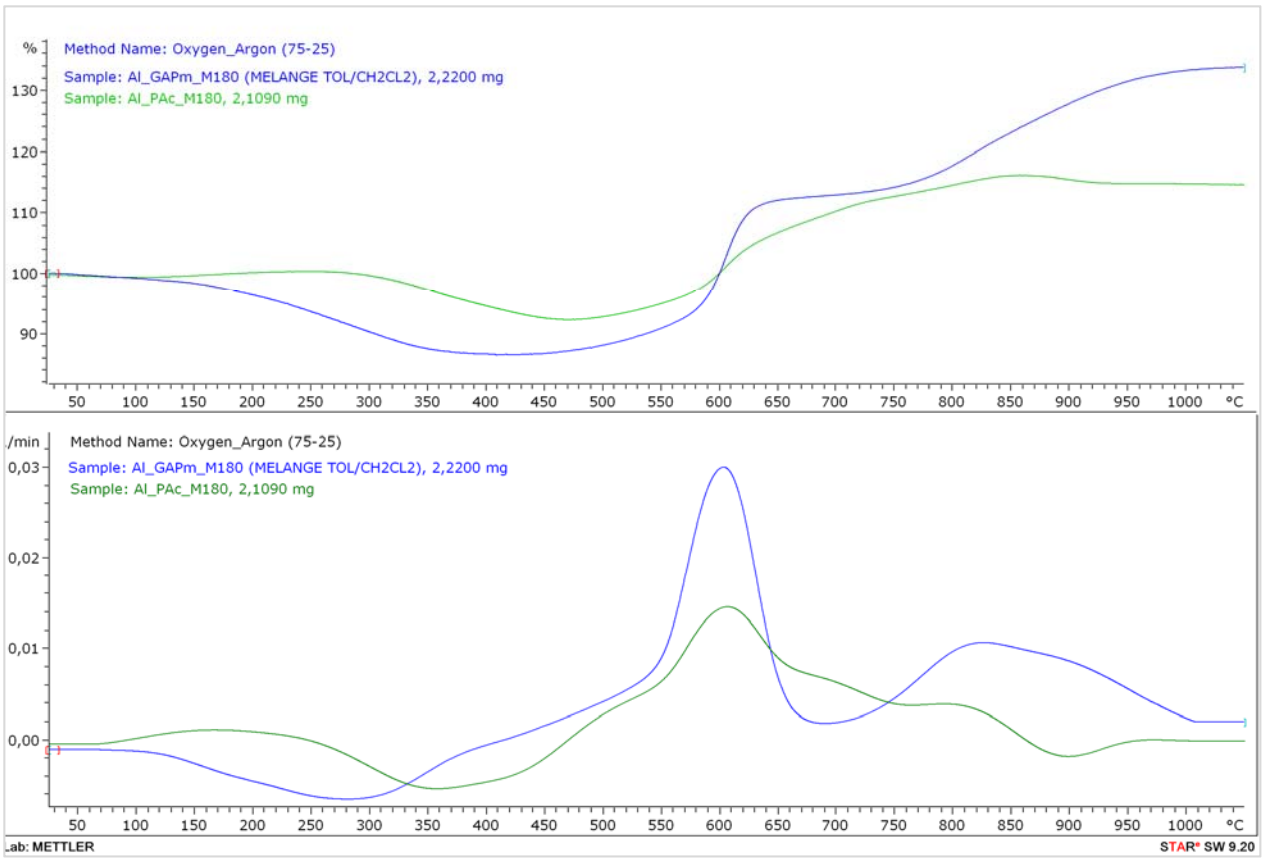

Figure 5-10: Comparison of experimental DTA-TGA curves measured for Al_GAPm_M180 and Al_PAC_M180 samples in oxygen environments.

The comparison of experimental DTA-TGA curves measured for both coated aluminum powders samples is shown in Figure 5-10. The modified GAPm-coated aluminum powders oxidize very rapidly and strongly, in both main oxidation stages. In contrast, the oxidation process for propiolic acid-capped aluminum sample was less effective than that of the GAPm. In Sossi et al., (2013) the fluoroelastomer capping of aluminum particles shifted the oxidation process of the metal encapsulated at the center of particles to higher temperature by ~20°C in comparison to hydrocarbon capping. That shows that hydrocarbon coatings are less effective than elastomer ones in terms of surface protection. In this study, the first peak of oxidation, for both samples, is almost at the same temperature, but the propiolic-capping sample showed a broad and less intense peak. In addition, in the second stage, after the melting point of the aluminum, in the range temperature from 650 to 1100°C, the oxidation reaction proceeded at a much slower pace. Probably, the poor protective action of propiolic capping leads a premature oxidation of this aluminum powder after

ball milling process. Calorimetric results also showed less energy release from these powders in comparison to aluminum coated with GAPm.

Finally, an additional evidence for the coating of aluminum particles with GAPm is given by the X-ray photoelectron spectrometry (XPS), which was used to measure elemental composition on aluminum surface. XPS analysis was performed on aluminum powders milled with modified glycidyl azide polymer (Al_GAPm_M180) and propiolic acid (Al_PAC_M180). The appearance of a nitrogen peak in XPS survey spectrum confirms the presence of GAPm molecules on aluminum surface, because the chemical difference in elemental composition of these organic layers is basically the presence of nitrogen atoms in GAPm molecules. No other nitrogen sources are expected to be present on the functionalized surface. And also, no such nitrogen peak was observed in the Al_PAC_M180 sample spectrographs as was expected.

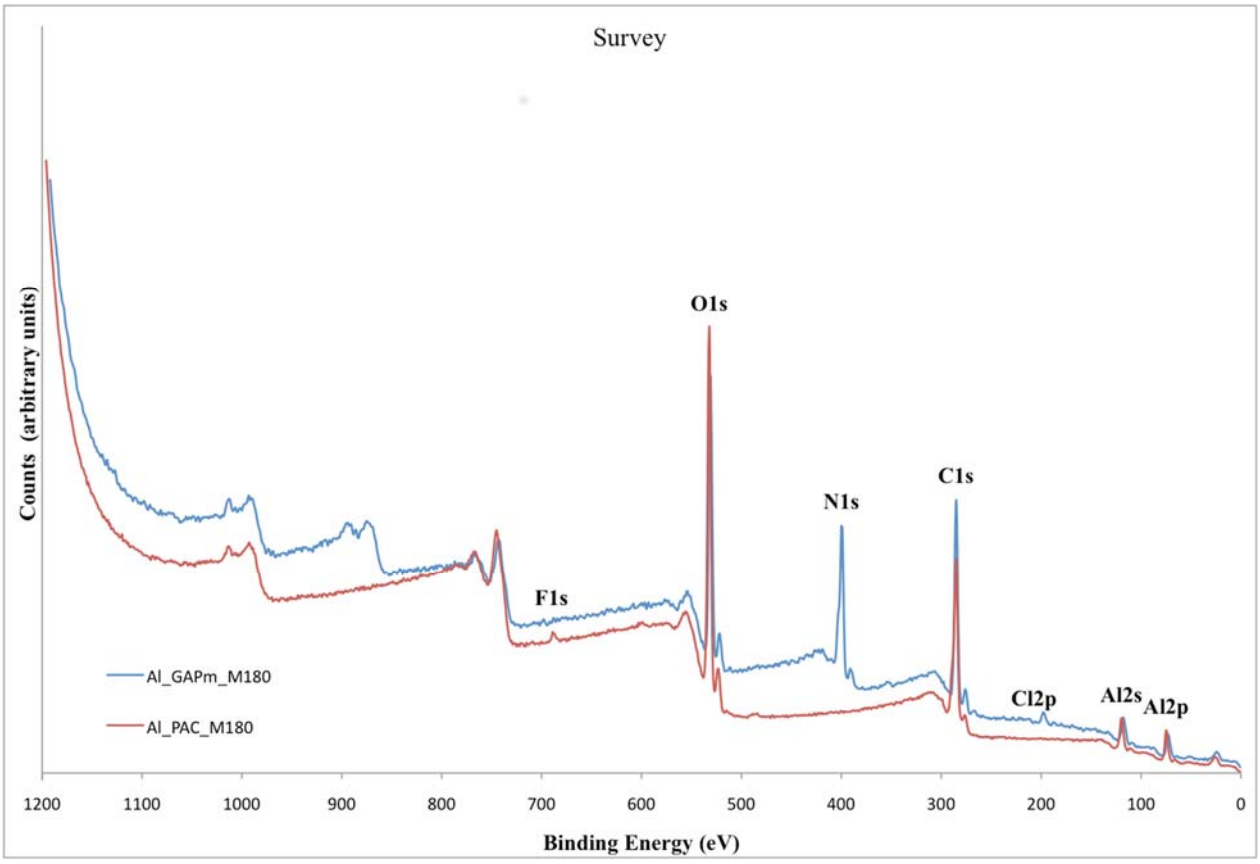

Figure 5-11: Survey spectrum XPS analysis of aluminum surfaces.

In order to confirm that the GAPm was successfully grafted onto aluminum surface, important regions of the XPS spectra were provided by both the N1s (Fig. 5-12A), C1s (f Fig. 5-12B) and Al2p (Fig. 5-12C) XPS regions. The high-resolution N1s data from GAPm-capped aluminum surface showed a broad peak centered at 400.6 eV, suggesting the presence of chemically distinct nitrogen atoms consistent with the formation of triazoles moiety and unreacted azide species (404.5 eV) ascribed by N1s D peak that correspond to the electron-deficient nitrogen in the azide group, which is in good agreement with the partial substitution of GAP.

XPS narrow scans of the C1s region for GAPm-capped aluminum particles shows five peaks fitting to assign contributions to the spectrum from carbons atoms in different environments, designated as C1sA (C=C, 284.5 eV), C1sB (C–C, 285.0 eV), C1sC (C–N (azide), C–O, 286.3 eV), C1sD (C–N, 287.1 eV (triazoles ring)) and C1sE (O–C=O, 289.1) as is shown in Figure 5-12B. Covalent bonds (C–O–Al) between particle surface and GAPm coating can be identified by a peak at 74.3 eV in the spectrum from aluminum atoms (Fig. 5-12C).

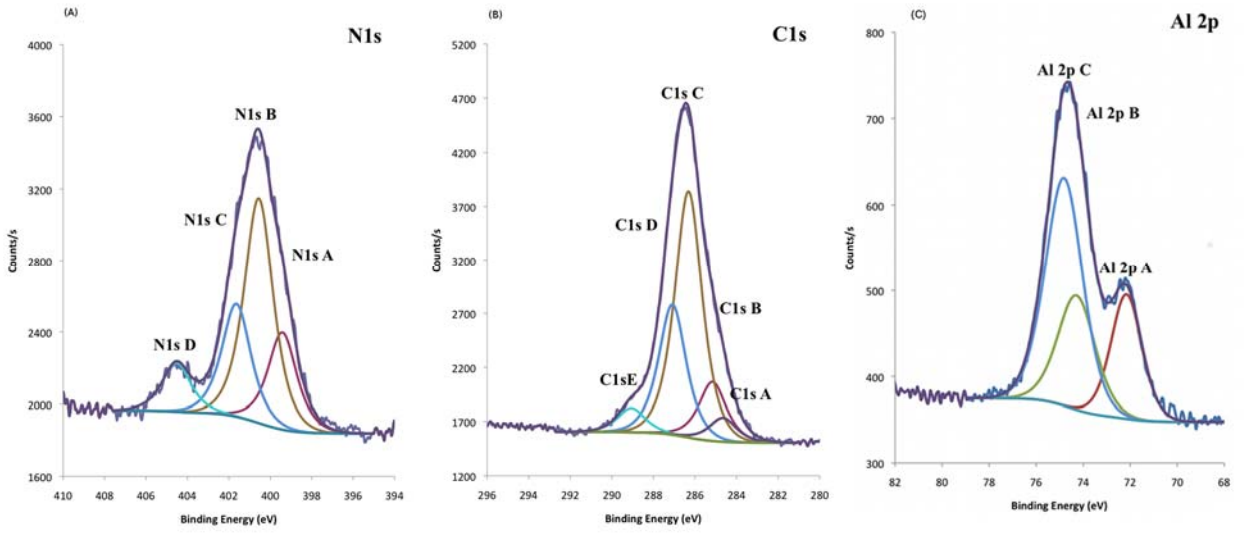

Figure 5-12: High-resolution XPS spectra of GAPm-capped aluminum powders. (A) N1s high-resolution data showing the partial formation of triazoles rings. (B) XPS narrow scans of the C1s region and (C) Al2p region.

In summary, the general XPS data from aluminum powders capped by GAPm and PAC can be compared in Table 5-2.

Table 5-2: XPS Analysis – Aluminum surfaces modified by organic coatings.

Name	Binding Energy (eV)	ASF	Atomic %	
			Al_GAP_M180	Al_PAC_M180
Al2p	74,5	0.185	6.7	9.5
C1s	285.0	0.250	42.3	53.6
N1s	339.4	0.420	23.9	-
O1s	532.1	0.660	26.0	35.9

5.3.3 Nanocomposite samples

Table 5-3 shows the combustion heat results obtained from aluminized-binders in the oxygen calorimeter bomb and its densities measured by gas pycnometer. The density of the binders is important in fuel applications because greater propellant densities can improve the vehicle performance. In general, the difference in density of the two different capping was not significant, but the capping with GAPm provided slight increases in binder density.

There was no significant variation in the experimental heat-of-combustion for samples made from propiolic acid-capped aluminum particles despite any increases in mass percentage. The highest value was 31.8±0.6 MJl^{-1} for the 30% w/w formulation.

Table 5-3: The heat of combustion measurements of aluminized-binders.

SAMPLES	GAP/BPS 100%	GAP/BPS Al_GAPm_M180			GAP/BPS Al_PAC_M180		
Metal powders w/w (%)	0.0	7.5	15	30	7.5	15	30
Density kg/m^3 (±0.1)	1299.0	1342.5	1385.4	1494.5	1338.2	1379.6	1489.1
Enthalpy kJ/g (±0.41)	22.68	22.25	21.96	23.09	21.88	21.50	21.37
Enthalpy MJ/l (±0.58)	29.47	29.87	30.42	34.51	29.28	29.04	31.84

The heat-of-combustion increases as a function of mass percentage in the formulation in the series of binders made from the aluminum powders coated with GAPm. The lowest value was 29.87±0.58 MJl^{-1} measured for 7.5% w/w formulation that is very close to the value of pure GAP/BSB binder (29.47 MJl^{-1}). The highest experimental value attains to 34.51±0.58 MJl^{-1}. It is a good assessment of the effect of aluminum capping with GAPm in comparison to hydrocarbon capping. In accordance with the difference in combustion behavior of the two series of binders, the visual examination of inside parts of calorimeter bomb (Fig.5-13) shows a higher formation of aluminum

oxide for the combustion test of GAPm-capped aluminum binders than the other ones. Similarly, there were also identified less unburned aluminum powders for this combustion tests.

Figure 5-13: Aluminum Oxide formation inside of oxygen calorimeter bomb Al_GAPm_M180/GAP_BPS binder (left) and Al_PAC_M180/GAP_BPS binder (right).

5.4 Conclusions

The work presented in this paper describes a method to produce aluminum-functionalized nanoparticles using the high-energy ball milling. The proposed procedure has been successfully applied to enhance the reactivity of aluminum powders coated by organic layer replacing the organic functionalized compound by an energetic polymer. The GAP-plasticizer chemically modified by partial substitution of azide groups was grafted onto aluminum surface in a simultaneous process of grinding and surface reaction. A series of combustion tests conducted in an oxygen calorimeter bomb demonstrated the better performance of GAPm-capped aluminum powders than the PAC-capped aluminum. More complete combustion and less residual unburned aluminum was observed in the combustion test leading to a highest combustion heat. The capping

of aluminum powders by the modified GAP showed to be a useful method to enhance the reactivity of aluminum powders.

5.5 References

Ciaramitaro, D. (2005). Triazole crosslinked in recyclable energetic compositions and method of preparing the same. US Patent 6,872,266. The United States of America as represented by the Secretary of the Navy, Washington, DC, USA.

Dubois, C., Désilets S., Nadeau G., & Gagnon, N. (2003). Chemical kinetics and heat transfer issues for a safe bench scale production of partially triazole substituted Glycidyl Azide Polymer (GAP). *Propellants, Explosives and Pyrotechnics* , 28: 107-113.

Dubois, C., Lafleur, P. G., & Roy, C. (2007). Polymer-grafted metal nanoparticles for fuel applications. *Journal of Propulsion and Power*, 23 (4) 651- 658.

Fecht, H. J., Hellstern, E., Fu, Z., & Johnson, W. L. (1990). Nanocrystalline metals prepared by high-energy ball milling. *Metallurgical Transactions A*, 21A, 2333-2337.

Fecht, H. J. (1995). Nanostructure formation by mechanical attrition. *Nanostructured Materials*, 6, 33-42.

Feng, H. T., Mintz, K. J., Augsten, R. A., & Jones, D. E. G. (1998). Thermal analysis of branched GAP. *Thermochimica Acta,* 311, 105-111.

Gao, Z., Walton, N. I., Malugin, A., Ghandehari, H., & Zharov, I. (2012). Preparation of dopamine-modified boron nanoparticles. *Journal of Materials Chemistry*, 22(3), 877-882.

Houser, T. J. and Humbert, D. K. (1973). Preparation and properties of a polymer formed from propargyl azide. *Macromolecules,* 6 (5), 786-787.

Keicher, T., Kuglstatter, W., Eisele, S., Wetzel, T., & Krause, H. (2009). Isocyanate-free curing of glycidyl azide polymer (GAP) with bis-propargyl-succinate (II). *Propellants, Explosives, Pyrotechnics*, 34(3), 210-217.

Koch, C. C., Scattergood, R. O., Youssef, K. M., Chan, E., & Zhu, Y. T. (2010). Nanostructured materials by mechanical alloying: new results on property enhancement. *Journal of Materials Science*, 45, 4725-4732.

Manzara, A. P. (1997). Azido polymers having improved brun rate. US Patent 5,681,904, Minnesota Mining and Manufacturing Company, St Paul, Minn., USA.

Reed Jr.,R. (2000). Triazole cross-linked polymers. US Patent 6,103,029. The United States of America as represented by the Secretary of the Navy, Washington, DC, USA.

Ringuette, S., Stowe, R., Dubois, C., Charlet, G., Kwok, Q., & Jones, D. E. G., (2006). Deuterium effect on thermal decomposition of deuterated GAP: 1. Slow thermal analysis with a TGA-DTA-FTIR-MS. *Journal of Energetic Materials*, 24 (4) , 307-320.

Sippel, T. R., Son, S. F. & Groven, L. J. (2013[a]). Modifying aluminum reactivity with poly(carbon monofluoride) via mechanical activation. *Propellants, Explosives, Pyrotechnics*, 38 (3), 321-326.

Sippel, T. R., Son, S. F. & Groven, L. J. (2013[b]). Altering reactivity of aluminum with selective inclusion of polytetrafluoroethylene through mechanical activation. *Propellants, Explosives, Pyrotechnics*, 38 (2), 286-295.

Sossi, A., Duranti, E., Paravan, C., Deluca, L. T., Vorozhtsov, A. B., Gromov, A. A., et al. (2013). Non-isothermal oxidation of aluminum nanopowder coated by hydrocarbons and fluorohydrocarbons. *Applied Surface Science*, 271, 337-343.

Tang, C., Lee, Y., & Litzinger, T. A. (1999). Simultaneous temperature and species measurements of the glycidyl azide polymer (GAP) propellant during laser-induced decomposition. *Combustion and Flame*, 117, 244-256.

Umbrajkar, S. M., Schoenitz, M., Jones, S. R., & Dreizin, E. L. (2005). Effect of temperature on synthesis and properties of aluminum-magnesium mechanical alloys. *Journal of Alloys and Compounds*, 402(1-2), 70-77.

Van Devener, B., Perez, J. P. L., Jankovich, J., & Anderson, S. L. (2009). Oxide-free, catalyst-coated, fuel-soluble, air-stable boron nanopowder as combined combustion catalyst and high energy density fuel. *Energy and Fuels*, 23(Compendex), 6111-6120.

Wang, T., Li, S., Yang, B., Huang, C. & Li, Y. (2007). Thermal decomposition of glycidyl azide polymer studied by synchrotron photoionization mass spectrometry. *J. Phys. Chem. B*, 111, 2449-2455.

Zhang, Z., Schoenitz, M. & Dreizin, E. L. (2012). Oxidation, ignition and combustion of Al-hydrocarbon composite reactive powders. *International Journal of Energetic Materials and Chemical Propulsion. 11(4), 353-373.*

Zhang, Z., Schoenitz, M. & Dreizin, E. L. (2013). Nearly pure aluminum powders with modified protective surface. *Combustion Science and Technology*, 185 (9),130-1377.

CHAPTER 6 ARTICLE 3: REACTIVITIES OF BORON AND BORON-MAGNESIUM ALLOY POWDERS COATED WITH A MODIFIED GLYCIDYL AZIDE POLYMER

Ricardo José Pontes Lima[1], Charles Dubois[1], Robert Stowe[2], Sophie Ringuette[2].

[1] *École Polytechnique de Montréal, Montreal, Canada*

[2] *Defence R&D Canada, Quebec City, Canada*

This paper has been submitted to Journal Energy and Fuels

Abstract

A study on the reactivity of boron and boron-magnesium alloy powders capped by modified glycidyl azide polymer is presented. Recent research has shown enhanced combustion efficiency of boron by the use of aluminum and magnesium as additive. In this work, high-energy ball milling was applied to fabricate intra-granular nano-composites from fine-particles of boron (1 – 2 μm) and magnesium powder. To further enhance the combustion properties of these powders, the particles were coated with an acid functionalized glycidyl azide - glycidyl triazole copolymer (GAPm), which resulted in the anchoring of the polymer chains on the particles. The combustion properties of as-milled powders were studied by thermal gravimetric analysis and calorimeter tests from a series of samples, in which magnesium content varies 0 to 20% w/w of metallic mixture. Focusing on studying the influence of the energetic protective coating of particles on these properties, we produced several boron and boron-magnesium powder samples varying the extent of coating with GAPm. The results showed the initial temperature of boron oxidation was decreased for as-milled boron particles, however the combustion efficiency diminished for unprotected particles. The coating process with modified glycidyl azide polymer increased the combustion efficiency that reached ~ 91%. From TGA experiments, the effect of embedded magnesium into boron based powders was characterized by a rise in weight gain rate, as revealed by a linear dependence on the magnesium content in the mixture, although the maximum combustion efficiency was achieved for the addition of 10% of magnesium powder in the composite that attained 87% of efficiency.

6.1 Introduction

The use of light metals, such as magnesium and aluminum as additives in boron formulations has been indicated as a means to enhance boron combustion efficiency. Recently, improvements of the combustion efficiency of boron were associated with the use of magnesium and aluminum as additives (Liu et al., 2014; Zhang et al., 2013). The boron ignition delay time and the energy loss by the formation of HOBO, which is indicated as the main problem in the boron combustion (Ulas et al., 2001; Yuong et al., 2006), were significantly decreased by the use of magnesium mechanically mixed with a boron powder (Liu et al., 2014). Similarly, the findings of the study conducted by Zhang et al. (2013) indicate that adding nano-aluminum increased significantly the burning rate of raw boron.

Despite these improved results on boron combustion other factors can also be controlled to enhance the performance of boron powders in propellant formulations and solid fuels. For example, the compatibility of the metal particles with the surrounding material and its dispersion during mixing in the polymeric matrix can play a critical role in the fabrication of solid fuels (Dubois et al., 2007). Also, the protection of these particles against premature oxidation should be improved since they might be stored for an extended period of time. One way to solve these problems is to coat the powders with a protective material that has an affinity for the binder system used.

Focusing on this issue, this study aims to investigate the effect of an energetic polymer coating of boron and magnesium-boron powders on their combustion properties. It is widely believed that energetic coatings such as a triazole -modified glycidyl azide polymer decreases the boron ignition delay time since an additional heat is produced close to the particles surface. In recent years, the glycidyl azide polymer (GAP) has been widely studied as an energetic binder for explosives, pyrotechnics and propellants. The GAP is characterized by the azide functional groups, which has a thermal decomposition to nitrogen gas and cyano groups releasing an enthalpy of 2473 kJ kg^{-1}.

To this end, we applied so-called mechanical milling to prepare ultrafine amorphous boron and Mg/B intra-granular mixture, from fine particles of boron and magnesium powder as starting materials. A number of studies have demonstrated the applicability of the mechanical milling to fabricate nanosized materials, amorphous alloys, intermetallic compounds and phase mixtures (Fecht et al., 1990; 1995; Koch et al., 2010), in which the powders, when mechanically milled in a

high-energy ball milling apparatus, are scaled down in size to the nanometer range, leading to large surface-area-to-volume ratios. Researchers have recently demonstrated that mechanical milling could be applied to coat the particles by the reactions of the freshly exposed metal surface with organic compounds (Devener et. al, 2009; Gao et al., 2012). Recently, we also presented an application of this method to produce nanosized aluminum flakes coating with GAPm (Lima et al., 2014).

In this study, the coating of metallic powders took place by adding a modified glycidyl azide polymer directly into the milling media. This is a versatile method that can be employed to obtain samples for various ratios of Mg/B combined with a range of energetic polymer coating thickness. These boron-rich composite powders were thoroughly examined by thermal gravimetric and differential thermal analysis. They were also incorporated into energetic binder, and then evaluated in subscale combustion tests using an oxygen calorimeter bomb.

6.2 Experimental procedures

6.2.1 Materials

The boron particles (boron, purity 99%, particle size 1–2 μm) used in our experiments were obtained from US Research Nanomaterials, Inc. The magnesium powder (96 μm) was used as additive material. The modified glycidyl azide polymer (GAPm) was prepared in our laboratory by chemical modification of 3M GAP plasticizer. It was then used without any further treatment to coat the milled-powders for all experiments. All the solvents were first dried by molecular sieve before being employed. Starting materials and milling balls were placed in a milling vial and sealed under argon to avoid premature oxidation. In order to reduce contamination, all chemicals and materials were handled in an argon-filled glove box at all times. A SPEX 8000M series shaker mill was used, with tungsten carbide (WC, $\rho = 14.5$ g cm^{-3}) vial and 3.16 mm diameter balls of the same material as the jars. The ball-to-powder mass charged ratio was adjusted by 120:1 for all experiments.

In order to establish a baseline for ball-milling experiments, boron powder was first milled without additives or organic compounds, for 120 minutes in hexanes. The resulted sample was identified as “as-milled boron”. The other ball-milling tests were performed to produce samples with varying

specific parameters. An experimental plan was conducted to obtain boron-rich composite powders as follows: boron powder was milled with different concentrations of GAPm during several milling times. In a second set of experiences, mixtures of boron and magnesium powders were also milled creating a range of Mg/B. The extent of coating with GAPm was kept constant at 16,67% w/w_{powder} for these experiments. Through this approach it became possible distinguish the benefits brought by the energetic coating or the magnesium addition on the combustion properties.

In order to provide standard milling parameters, the mass of powders, ball-to-powders mass charge ratio, and the volume of solvent were kept constant for all the experiments. Previous milling tests showed that the changing these parameters could influence ball-milling results. The percentage of GAPm was ranged from 0 to 50% (based weight). The magnesium/boron mass ratio was adjusted to obtain concentrations of 5, 10 and 20% w/w of magnesium in the samples. All other conditions of the first milling test were otherwise maintained. The detailed nomenclature of the composites is reported in Table 6-1. The ball-milling parameters setup for this study is also presented.

Table 6-1: Boron-rich composite samples

Sample Abbreviations	Mg content % (w/w_p)	GAPm coating % (w/w_{powder})	Milling time [min]	Ball-to-powder mass ratio
As-milled boron	0	0	120	1:120
$B\_(GAPm)_{16\%}\_M120$	0	16.67	120	1:120
$B\_(GAPm)_{33\%}\_M120$	0	33.37	120	1:120
$B\_(GAPm)_{50\%}\_M120$	0	50.00	120	1:120
$(Mg/B)_{5\%}$_GAPm_M120	5	16.67	120	1:120
$(Mg/B)_{10\%}$_GAPm_M30	10	16.67	30	1:120
$(Mg/B)_{10\%}$_GAPm_M60	10	16.67	60	1:120
$(Mg/B)_{10\%}$_GAPm_M120	10	16.67	120	1:120

$(Mg/B)_{20\%}$_GAPm_M120	20	16.67	120	1:120

6.2.2 Boron-rich energetic binders

Energetic binders enriched with boron and magnesium/boron powders were produced by the curing reaction of GAP plasticizer (GAP700, 700g mol^{-1}) with bis-propargyl succinate (BPS). The following procedure was applied for producing all the binder samples. Sufficient amounts of GAP and BPS were calculated to obtain a molar ratio of 0.25 ([C≡C]/[N_3]) and weighed separately. The appropriated amounts for each formulation of metal powders were poured into the GAP and homogenized for 30 min at ambient temperature. The BPS was added in the pre-mixed formulation and homogenized. The final formulation was cast into plastic molds (3 x 19 x 76 mm), degassed during 1 hour at 45 °C and cured at the same temperature for one day. Complete curing was achieved at 65 °C for another 1 day. Figure 6-1 shows the samples of cured binders. The yellow transparent sample was obtained from pure GAP plasticizer and dark brown sample resulted of boron-rich energetic binders.

Figure 6-1: (A) GAP/BPS energetic binder, (B) boron-rich energetic binder

The heat of combustion of these boron-rich energetic binders was measured in an oxygen calorimeter bomb (PARR calorimeter bomb) operated at 30 atmospheres. The thermal mass of the calorimeter was determined to be 10482±101 JK^{-1} prior to the calorimetric measurements through the combustion of standardized benzoic acid in a pure oxygen atmosphere.

The measurements of metal-binder densities were carried out with a gas pycnometer (AccuPyc 1340 Micromeritics apparatus) operated under helium at room temperature.

6.2.3 Thermal gravimetric analysis

Thermal analysis experiments were conducted by using a Mettler Toledo apparatus. A heating rate of 10 °C/min and a flow rate of 50 ml/min of pure dry oxygen were used. In each non-isothermal experiment operated over the 25 – 1050 °C temperature range, approximately 3 mg of the samples was placed in a 70μl alumina crucible. The initial oxidation temperature, the weight gain rate, and the temperature at a maximum oxidation rate of boron samples were determined using thermal gravimetric and differential thermal analysis to investigate the effects of magnesium addition and the coating with GAPm on the thermal oxidation characteristics of boron powders.

6.2.4 X-ray Photoelectron Spectroscopy (XPS)

The chemical composition of boron particle surfaces was carried out using X-ray photoelectron spectroscopy (XPS). XPS spectra were collected using the Mg Kα X-ray source on a VG Scientific ESCALAB 3 M KII XPS spectrometer. The electron beam power was 216 W (12 kV, 18mA). Both low-resolution survey and high-resolution scans of energy ranges were done. High-resolution spectra were taken with 20 eV pass energy and a resolution of 0.05 eV. The Shirley method was used to subtract background noise and Wagner sensitivity factors for quantitative analysis.

6.3 Results and discussion

This study aimed to evaluate the potential of the coatings on boron and boron-magnesium powders with an energetic polymer as a means of enhancing its combustion properties. To assess this potential improvement, several experimental variables were investigated. The main factor to be examined was the combustion behavior in oxygen rich environments. In view of this factor, two experimental methods were given priority. First, the combustion efficiency was calculated from the heat of combustion of the solid fuels enriched with these powders and compared to theoretical values. The second method was the thermal gravimetric analysis, which was performed in a non-isothermal test (10°C min^{-1}) under pure oxygen providing a summary of the differences in the oxidation process of powders.

6.3.1 The effect of boron particles coated with GAPm

The heat of combustion of different formulations of boron-rich solid fuels was measured in an oxygen calorimeter bomb. Three concentrations of GAPm coatings were analyzed (16, 33 and 50%w/w_{powder}) and the powder content in the binder was adjusted to obtain 15 and 30% w/w.

The results showed that the combustion efficiency of boron-rich binders samples produced from GAPm-capped boron powder reaches approximately 91% (B_(GAPm)$_{50\%}$_15% sample) whereas the lowest efficiency was 75.8% (B_(GAPm)$_{16\%}$_30%). A correlation between the combustion efficiency and the weight fraction of GAPm coating is found in the samples composed of 15% of powders, but this tendency is observed to the same extent for the samples made with 30% w/w of powders, in which the maximum value of efficiency seems to be limited at ~85%.

Table 6-2 reports all the results obtained from the oxygen bomb calorimeter experiments. The first data in this table reports the values of boron containing solid fuels to which boron powders were milled without GAPm or Mg adding. That is a reference data for comparative combustion performance of the others formulations. Herein, the efficiency of combustion reports the ratio of the energy released by the solid fuel compared to its expected theoretical value.

Table 6-2: Combustion efficiency of boron containing solid fuels

Sample abbreviations (binders)	Powder content w/w [%]	Binder Density [kg L^{-1}]		Heat-of-combustion [MJ L^{-1}]		Yield [%]
		Calculated	Measured ±0.010	Calculated	Measured ±1.05	
As-milled boron powder*	15	1.464	1.482	40.50	31.10	76.8
	30	1.618	1.638	53.57	32.11	58.1
$B\_(GAPm)_{16\%}$	15	1.438	1.415	38.46	32.87	85.5
$B\_(GAPm)_{33\%}$	15	1.412	1.415	36.51	32.42	88.8
$B\_(GAPm)_{50\%}$	15	1.386	1.390	34.58	31.45	91.0
$B\_(GAPm)_{16\%}$	30	1.567	1.556	49.01	37.13	75.8
$B\_(GAPm)_{33\%}$	30	1.515	1.527	44.56	38.04	85.4
$B\_(GAPm)_{50\%}$	30	1.464	1.474	40.32	33.85	83.9
$(Mg/B)_{5\%}\_(GAPm)_{16\%}$	30	1.559	1.580	48.14	36.24	75.3
$(Mg/B)_{10\%}$ $(GAPm)_{16\%}$	30	1.552	1.571	47.25	34.81	73.7
$(Mg/B)_{20\%}\_(GAPm)_{16\%}$	30	1.537	1.566	45.51	33.45	73.5
$(Mg/B)_{10\%}\_(GAPm)_{33\%}$	30	1.503	1.573	43.30	37.50	86.6
$(Mg/B)_{20\%}\_(GAPm)_{33\%}$	30	1.491	1.584	41.95	35.62	84.9

* Boron milled without GAP-m, nor magnesium adding.

The expected values to the heat of combustion of metal-rich binders were calculated from theoretical data of boron, magnesium and measured values of GAP/BPS-Binder 0.25 molar ratio (Table 6-3) and considering its mass percent in the mixture.

Table 6-3: Combustion data of fuels

Fuels	Density [kg L^{-1}]	Heat-of-combustion [kJ g^{-1}]
GAP/BPS 1:0.25 molar	1.309 ±0.010 *	22.22 ±0.40 *
Boron	2.340	58.50
Magnesium	1.740	25.02

* Measured

It should be noted that the increase of GAPm coatings diminishes the heat of combustion of composite because GAPm releases a lower heat than boron. A similar effect is noted to the density of binders.

In general, the results reveal that the combustion of all boron-rich energetic binders was incomplete in the conditions of the test. In fact, as can be seen in Figure 6-2, there was unburned metallic boron in the crucible after the combustion test. The residues of boron-binders from the crucible were collected and analyzed. The white powders were chemically identified as boron oxide (B_2O_3) and the surface analysis (XPS) of black residues revealed that is composed of B (15.4%), C (54.6%), N (2.5%), O (27.3%) and traces of W (0.2%).

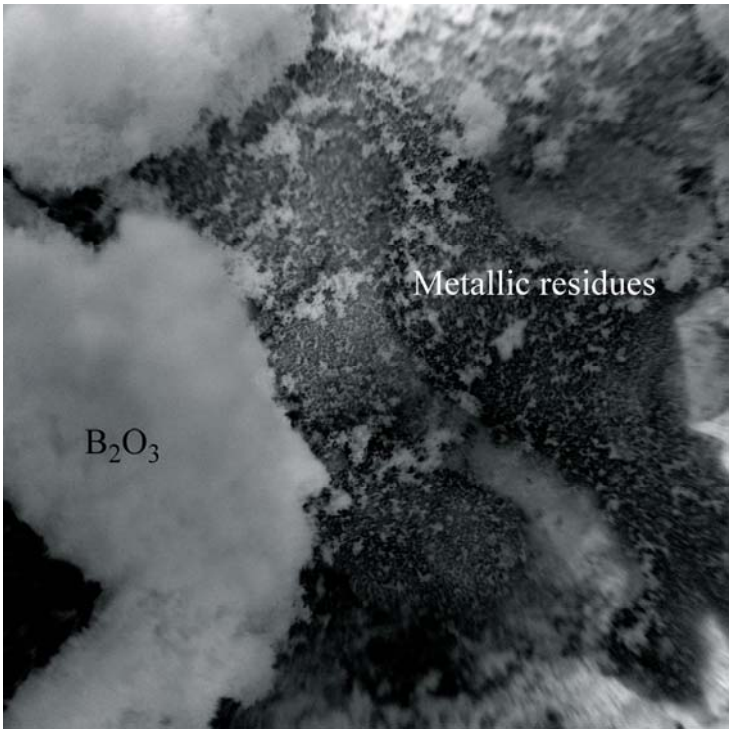

Figure 6-2: Image of combustion residues of boron-rich energetic binders

Further measurements and an in-depth analysis would be needed to determine the chemical composition of black solid residues because the carbonaceous residues from the decomposition of GAP should represent the major proportion on surface. However the presence of boron suggests the actual composition of the metallic residue, as well as, the traces of tungsten indicates the contamination of the material of balls.

6.3.2 The effect of adding of Mg into boron particles coated with GAPm

Boron-magnesium powders coated with GAPm were used in solid fuels formulations obtaining 30% w/w of binder weight. Regarding the effect of magnesium in the mixture, three different ratios of magnesium/boron were investigated (5, 10 and 20%). The adding of magnesium powders favors more complete fuel combustion as compared to B-binders (without GAPm coating). This trend is consistent with other studies (Liu et al., 2014). However, contrary to what was reported by Liu et al. (2014), our results revealed no significant dependence of the combustion efficiency on the magnesium content. The average efficiency was approximately 74%, a lesser value than what is

observed with GAPm-capped boron powders. An increase in the amount of GAPm grafted on B/Mg particles improved the efficiency from 73.7 to 86.6 and 73.5 to 84.9% (samples with 10 and 20% of Mg, respectively).

This lack of correlation between the combustion efficiency and the magnesium content was unexpected. We propose the following explanation about it. First, it is important to emphasize that there are differences in the methods used to obtain the B/Mg mixtures. Liu et al. (2014) reports that they used a mortar to blend the powders for 20 minutes; herein, the high-energy ball milling was applied to prepare the composites for 2 hours. It is reasonable expect that in these conditions the boron could have partially reacted with magnesium to form boride compounds (Habler et al., 2003). Boride compounds release lower heat in the combustion process than boron (e.g. $\Delta H_{[MgB_2]}$ = 38.8 kJ g^{-1}). Consequently, the total heat released by the composite could be attenuated by the presence of these products in the mixture. Second, since ultrafine powders of magnesium and boron are very sensitive to oxygen, small amount of these powders could be oxidized by the first contact with oxygen environment. We tend to believe that to a certain degree the oxidation has been occurred because an increasing of GAPm in the composite enhanced the results, which means there was a better protection against premature oxidation.

In order to confirm the above explanations, the chemical composition of particle surface was investigated by X-ray photoelectron spectroscopy (XPS). A summary of XPS data obtained from several samples of as-milled powders coated with GAPm compared to as-milled boron is reported in Table 6-4.

Table 6-4: XPS analysis of boron-rich composite powders

Name	Binding Energy (eV)	ASF	Atomic %				
			As-milled boron	Boron $(GAPm)_{16\%}$	$(Mg/B)_{5\%}$ $(GAPm)_{16\%}$	$(Mg/B)_{10\%}$ $(GAPm)_{16\%}$	$(Mg/B)_{20\%}$ $(GAPm)_{16\%}$
W 4f	33.6	2.750	2.2	0.3	0.4	0.2	0.1
Al 2p	73.1	0.185	—	—	—	1.4	—
Mg 2s	89.1	0.180	—	—	1.9	2.3	5.7
B 1s	187.3	0.130	36.5	15.2	25.2	20.9	20.8
C 1s	284.8	0.250	14.6	40.5	30.4	36.7	26.1
N 1s	399.9	0.420	—	16.1	6.7	4.5	5.3
O 1s	531.8	0.660	40.9	6.8	33.6	32.6	39.0
F 1s	687.3	1.000	1.8	0.6	1.4	1.4	2.8
Co 2p	782.4	3.800	4.0	0.5	0.4	—	—

An important peak of C 1s at 284.8 eV (40.9%) and the N 1s peak (399.9 eV, 16.1 %) were detected for GAPm-coated boron samples and attributed to the GAPm molecules, which denotes the success of capping boron particles. As a consequence of this protective capping, the oxygen peak (O 1s 531.8 eV) was significantly diminished from 40.9 to 6.8%, suggesting that the formation of boron oxides and boron sub-oxides was decreased. However, the intensity of oxygen peak was increased with B/Mg samples, which seems to confirm a possible premature oxidation in these samples.

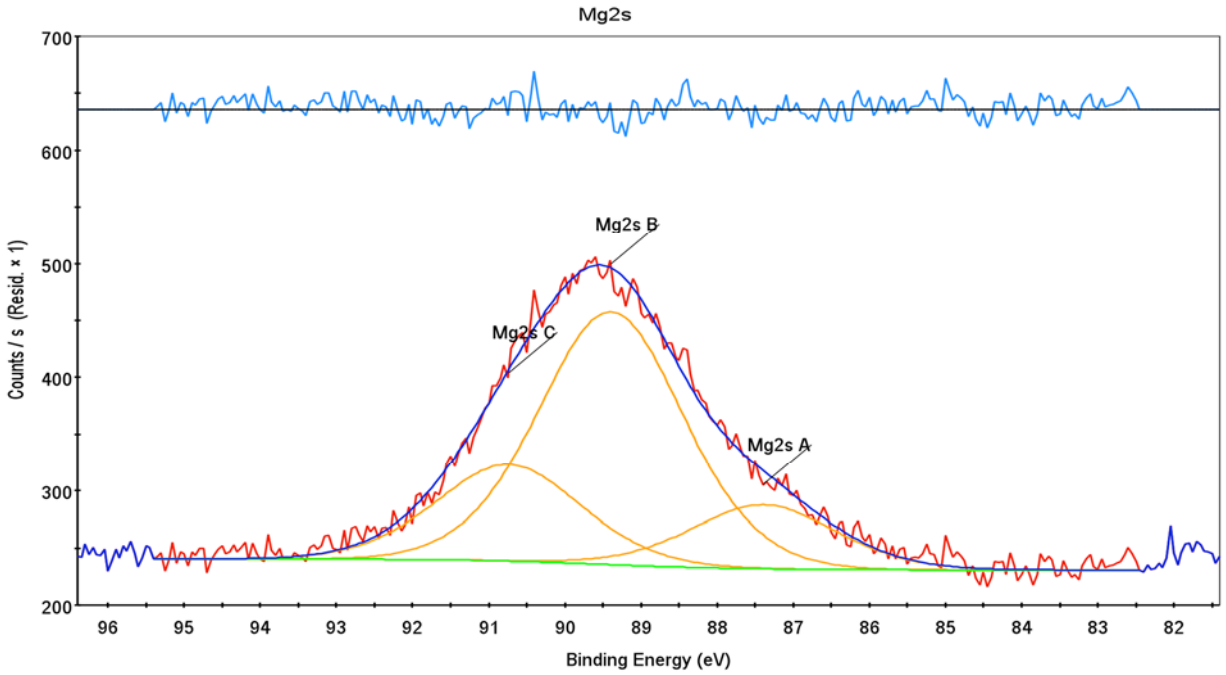

Figure 6-3: High-resolution XPS spectra data of $(Mg/B)_{20\%}$ $(GAPm)_{16\%}$ sample showing the XPS narrow scans of the Mg 2s region (yellow lines).

The high-resolution Mg 2s data from GAPm-capped boron-magnesium samples also confirms both the B—Mg bond and the partial oxidation of magnesium. As seen in the Mg 2s photoelectron spectra (Fig.6-3) a broad peak centered at 89.1 eV suggests the presence of chemically distinct magnesium atoms consistent with the formation of magnesium diboride (90.7 eV) ascribed by Mg2s C and magnesium oxide (89.4 eV) designated as Mg2s B (Talapatra et al., 2005), as showed in Figure 6-3.

XPS spectra also showed traces of tungsten (33.6 eV) and cobalt (782.4 eV), which arise from tungsten carbide balls and milling vial (main composition WC, Co), however, it is interesting to note that the intensity of W 4f and Co 2p was decreased to the GAPm-coated powders and B/Mg samples. The addition of polymer acts as process control agent (surfactant) reducing the surface tension, and as the magnesium is more ductile than boron it reduces the shear forces on the balls. Clearly both these effects have contributed to reduce the attrition of powders on balls and walls of milling container resulting less contamination.

6.3.3 TGA experiments

The thermal gravimetric analysis confirms the results obtained from the bomb calorimeter experiments. Table 6-5 resumes the TGA data obtained from the boron powder composites. Although smaller values were observed in the combustion efficiency of powders in comparison to metal binders, they are close to the values achieved before (Table 6-2). In general, the oxidative process is controlled by the gas diffusion that could be reduced by agglomeration of metal powders and oxides formed into the crucible, thus attenuating the oxidation process.

Table 6-5: TGA data of oxidative process of powders

Powder abbreviations	T_{onset} [° C]	$T_{ox\ peak}$ [° C]	Weight gain rate [% min^{-1}]	Total weight [%]	Calculated weight * [%]	Yield [%]
As-milled boron	576.42	616.84	5.82	148.93	322.00	22.04
$B\_(GAPm)_{16\%}$	568.96	588.51	26.78	167.84	268.33	45.68
$B\_(GAPm)_{33\%}$	600.24	642.01	7.59	149.27	214.67	55.81
$B\_(GAPm)_{50\%}$	620.17	654.18	5.66	128.89	161.00	71.07
$(Mg/B)_{5\%}\_(GAPm)_{16\%}$	606.11	652.51	6.92	173.59	261.83	52.30
$(Mg/B)_{10\%}\ (GAPm)_{16\%}$	691.69	717.01	25.15	188.30	252.33	63.77
$(Mg/B)_{20\%}\_(GAPm)_{16\%}$	705.10	710.84	44.09	163.23	242.33	57.24
$(Mg/B)_{10\%}\_(GAPm)_{33\%}$	671.65	699.18	15.17	162.34	204.27	71.67
$(Mg/B)_{20\%}\_(GAPm)_{33\%}$	691.86	697.18	32.39	149.91	193.87	70.30

* Calculated from the metal contents in the sample and considering complete decomposition of GAPm up to 1050 °C

In regard to the influence of the thickness of coating on the combustion, the TGA results could be likened to what was found in the calorimeter tests. The yield of oxidation reaction of powders has an increasing dependence on the thickness of coatings, whereas the same random variations of values are observed to boron-magnesium powders. However, thicker coatings seem to mitigate the

rate of weight gain. On the other hand, increasing the magnesium content led to the highest weight gain rates as illustrated in Table 6-5. We observed that this is the major contribution of magnesium addition in the boron composites as will be discussed hereafter.

As mentioned above, the alloys of magnesium and boron have the highest oxidation rates, increasing with magnesium content in the sample. In this study, this was the major outcome for the addition of magnesium in boron formulations, which can be argued as a factor decreasing the boron ignition delay time. In fact, since magnesium ignites more readily than boron, it induces the ignition of boron. As has been pointed out by Liu et al. (2014), magnesium quickly reacts with oxygen and releases a large amount of heat thus promoting boron ignition. However, to a certain point, there is a mutual competition relation between the reaction of magnesium and oxygen and boron-oxygen reaction, which might also explain the random variations in the final oxidation degree of TGA experiments.

6.3.4 The effect of milling time

Boron and boron-magnesium alloy powders were obtained from ball milling process in which the milling time plays an important role. The decrease of the internal grain size is an implicit result of the raise in milling time. Previous studies have shown the correlation between the internal grain size and the metal properties such as the melting point (Eckert et al. 1993). In light of these findings, it seems reasonable to investigate the effect of the milling time on the combustion properties. TGA curves illustrated in Figure 6-4 shows the comparison between the oxidative behaviors of the B/Mg samples milled at three different durations (30, 60 and 120 minutes).

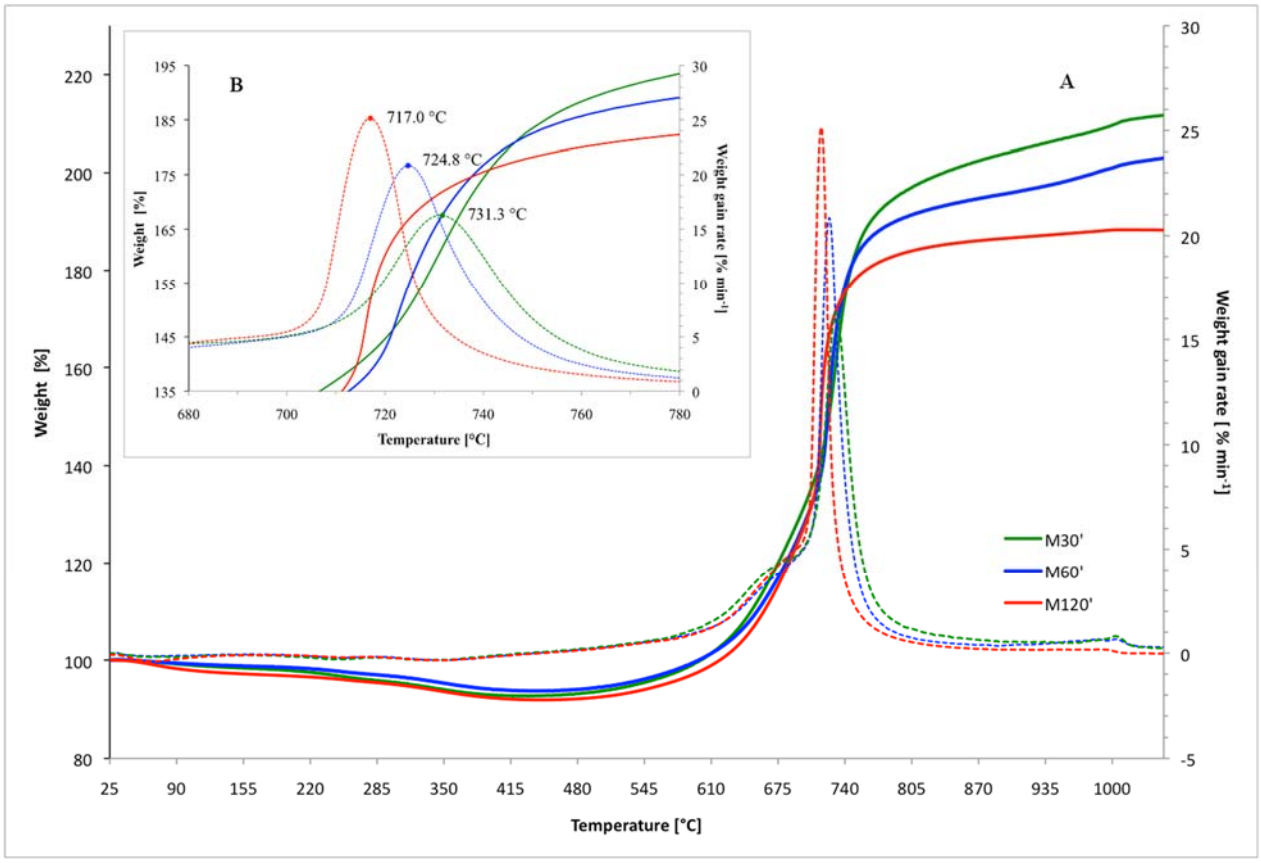

Figure 6-4: Comparison of TGA results of samples obtained by progressive increase in milling-time (A) solid lines TGA and dashed lines DTG. The differences in the temperature of maximum rate of weight gain (B).

Even if the raise in milling time appears to mitigate the final degree of oxidation, it was shifted down the temperature of maximum point of oxidation (Fig. 6-5A) and caused a steady rise in the weight gain rate (Fig. 6-5B). This is consistent with thermodynamic models for the size effect of the combustion properties of small particles.

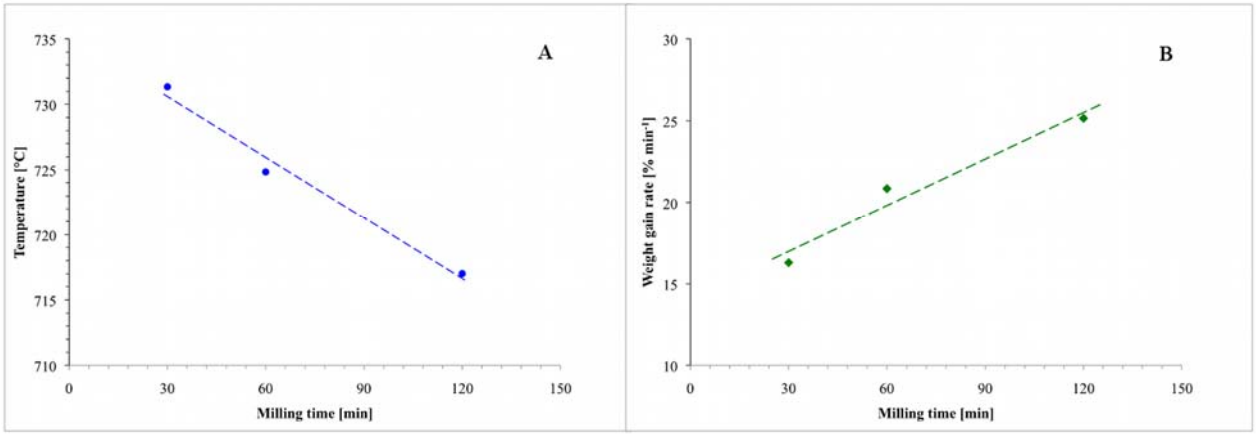

Figure 6-5: Linear dependence of T_m (A) and weight gain rate on milling time (B).

6.4 Conclusion

The present experimental study demonstrated the effect of the energetic coating of boron and boron-magnesium alloy powders produced by high-energy ball milling on its combustion properties. Considering the data presented herein, it is clear that the protective energetic capping has enhanced the combustion properties of powders. This study achieved the goal of providing parameters to compare different formulations of boron and boron-magnesium alloys coated by GAPm. It should be pointed out that the adding of magnesium into these formulations provides better results in boron combustion, as was shown by the high oxidation rates in TGA, but it needs a good protection of particles against premature oxidation. The capping of powders with the modified glycidyl azide polymer appears as an important means to achieve these improvements.

In regards to future researches, our findings only highlight the importance of the coating of powders with modified glycidyl azide polymer. Future studies will be necessary to further determine the performance of these novel fuels. Other burning tests will be essential to establish the effectiveness of the fuels on the boron ignition delay time and burning regression rates.

REFERENCES

Dubois, C., Lafleur, P. G., & Roy, C. (2007). Polymer-grafted metal nanoparticles for fuel applications. *Journal of Propulsion and Power*, 23 (4) 651- 658.

Eckert, J., J. C. Holzer, *et al.* (1993). "Melting behavior of nanocrystalline aluminum powders." *Nanostructured Materials* 2, 407-407.

Fecht, H. J., Hellstern, E., Fu, Z., & Johnson, W. L. (1990). Nanocrystalline metals prepared by high-energy ball milling. *Metallurgical Transactions A*, 21A, 2333-2337.

Fecht, H. J. (1995). Nanostructure formation by mechanical attrition. *Nanostructured Materials*, 6, 33-42.

Gao, Z., Walton, N. I., Malugin, A., Ghandehari, H., & Zharov, I. (2012). Preparation of dopamine-modified boron nanoparticles. *Journal of Materials Chemistry*, 22(3), 877-882.

Guo, Y., Zhang, W., Zhou, X. & Bao, T. (2012). Magnesium boride sintered as high-energy fuel. *Journal of Thermal Analysis and Calorimetry*,1-5.

Hacler, W., Rodig, C., Fischer, C., Holzapfel, B., Perner, O., Eckert, J., Nenkov, K. & Fuchs, G. (2003). Low temperature preparation of MgB2 tapes using mechanically alloyed powder. *Superconductor Science and Tecnology*, 16, 281-284.

Koch, C. C., Scattergood, R. O., Youssef, K. M., Chan, E., & Zhu, Y. T. (2010). Nanostructured materials by mechanical alloying: new results on property enhancement. *J Mater Sci*, 45, 4725-4732.

Lima, R. J. P., Dubois, C., Stowe, R. & Ringuette, S. (2014). Enhanced reactivity of aluminum powders by capping with a modified glycidyl azide polymer. *International Journal of Energetic Materials and Chemical Propulsion. (In press)*

Liu, J-Z., Xi J-F., Yang, W-J., Hu Y-R., Zhan Y-W., Wang, Y. & Zhou, J-H. (2014). Effect of magnesium on the burning characteristics of boron particles. *Acta Astronautica*, 96, 89-96.

Ulas, A. Kuo, K. K. (2001). Ignition and combustion of boron particles in fluorine containing environments. *Combustion and Flame*,127, 1935-1957.

Van Devener, B., Perez, J. P. L., Jankovich, J., & Anderson, S. L. (2009). Oxide-free, catalyst-coated, fuel-soluble, air-stable boron nanopowder as combined combustion catalyst and high energy density fuel. *Energy and Fuels*, 23(Compendex), 6111-6120

Young, G., Balar, R., Krasel, M., Yu, K. (2006). Effect of nanoparticles in airbreathing combustion. 14th AIAA/AHI International Space Planes and Hypersonics Systems Technologies Conference, November 6, 2006 - November 9, 2006, Canberra, Australia, American Institute of Aeronautics and Astronautics Inc.

Zhang, B., Huang, C. Yan, S., Li, Y. & Cheng, Y. (2013). Enhanced reactivity of boron, through adding nano-aluminum and wet ball milling. *Apllied Surface Science.*

GENERAL DISCUSSION

This work concerns the application of metal as fuels or additives in high-energy condensed systems. As we mentioned earlier, considerable improvements can be achieved in combustion processes by reducing the metal particle sizes. However, nanosized particles need special treatments to ensure a high combustion efficiency. This topic has been addressed in several previous studies that have proposed different ways to enhance the combustion of metal nanoparticles. In this study, one novel promising option of producing metal nanoparticles for fuel application is presented: the synthesis of metal-energetic polymer nanocomposites. This procedure overturns the more conventional methods in which non-energetic coatings are deposited onto metal particles. Instead, herein an energetic polymer was applied that releases a significant amount of heat in combustion processes, promoting boron ignition. In addition, the dispersion of powders in an azide-based binder for the final composite material is facilitated because of a smaller enthalpy of mixing.

The high-energy ball milling process was used to fabricate different samples of nanosized metal powders coated with organic compounds (propargyl species) and a modified glycidyl azide polymer (GAPm). In light of the findings of the review literature, this work was aimed at determining a new route to produce metal-polymer composites for the fuel applications. It should be noted that the metal-polymer composites showed significant new characteristics such as the enhanced heat of combustion, stability, and safer handling in the air, as a consequence of the change of size and shape of particles, and also the features provided by the energetic capping on the particles. The results confirm that the metal powders were coated successfully. The comparative study conducted in the first part of this work showed the versatility of the experimental method. In fact, high-energy ball milling proved to be a remarkable technique to obtain new composite material with great reproducibility. Since it proceeds in one step, it could easily be scaled-up.

The major difficulty found to produce the energetic-coated metal particles concern the boron milling. The level of contamination from milling media was very high in the first experiments. Great efforts were needed to understand and develop a procedure able to produce composites with low contamination. Other drawbacks detected for the simultaneous milling process was solved by changes to the experimental method, such as the direct capping of particles with modified glycidyl azide polymer. This change in the milling process prevents an additional step to graft the energetic

polymer. Also, it was helpful to diminish the contamination level in the boron ball milling. Moreover, an enhancing of the heat transfer of shaker mill was done by the modified by the addition of a new external fan to cool and the set of finned aluminum heat sinks placed on the vial.

Considering that the main goal of this thesis was to enhance the combustion properties of metal powder, in general, the metal particles and metal alloy presented showed a good performance in the oxidation and combustion tests. This change in behavior was principally attributed to the capping of particles, for which it was introduced a new energetic compound resulting from the chemical modification of the glycidyl azide polymer. In comparison to propargyl-capped aluminum powders, the samples coated with GAPm exhibit more complete combustion and less residual unburned aluminum leading to maximum combustion heat.

The modified energetic polymer was characterized by experimental analysis, such as ATR-FTIR, DCS and XPS analyses that also confirm the grafting of GAPm molecules onto metal particles. The samples of metal-polymer composite produced with GAPm-coated powders showed higher densities (ρ_{max} = 1.494 g cm^{-3}) than classic solid fuels (e. g. HTPB, ρ = 0.920 g cm^{-3}). They have also high combustion heats, for which the highest volumetric heat combustion measured was 34.51 ± 0.58 MJ L^{-1}.

The third part of this work concerned boron and boron/magnesium alloy. The results showed that the energetic coating contributed to enhancing the combustion performance for both the boron and the boron/magnesium powders. Different formulations of boron and boron-magnesium alloys coated by GAPm were investigated. The sampling includes variations in the GAPm coatings, different ratios of magnesium/boron, and different milling times. The systematic analysis in TGA and combustion tests on these samples provides the parameters to compare the combustion behaviors. Unexpected findings should be pointed out for the formulations in which magnesium powders were added. Despite the high rates of non-isothermal oxidation, it was expected that the dependence of the combustion efficiency on the magnesium content did not occur. However, considering their high rate of oxidations that could be argued as an impact factor on the boron ignition delay time, these formulations exhibit better results for boron combustion. Even so, they need better protection against premature oxidation.

Some technical limitations, such as the scale-up of processes that could provide sufficient amount of binders for measurements and combustion tests, prevented further characterization of the new

solid fuels, which could demonstrate more clearly the benefits produced. In fact, initial tests to scale up aluminized-binders led to very porous samples that prevented burning rate measurements. No further investigations were done to determine what caused the bubbles in the samples; however, it was believed that some incompatibility of the ingredients in the formulations occurred. More development will be necessary to achieve a stable formulation. However, burning rate measurements and combustion tests by laser induction are important characterizations that could further highlight the potential of these fuels, and small-scale rocket motor tests are also missing.

CONCLUSION, PERSPECTIVES AND RECOMMENDATIONS

Conclusion

The first contribution of this thesis is the development of a method to coat metal particles with an energetic polymer, as a mean of enhancing their combustion properties. With respect to the incorporation of these composite powders into an energetic polymer matrix, the grafted polymer contributed to a better dispersion, which in turn resulted in a more complete combustion. High combustion enthalpies found in the new metal composites are very encouraging for the development of new metallic composite fuels. The high volumetric heat of combustion qualifies these composites as potential candidates in volume-limited applications such as rocket propulsion systems.

The experiments conducted during this thesis project showed that high-energy ball milling is a very versatile method to obtain nanosized metal structures in a variety of sizes and shapes, while allowing for several types of organic coatings.

Characterization of composite powders and binders was limited by the laboratory facilities - for example, the lack of an ignition laser apparatus. Also, it is necessary to scale up the process to produce sufficient amount of binders for burning rate tests. Despite these limits, it is believed that its findings may contribute to innovation in the field of metal fuel formulation containing boron and boron alloys.

In regards to future research, the findings presented herein only highlight the usefulness of coating of powders with modified glycidyl azide polymer. Future studies will be necessary to further determine the performance of these novel fuels. Other burning tests will be essential to establish the effectiveness of the fuels, such as the linear regression rates.

PERSPECTIVES AND RECOMMENDATIONS

Following the results presented in this thesis, a number of new research opportunities could be pursued to bring these novel metal-polymer composites closer to fuel applications. First, *“the influence of the energetic capping on the regression rates of solid fuels”* should be investigated. Based on the results presented from non-isothermal oxidation in TGA experiments, one can

anticipate a great improvement of the regression rates of GAPm-capped metal solid fuels. Secondly, future studies will be necessary to determine the impact of the energetic coating on " *the ignition delay time of GAPm-capped boron and boron/magnesium particles"*.

Considering the experimental method applied to achieve the objectives: *high-energy ball milling*, certain operational parameters had to be maintained constant for the sake of facilitating data interpretation and reducing the number of experiments. Therefore, an improved reduction of particle sizes could have been reached by the variation of some of these parameters. For example, the size and number of mill balls were kept constant, but a variation in number would have a direct impact on the milling energy. Moreover, the use of different sizes of balls in the same vial could create a random motion of balls and improve the size reduction process.

REFERENCE LIST

Abe, H., Naito, M., Nogi, K., Matsuda, M., Miyake, M., Ohara, S., et al. (2003). Low temperature formation of superconducting MgB2 phase from elements by mechanical milling. *Physica C: Superconductivity and its Applications*, 391(2), 211-216.

Altman, D. & Holzman, A. (2007). Overview and History of hybrid rocket propulsion. In Chiaverini, M. J., Kuo, K. K. (ed), *Fundamentals of hybrid rocket combustion and propulsion.* (1st, p. 1-36) American Institute of Aeronautics and Astronautics, Inc., Reston, Virginia.

Balaz, P. (2008). High-energy milling. In *Mechanochemistry in nanoscience and minerals engineering.*(1st, 103-132). Berlin, springer-Verlag Berlin Heidelberg.

Bretherick, L. (1990). Bretherick's handbook of reactive chemical hazards (4th Ed.). Bodmin, Cornwall: Butterworth & Co. (publishers) Ltd.

Castro, C. L. & Mitchell, B. S. (2002). Nanoparticles from mechanical attrition. In Bataron, M-I. (Ed), *Synthesis, functionalization and surface treatment of nanoparticles.* (1st, 1-15). US Americam Scientific Publishers.

Cheng, Q. (2005). Method of preparing aluminum nanorods. US.**2005/0274226 Al**.

Chiaverini, M. J., Serin, N., Johnson, D. K., Lu, Y.-C., Kuo, K. K., & Risha, G. A. (2000). Regression rate behavior of hybrid rocket solid fuels. *Journal of Propulsion and Power, 16*(Compendex), 125-132.

Chiaverini, M. (2007). Review of solid-fuel regression rate behaviour in classical and nonclassical hybrid rocket motors. In Chiaverini, M. J., Kuo, K. K. (ed), *Fundamentals of hybrid rocket combustion and propulsion.* (1st, p. 37-125) American Institute of Aeronautics and Astronautics, Inc., Reston, Virginia.

Davis, R. M., Mcdermott, B. & Koch, C. C. (1988). Mechanical alloying of brittle materials. *Metallurgical Transactions A*, 19A, 2867-2874.

Devener, B., Perez, J. P. L., Jankovich, J., & Anderson, S. L. (2009). Oxide-free, catalyst-coated, fuel-soluble, air-stable boron nanopowder as combined combustion catalyst and high energy density fuel. *Energy and Fuels*, 23(Compendex), 6111-6120

Dubois, C., Lafleur, P. G., & Roy, C. (2007). Polymer-grafted metal nanoparticles for fuel applications. *Journal of Propulsion and Power*, 23 (4) 651- 658.

Eckert, J., J. C. Holzer, *et al.* (1993). Melting behavior of nanocrystalline aluminum powders. *Nanostructured Materials* 2, 407-407.

Evans, B., Favorito, N. A., & Kuo, K. K. (2006). *Oxidizer-type and aluminum-particle addition effects on solid-fuel burning behavior*. Paper presented at the AIAA/ASME/SAE/ASEE 42nd Joint Propulsion Conference, July 9, 2006 - July 12, 2006, Sacramento, CA, United states.

Fecht, H. J., Hellstern, E., Fu, Z., & Johnson, W. L. (1990). Nanocrystalline metals prepared by high-energy ball milling. *Metallurgical Transactions A*, 21A, 2333-2337.

Fecht, H. J. (1995). Nanostructure formation by mechanical attrition. *Nanostructured Materials*, 6, 33-42.

Fedorov, S. G., Guseinov, Sh. L., & Storozhenko, P. A. (2010). Nanodispersed metal powders in high-energy condensed systems. *Nanotechnologies in Russia*, 5, (9-10) 565-582.

Galfetti, L., De Luca, L. T., Severini, F., Meda, L., Marra, G., Marchetti, M., . . . Bellucci, S. (2006). Nanoparticles for solid rocket propulsion. *Journal of Physics Condensed Matter, 18*, S1991-S2005.

Galfetti, L., De Luca, L. T., Severini, F., Meda, L. & Marra, G. (2007). Pre and post-burning analysis of nano-aluminized solid rocket propellants. *Aerospace Science and Technology*, 11, 26-32.

Gao, Z., Walton, N. I., Malugin, A., Ghandehari, H., & Zharov, I. (2012). Preparation of dopamine-modified boron nanoparticles. *Journal of Materials Chemistry*, 22 (3), 877-882.

Gumbel, A., Eckert, J., Fuchs, G., Nenkov, K., Muller, K. H., & Schultz, L. (2002). Improved superconducting properties in nanocrystalline bulk MgB2. *Applied Physics Letters, 80*(15), 2725-2727.

Grumov, A. A., Ilyin, A. P., Foerter-Barth, U. & Teipel, U. (2006). Effect of the passivation coating type, particle size, and storage time on oxidation and nitridation of aluminum powders. *Combustion, Explosion, and Shock Waves*,42 (2) , 177-184.

Hacler, W., Rodig, C., Fischer, C., Holzapfel, B., Perner, O., Eckert, J., Nenkov, K. & Fuchs, G. (2003). Low temperature preparation of MgB2 tapes using mechanically alloyed powder. *Superconductor Science and Tecnology*, 16, 281-284.

Hori, K. (2009). Application of glycidyl azide polymer to hybrid rocket motor. 45th AIAA/ASME/SAE/ASEE Joint Propulsion Conference and Exhibit, August 2, 2009 - August 5, 2009, Denver, CO, United states, American Institute of Aeronautics and Astronautics Inc.

Huang, Y., Risha, G. A., Yang, V., & Yetter, R. A. (2009). Effect of particle size on combustion of aluminum particle dust in air. *Combustion and Flame, 156*(Compendex), 5-13.

Hussain, I., Brust, M., Papworth, A. J., & Cooper, A. I. (2003). Preparation of acrylate-stabilized gold and silver hydrosols and gold-polymer composite films. *Langmuir, 19*, 4831-4835.

Hwang, S., Nishimura, C., & McCormick, P. G. (2001). Mechanical milling of magnesium powder. Materials Science & Engineering A (Structural Materials: Properties, Microstructure and Processing), A318(1-2), 22-33.

Hwang S. and McCormick, P. G. (1999). The synthesis and properties of nanocrystalline magnesium produced by ball milling.

Ivanov, V. G. & Gavrilyuk, O. V. (1999). Specific Features of the oxidation and self-ignition of electroexplosive ultradisperse metal powders in air. *Combustion, Explosion, and Shock Waves*, 35(6), 648 -655.

Jiang, X., Trunov, M. A., Schoentz, M., Dave, R. N., & Dreizin, E. L. (2008). Mechanical alloying and reactive milling in a high energy planetary mill. 44th AIAA/ASME/SAE/ASEE Joint Propulsion Conference & Exhibit 21- 23 July 2008, Hartford, CT.

Keicher, T., Kuglstatter, W., Eisele, S., Wetzel, T., & Krause, H. (2009). Isocyanate-free curing of glycidyl azide polymer (GAP) with bis-propargyl-succinate (II). *Propellants, Explosives, Pyrotechnics*, 34(3), 210-217.

Koch, C. C. (1993) The synthesis and structure of nanocrystalline materials produced by mechanical attriton: a review. *Nanostructured Materials* 2, 13-22.

Koch, C. C., Scattergood, R. O., Youssef, K. M., Chan, E., & Zhu, Y. T. (2010). Nanostructured materials by mechanical alloying: new results on property enhancement. *J Mater Sci*, 45, 4725-4732.

Kotov, Y. (2003). Electric explosion of wires as a method for preparation of nanopowders. *Journal of Nanoparticle Research, 5*(5-6), 539-550.

Kotov, Y. (2009). The electrical of wire: a method for the synthesis of weakly aggregated nanopowders. *Nanotecnologies in Russia,* 4(7-8), 415-424.

Kwon, Y-S., Gromov, A. A., Ilyin A. P. (2002). Reactivity of superfine aluminum powders stabilized by aluminum diboride. *Combustion and Flame,* 131, 349-352.

Kwon, Y-S., Gromov, A. A., Ilyin A. P., Rim, G-H. (2003). Passivation process for superfine aluminum powders obtained by electrical explosion of wires. *Applied Surface science,* 211, 57-67.

Kwon, Y-S., Gromov, A. A., Strokova, J. I. (2007). Passivation of the surface of aluminum nanopowders by protective coatings of the different chemical origin. *Applied Surface Science,* 253, 5558-5564.

Kuo, K.K., Risha, G.A., Evans, B. J., & Boyer, J. E., (2004). Potential usage of energetic nano-sized powders for combustion and rocket propulsion. Published in Symposium Proceeding, Volume 800: Synthesis, Characterization and Properties of Energetic/Reactive Nanomaterials, Edited by Ronald Armstrong, et al. pp. 3-14.

Lengelle, G. (2007). Solid-fuel pyrolysis phenomena and regression rate, part 1: mechanisms. *Progress in Astronautics and Aeronautics*, *218*, 127.

Lima, R. J. P., Dubois, C., Mader, O., Stowe, R., & Ringuette, S. (2010). Boron Nanoparticle-Rich Fuels for Gas Generators and Propellants. *International Journal of Energetic Materials and Chemical Propulsion*, 9(5), 1-10.

Liu, J. Z., Xi J. F., Yang, W. J., Hu Y. R., Zhan Y. W., Wang, Y. & Zhou, J. H. (2014). Effect of magnesium on the burning characteristics of boron particles. *Acta Astronautica,* 96, 89-96.

Liu, L. L., He, G. Q. & Wang, Y. H. (2013). Thermal reaction characteristics of the boron used in the fuel-rich propellant. *Journal of Thermal Analysis and Calorimetry,* 114(3), 1057-1068.

Martirosyan, K. S., Wang, L., Vicent, A. & Luss, D. (2009). Nanoenergetic gas-generators: design and performance. *Propellants, Explosives and Pyrotechnics,* 34, 532–538.

Mahanta A. K. & Pathak D. D. (2012). HTPB-polyurethane: a versatile fuel binder for composite solid propellant, polyurethane, Dr. Fahmina Zafar (Ed.), ISBN: 978-953-51-0726-2, InTech, DOI: 10.5772/47995. Available from: http://www.intechopen.com/books/polyurethane/htpb-polyurethane-a-versatile-fuel-binder-for-composite-solid-propellant

Maurice, D. R. & Courtney, T. H. (1990). The physics of mechanical alloying: a first report. *Metallurgical Transactions A,* 21 (A), 289-303.

Meda, L., Marra, G., Galfetti, L., Inchingalo, S., Severini, F., & De Luca, L. (2005). Nanocomposites for rocket solid propellants. *Composites Science and Technology*, 65(5), 769-773.

Mullen, J. C. & Brewster, M. Q. (2008). *Characterization of aluminum at the surface of fine-AP/HTPB composite propellants.* Paper presented at the 44th AIAA/ASME/SAE/ASEE Joint Propulsion Conference & Exhibit 21 - 23 july 2009.

Nagashima, M.; Maji, K.; Hayakawa, M. (2001). Fabrication of Al2O3/ZrO2 micro/nano-composite prepared by high energy ball milling. *Materials Transactions*, 42, (6), 1119-1123.

Pickering, A. L., Mitterbauer, C., Browning, N. D., Kauzlarich, S. M., & Power, P. P. (2007). Room temperature synthesis of surface-functionalized boron nanoparticles. *Chemical Communications*, 6, 580-582.

Risha, G. A., Evans B. J., Boyer, E. & Kuo, K. K. (2007). Metals, Energetics additives, and special binders used in solid fuels for hybrid rockets. In Chiaverini, M. J., Kuo, K. K. (ed), *Fundamentals of hybrid rocket combustion and propulsion.* (1st, p. 416-456). American Institute of Aeronautics and Astronautics, Inc., Reston, Virginia.

Roy, C., Dubois, C., Lafleur, P. & Brousseau, P. (2004). The dispersion and polymer coating of ultrafine aluminum powders by Ziegler-Natta reaction. *Materials Research Society Symposium proceedings,* 800, 79-84.

Sabourin, J. L., Risha, G. A., Yetter, R. A., Son, S. F., & Tappan, B. C. (2008). Combustion characteristics of nanoaluminum, liquid water, and hydrogen peroxide mixtures. *Combustion and Flame, 154*, 587-600.

Shteinberg, A. S., Lin, Y.-C., Son, S. F., & Mukasyan, A. S. (2010). Kinetics of high temperature reaction in Ni-Al system: Influence of mechanical activation. *Journal of Physical Chemistry A,* 114(20), 6111-6116.

Si, P. Z., Zhang. M., You, C. Y., Geng, D. Y., Zhao, X. G., et al. (2003). Amorphus boron nanoparticles and BN encapsulating boron nano-peanuts prepared by arc-decomposing diborane and nitriding. *Journal of Materials Science*, 38(4), 686-692.

Sippel, T. R., Son, S. F. & Groven, L. J. (2013[a]). Modifying aluminum reactivity with poly(carbon monofluoride) via mechanical activation. *Propellants, Explosives, Pyrotechnics*, 38 (3), 321-326.

Sippel, T. R., Son, S. F. & Groven, L. J. (2013[b]). Altering reactivity of aluminum with selective inclusion of polytetrafluoroethylene through mechanical activation. *Propellants, Explosives, Pyrotechnics*, 38 (2), 286-295.

Sossi, A., Duranti, E., Paravan, C., Deluca, L. T., Vorozhtsov, A. B., Gromov, A. A., et al. (2013). Non-isothermal oxidation of aluminum nanopowder coated by hydrocarbons and fluorohydrocarbons. *Applied Surface Science*, 271, 337-343.

Sun, J., & Simon, S. L. (2007). The melting behavior of aluminum nanoparticles. *Thermochimica Acta, 463*(1-2), 32-40.

Talapatra, A., Bandyopadhyay, S. K., Sen, P., Barat, P., Mukherjee, S., & Mukherjee, M. (2005). X-ray photoelectron spectroscopy studies of MgB 2 for valence state of Mg. *Physica C: Superconductivity*, *419*(3), 141-147.

Umbrajkar, S. M., Schoenitz, M., Jones, S. R., & Dreizin, E. L. (2005). Effect of temperature on synthesis and properties of aluminum-magnesium mechanical alloys. *Journal of Alloys and Compounds*, 402(1-2), 70-77.

Urakaev, F. K., & Shevchenko, V. S. (2004). Synthesis of boron-rich solids of light metals in mechanochemical reactors. *Journal of Materials Science*, 39, 5507-5509.

Wada, Y., Y. Seike, *et al.* (2009). Combustion model of tetra-ol glycidyl azide polymer. 32nd International Symposium on Combustion, August 3, 2008 — August 8, 2008, Montreal, QC, Canada, Elsevier Ltd.

Ward, T. S., Chen, W., Schoenitz, M., Dave, R. N., Dreizin E. L. (2005). A study of mechanical alloying processes using reactive milling and discrete element modeling. *Acta Materialia*, 53, 2909-2918.

White, J. D. E., Reeves, R. V., Son, S. F., & Mukasyan, A. S. (2009). Thermal explosion in Ni-Al system: Influence of mechanical activation. *Journal of Physical Chemistry A*, 113(48), 13541-13547.

Wood, T. D., Pfeil, M. A., Pourpoint, T. L., Tsohas, J., Son, S. F., Connell, T. L., . . . Yetter, R. A. (2009). *Feasibility Study and Demonstration of an Aluminum and Ice Solid Propellant.* Paper presented at the 45th AIAA/ASME/SAE/ASEE Joint Propulsion Conference & Exhibit 2 - 5 august 2009.

Yeh, C. L. & Kuo, K. K. (1996). Ignition and combustion of boron particles. *Progression in Energy and Combustion Science,* 22, 511-541.

Yetter, R. A., Risha, G. A., Son, S. F. (2009). Metal particle combustion and nanotechnology. *Proceeding of the Combustion Institute,* 32, 1819-1838.

Young, G., Balar, R., Krasel, M. & Yu, K. (2006). *Effect of nanoparticles additives in airbreathing combustion.* Paper presented at the 14th AIAA/AHI International Space Planes and Hypersonic Systems and Technologies Conference 6 - 9 november 2006.

Zhang, Z., Schoenitz, M. & Dreizin, E. L. (2012). Oxidation, ignition and combustion of Al-hydrocarbon composite reactive powders. *International Journal of Energetic Materials and Chemical Propulsion. 11(4), 353-373.*

Zhang, Z., Schoenitz, M. & Dreizin, E. L. (2013). Nearly pure aluminum powders with modified protective surface. *Combustion Science and Technology*, 185 (9),130-1377.

Zhang, B., Huang, C., Yan, S., Li, Y. & Cheng, Y. (2013) Enhanced reactivity of boron, through adding nano-aluminum and wet ball milling. *Apllied Surface Science.* Article in press.

ANNEXE 1 – ON THE CONTAMINATION OF AS-MILLED BORON POWDERS

As was mentioned in this word, the major difficulty found to produce the energetic-coated metal particles concern the boron milling, because the level of contamination from milling media was very high in the first experiments. The W and Co, clearly coming from the cobalt-cemented tungsten carbide milling jar and balls, was identified in an XPS analysis of the as-milled boron powders. However, the contamination can be qualitatively analyzed using a simple method to verify the magnetic property of as-milled powder. Because the cobalt-cemented tungsten carbide is strongly magnetic, it is simple to identify the presence of this material using a magnetic stir bar (See Fig. Annexo-1.1)

Figure Annexo-1.1: Magnetic property of contaminated boron powder

Devener et al. (2009) describing a method to remove the contamination based on their magnetic property. The particles were suspended in a hydrocarbon (hexane or JP-5), then “ cleaned” by simply stirring the liquid using a magnetic stir bar. The magnetic was periodically removed, wiped clean with a lint-free cloth, and the process was repeated until the magnet appeared clean under visual inspection. We have tried to apply this method with our samples, but it has not functioned. TEM images of as-milled boron powders reveal that the tungsten particles are interspersed between boron particles throughout the sample (Fig. Annexo-1.2). Dark areas in TEM images were identified by Energy-dispersive X-ray spectroscopy (EDS) as a main content of tungsten and

cobalt. Thus, the contamination is intimately mixed that was not possible to remove it by physical techniques.

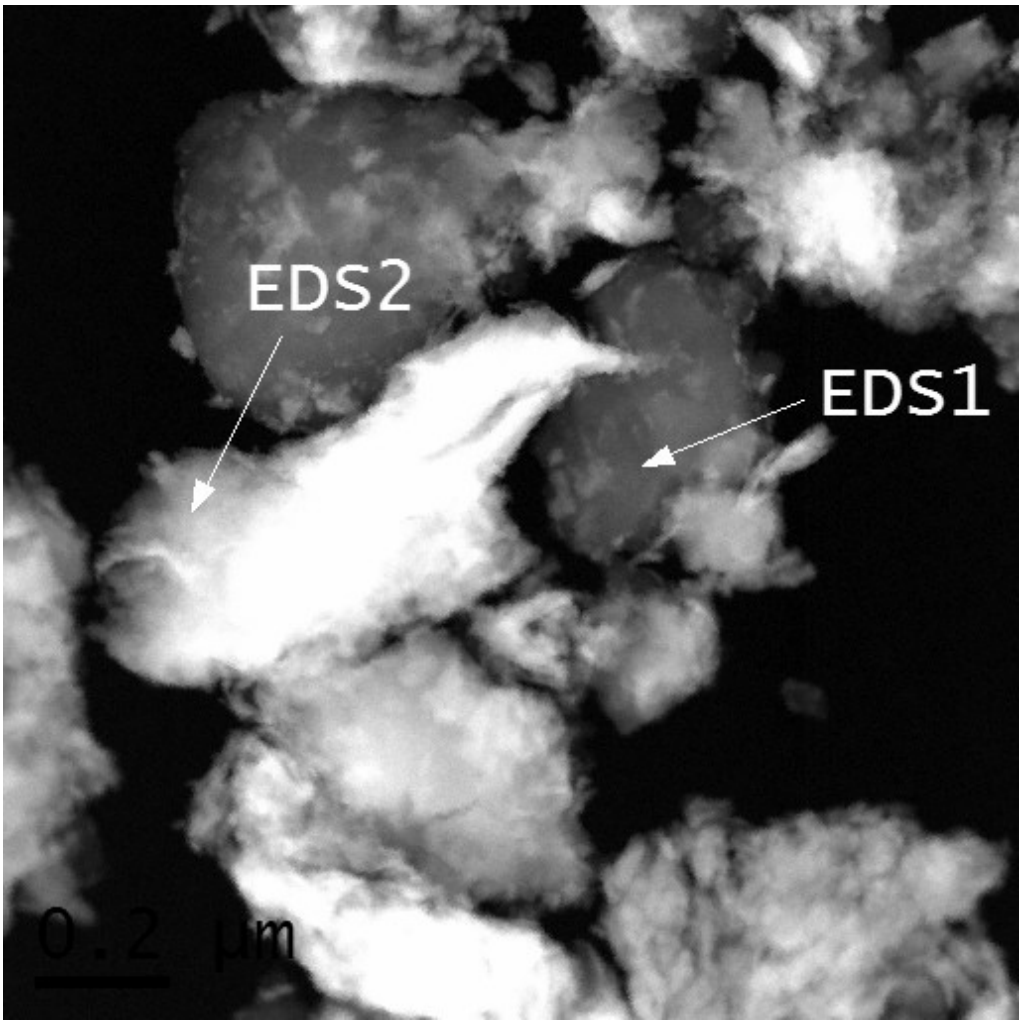

Figure Annexo-1.2: TEM images of as-milled boron powders

The logical issue to this shortcoming is to prevent or diminish the contamination during the milling processes. As the boron is very hard material (i.e. Mohs hardness ~ 9.5) and very abrasive material, it was necessary diminish the shear and attrition with the balls and inner walls of the vial. In the ball milling process, the solvents and organic compounds added could act as “process control agent” (PCA), which means a material that has the property to facilitate the dispersion of powders and lubricate the surface of balls and inner walls, thus facilitates the milling processes. Different solvents were tested, and the same polymer used to coat the particles was used as a means to achieve le better lubrication of balls. Also, the mixture of magnesium powders with boron seams to diminish the levels of contamination because magnesium is a ductile material.

The XPS analysis was used for more accurate measurement of the levels of contamination. Because atomic composition changes with the organic capping adding to the particles, it is essential that a ratio between atomic species analyzed be established, for comparison purpose of different samples. To achieve a better comparison between the as-milled powder samples, it was used the ratio of W/B (i.e. the atomic % of W divided by B atomic %). Table Annexo-1.1 shows some XPS results of different as-milled boron samples.

Table Annexo-1 1: Ratio of W/B atomic% of as-milled boron samples.

	Boron	B_PGA	B_GAPm	$(Mg/B)_{5\%}$ GAPm	$(Mg/B)_{10\%}$ GAPm	$(Mg/B)_{20\%}$ GAPm
W/B (10^2)	6.0	5.6	1.9	1.5	0.9	0.4

Clearly, the effect of addition of the polymer results in less contamination of powders, in comparison of pure boron and of the propargyl alcohol. Also, as was expected, the addition of magnesium powders influences the milling process, reducing the shear and attrition, which results in a smaller level of contamination.

In conclusion, because boron is a very abrasive material and leads a high levels of contamination in ball milling processes, it is necessary the additional PCA for a better milling process. This PCA, sometimes, can be the same organic compound used for coating particles.